Bioinorganic Chemistry and Applications

Metals in Medicine

Guest Editors: Goran N. Kaluđerović,
Santiago Gómez-Ruiz, Danijela Maksimović-Ivanić,
Reinhard Paschke, and Sanja Mijatović

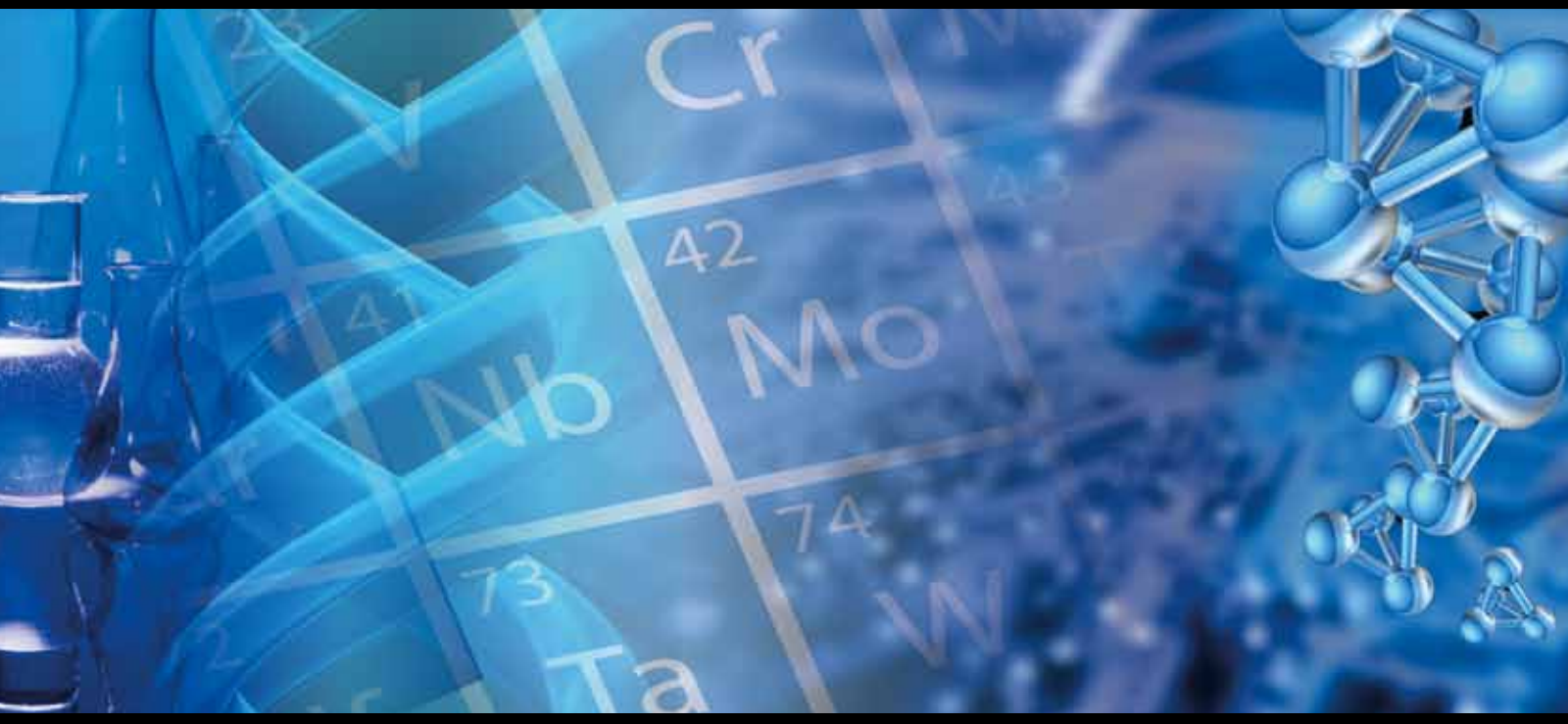

Metals in Medicine

Metals in Medicine

Guest Editors: Goran N. Kaluđerović, Santiago Gómez-Ruiz, Danijela Maksimović-Ivanić, Reinhard Paschke, and Sanja Mijatović

Editorial Board

Contents

Hindawi Publishing Corporation
Bioinorganic Chemistry and Applications
Volume 2012, Article ID 705907, 2 pages
doi:10.1155/2012/705907

Editorial
Metals in Medicine

Goran N. Kaluđerović,[1] Santiago Gómez-Ruiz,[2] Danijela Maksimović-Ivanić,[3] Reinhard Paschke,[4] and Sanja Mijatović[3]

[1] *Institut für Chemie, Martin-Luther-Universität Halle-Wittenberg, Kurt-Mothes-Straße 2, 06120 Halle, Germany*
[2] *Departamento de Química Inorgánicay Analítica, ESCET, Universidad Rey Juan Carlos, 28933 Móstoles, Spain*
[3] *Institute for Biological Research "Sinisa Stankovic," University of Belgrade, Bulevar despota Stefana 142, 11060 Belgrade, Serbia*
[4] *Biozentrum, Martin-Luther-Universität Halle-Wittenberg, Weinbergweg 22, 06120 Halle, Germany*

Correspondence should be addressed to Goran N. Kaluđerović, goran.kaluderovic@chemie.uni-halle.de

Received 3 July 2012; Accepted 3 July 2012

Metals in medicine are bridging the areas of inorganic chemistry and medicine. Metal-based materials, metallodrugs, and agents for treating and detecting diseases, their synthesis, structure, and general properties, as well as biological applications on cellular and living system level, are of great importance. The mechanisms of action and the roles of these metal compounds in cellular regulation and signaling in health and diseases are of principal interest. These areas are linked by the need to involve researchers having a deep understanding of inorganic chemistry in medically relevant research. This special issue presents a collection of papers dealing with different compounds/materials investigated for antitumoral, antimicrobial, and antifungal activity as well as DNA binding study.

Y. Li et al. reported on the efficient and specific method for the determination of diphenyl-di-(2,4-difluobenzohydroxamato)tin(II), DPDFT, in rat plasma. Their preliminary studies indicated nonlinearity pharmacokinetics in the investigated dose ranges in rats and that the concentration-time curves of DPDFT in rat plasma could be fitted to two-compartment model. Additionally, results hinted that DPDFT might accumulate in certain organs, thus producing the toxicity, or could be quickly metabolized in the plasma into active antitumoral constituents.

The synthesis and characterization of novel salicylaldehyde-derived ligands and corresponding Cu(II), Co(II), Ni(II), and Zn(II) complexes are described by Kursunlu et al. Ligands bearing chlorine, bromine and –OH substituents showed moderate inhibition activity against some Gram-positive and Gram-negative bacteria including methicillin-resistant *Staphylococcus aureus*. Ni(II) and Zn(II) complexes were generally more effective against tested bacteria than Cu(II) and Co(II) complexes.

In the work of A. A. Al-Amiery et al., significant antifungal activity of Cu(II), Co(II), and Ni(II) complexes with (*Z*)-2-(pyrrolidin-2-ylidene)hydrazinecarbothioamide and chloride ligands is described. The complexes were found to be superior antioxidants compared to ascorbic acid.

Zietz et al. evaluated Cu release characteristics from Cu doped titanium alloy (Ti_6Al_4V) of antimicrobial implant surfaces *in vitro* according to the storage fluid and surface roughness. Plasma immersion ion implantation of Cu (Cu-PIII) and pulsed magnetron sputtering process of a titanium copper film (Ti-Cu) were applied to Ti_6Al_4V samples with different surface finishing of the implant material (polished, hydroxyapatite, and corundum blasted). The Cu concentration in the supernatant was measured using atomic absorption spectrometry.

M. Rezaee et al. investigated the optimum experimental conditions to prepare dry thin films of Pt compounds bound to plasmid DNA on a Ta substrate. Their results show that used conditions can induce damage to DNA and highly sensitize them to manipulations required to form thin films and recover DNA from the Ta substrate. The concentration of intact DNA increases significantly in the film samples when used lower incubation temperature and shorter incubation time. Thus, the optimum condition is obtained from

equilibrium between temperature, time, and Pt-compounds concentration during the DNA platination reaction.

In the review by S. Gómez-Ruiz et al., the mode of action of cisplatin against tumor cells as well as a brief outlook on the metallocene compounds as antitumor drugs and future tendencies for the use of the latter in anticancer chemotherapy are summarized. The authors reported on the molecular mechanisms of cisplatin interaction with DNA, DNA repair mechanisms, and cellular proteins. Molecular background of the sensitivity and resistance to cisplatin as well as its influence on the efficacy of the antitumor immune response were evaluated. Moreover, the use and mechanism of some metallocenes (titanocene, vanadocene, molybdocene, ferrocene and zirconocene) with high antitumor activity are reported.

Acknowledgments

The authors thank the referees who devoted considerable time and effort for reviewing the papers. Furthermore, they would like to express their gratitude to Mr. Noran El-Zoheary and other editorial assistants of Bioinorganic Chemistry and Applications for their help in many practical problems and for great help during the organization of the special issue.

Goran N. Kaluđerović
Santiago Gómez-Ruiz
Danijela Maksimović-Ivanić
Reinhard Paschke
Sanja Mijatović

Hindawi Publishing Corporation
Bioinorganic Chemistry and Applications
Volume 2012, Article ID 140284, 14 pages
doi:10.1155/2012/140284

Review Article

On the Discovery, Biological Effects, and Use of Cisplatin and Metallocenes in Anticancer Chemotherapy

Santiago Gómez-Ruiz,[1] Danijela Maksimović-Ivanić,[2] Sanja Mijatović,[2] and Goran N. Kaluđerović[3]

[1] *Departamento de Química Inorgánica y Analítica, E.S.C.E.T., Universidad Rey Juan Carlos, 28933 Móstoles, Spain*
[2] *Institute for Biological Research "Sinisa Stankovic", University of Belgrade, Boulevard of Despot Stefan 142, 11060 Belgrade, Serbia*
[3] *Institut für Chemie, Martin-Luther-Universität Halle-Wittenberg, Kurt-Mothes-Straße 2, 06120 Halle, Germany*

Correspondence should be addressed to Goran N. Kaluđerović, goran.kaluderovic@chemie.uni-halle.de

Received 11 March 2012; Accepted 19 May 2012

Academic Editor: Zhe-Sheng Chen

The purpose of this paper is to summarize mode of action of cisplatin on the tumor cells, a brief outlook on the metallocene compounds as antitumor drugs as well as the future tendencies for the use of the latter in anticancer chemotherapy. Molecular mechanisms of cisplatin interaction with DNA, DNA repair mechanisms, and cellular proteins are discussed. Molecular background of the sensitivity and resistance to cisplatin, as well as its influence on the efficacy of the antitumor immune response was evaluated. Furthermore, herein are summarized some metallocenes (titanocene, vanadocene, molybdocene, ferrocene, and zirconocene) with high antitumor activity.

1. Cisplatin

Since 1845, when Italian doctor Peyrone synthesized cisplatin (Figure 1), through Rosenberg's discovery of cisplatin antiproliferative potential [1], and subsequent approval for clinical usage in 1978, this drug is considered as most promising anticancer therapeutic [2, 3]. Cisplatin is highly effective against testicular, ovarian, head and neck, bladder, cervical, oesophageal as well as small cell lung cancer [4].

For more than 150 years, first exaltation about this "drug of the 20th century" was replaced with discouraging data about its toxicity and ineffectiveness got from clinical practice. It was found that cisplatin induced serious side effects such as nephrotoxicity, neurotoxicity, ototoxicity, nausea, and vomiting [5]. General toxicity and low biological availability restricted its therapeutically application. In addition, it is known that some tumors such as colorectal and nonsmall lung cancers are initially resistant to cisplatin while other like ovarian and small cell lung cancers easily acquired resistance to drug [6]. Numerous examples from *in vitro* studies confirmed that exposure to cisplatin often resulted in development of apoptotic resistant phenotype [7–9]. Following this, development of cisplatin resistant cell lines is found useful for testing the efficacy of future cisplatin modified drugs and on the other hand for evaluation of mechanisms involved in development of resistance. For better understanding of unresponsiveness to cisplatin, it is necessary to define the exact molecular targets of drug action from the moment of entering tumor cell. It is proposed the intact cisplatin which avoided bounding to plasma proteins enter the cell by diffusion or active transport via specific receptors (Figure 2) [10, 11]. Cisplatin is able to use copper-transporting proteins to reach intracellular compartments [12–14]. In addition, regarding to its chemical reactivity, cisplatin can influence cell physiology even through interaction with cell membrane molecules such as different receptors.

1.1. Cisplatin and DNA. Although it is known that DNA is a major target for cisplatin, only 5–10% intracellular concentration of cisplatin is found in DNA fraction while 75–85% binds to nucleophilic sites of intracellular constituents like thiol containing peptides, proteins, replication enzymes, and RNA [6, 15–17]. This preferential binding to non-DNA targets offers the explanation for cisplatin resistance but

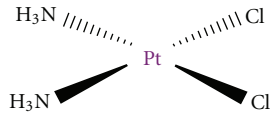

Figure 1: Cisplatin.

also its high toxicity. Prerequisite of efficient formation of cisplatin DNA adducts is hydratization of cisplatin enabled by low chloride ions content inside the cells [18]. N7 of guanine and in less extend adenine nucleotide are targeted by platinum [19]. Binding of cisplatin to DNA is irreversible and structurally different adducts are formed. The adducts are classified as intrastrand crosslinking of two nucleobases of single DNA strand, interstrand crosslinking of two different strands of one DNA molecule, chelate formation through *N*- and *O*-atoms of one guanine, and DNA-protein crosslinks [20, 21]. Cisplatin forms about 65% pGpG-intrastrand crosslinks, 25% pApG-intrastrand crosslinks, 13% interstrand or intrastrand crosslinks on pGpXpG sequences, and less than 1% of monofunctional adducts (Figure 3) [22]. Crucial role of 1,2-intrastrand crosslinks in antitumor potential of the cisplatin is supported by two facts. First, high mobility group proteins (HMG) specifically recognize this type of cisplatin-DNA interaction and second, these adducts are less efficiently removed by repair enzymes [17]. In addition, important mediators of cisplatin toxicity are ternary DNA-platinum-protein crosslinks (DPCL) whose frequency is dependent from the cell type as well as the type of the treatment. DPCLs inhibited DNA polymerization or their own removal by nucleotide excision repair system more potently than other DNA adducts [17]. In fact, cisplatin DNA adducts can be repaired by nucleotide excision repair proteins (NER), mismatch repair (MMR), and DNA-dependent protein kinases protein [17].

1.2. DNA Repair Mechanism. Nucleotide excision repair proteins are ATP-dependent multiprotein complex able to efficiently repair both inter as well as intrastrand DNA-cisplatin adducts. Successful repair of 1,2-d(GpG) and 1,3-d(GpNpG) intrastrand crosslinks has been found in different human and rodent NER systems [23, 24]. This repair mechanism is able to correct the lesions promoted by chemotherapeutic drugs, UV radiation as well as oxidative stress [17]. Efficacy of NER proteins varying in different type of tumors and is responsible for acquirement of cisplatin resistance. Low level of mentioned proteins is found in testis tumor defining their high sensitivity to cisplatin treatment. Oppositely, ovarian, bladder, prostate, gastric, and cervical cancers are resistant to cisplatin based therapy due to overexpression of several NER genes [25, 26].

Mismatch repair (MMR) proteins are the post replication repair system for correction of mispaired and unpaired bases in DNA caused by DNA Pt adducts. MMR recognized the DNA adducts formed by ligation of cisplatin but not oxaliplatin [27–30]. Defective MMR is behind the resistance of ovarian cancer to cisplatin and responsible for the mutagenicity of cisplatin [31].

DNA dependent protein kinase is a part of eukaryotic DNA double strand repair pathway. This protein is involved in maintaining of genomic stability as well as in repair of double strand breaks induced by radiation [31]. In ovarian cancer presence of cisplatin DNA adducts inhibited translocation of DNA-PK subunit Ku resulting in inhibition of this repair protein [32].

Special attention is focused on recognition of cisplatin-modified DNA by HMG proteins (HMG). It is hypothesized that HMG proteins protected adducts from recognition and reparation [17, 31]. Moreover, it was postulated that these proteins modulate cell cycle events and triggered cell death as a consequence of DNA damage. One of the members from this group marked as HMGB1 is involved in MMR, increased the p53 DNA-binding activity and further stimulated binding of different sequence specific transcription factors [33]. Few studies revealed that cisplatin sensitivity was in correlation with HMGB level, while other studies eliminated its significance in response to cisplatin treatment. Contradictory data about the relevance of HMG proteins in efficacy of cisplatin therapy indicated that this relation is defined by cell specificity.

1.3. Cytotoxicity of Cisplatin. Other non-HMG nuclear proteins are also involved in cytotoxicity of cisplatin. Presence of cisplatin DNA adducts is able to significantly change or even disable the primary function of nuclear proteins essential for transcription of mammalian genes (TATA binding protein, histon-linker protein H1 or 3-methyladenine DNA glycosylase mammalian repair protein) [34–36].

Although cytotoxicity of cisplatin is usually attributed to its reactivity against DNA and subsequent lesions, the fact that more than 80% of internalized drug did not reach DNA indicated the involvement of numerous non-DNA cellular targets in mediation of cisplatin anticancer action [6]. As a consequence of exposure to cisplatin, different signaling pathways are affected. There is no general concept applicable to all types of tumor. It is evident that response to cisplatin is defined by cell specificity. Numerous data revealed changes in activity of most important signaling pathways involved in cell proliferation, differentiation and cell death such as PI3K/Akt, MAPK as well as signaling pathways involved in realization of death signals dependent or independent of death receptors [33]. It is very important to note that alteration in signal transduction upon the cisplatin treatment could be the consequence of both, DNA damage or interaction with exact protein or protein which is relevant for appropriate molecular response. Some of the interactions between protein and cisplatin are already described. Therefore, it was found that cisplatin directly interacts with telomerase, an enzyme that repairs the ends of eukaryotic chromosomes [31, 37]. In parallel, cisplatin-induced damage of telomeres which are not transcribed and therefore hidden from NER. Other important protein targeted by cisplatin is small, tightly folded molecule known as ubiquitin (Ub) [38]. Ub is implicated in selective degradation of short-lived cellular proteins [39]. It has been hypothesized that direct interaction of cisplatin with this protein presented a strong signal for cell death [40]. Two binding sites were identified as target

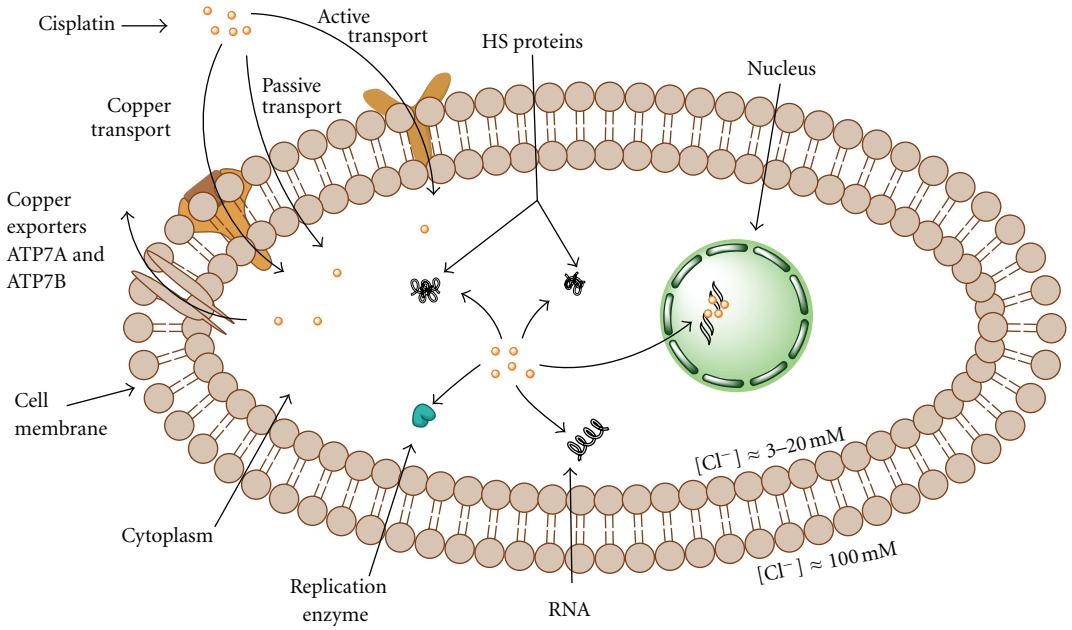

Figure 2: Cisplatin and the cell: transport/export and targets.

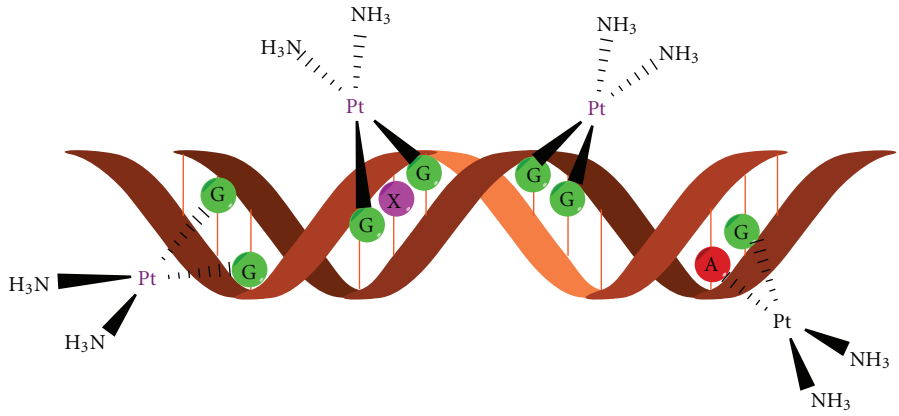

Figure 3: DNA adduct formation with cisplatin moiety.

for cisplatin ligation: *N*-terminal methionine (Met1) and histidine at position 68, while the drug makes at least four types of adducts with protein [38]. This resulted in disturbed proteasomal activity and further cell destruction. Having in mind that proteasomal inactivation by specific inhibitors showed promising results in cancer treatment, this aspect of cisplatin reactivity can be leading cytotoxic effect even to be more powerful than DNA damage [41]. One of the crucial molecules involved in propagation of apoptotic signal through depolarization of mitochondrial potential—cytochrome c is also targeted by cisplatin on Met65 [42]. Further, on the list of protein or peptide targets for cisplatin are glutathione and metallothioneins, superoxide dismutase, lysozyme as well as extracellular protein such as albumin, transferrin, and hemoglobin [43]. Some of mentioned interactions served as drug intracellular pool while their biological relevance is still under investigation.

1.4. Activation of Signaling Pathways Induced with Cisplatin. DNA damage induced by cisplatin represent strong stimulus for activation of different signaling pathways. It was found that AKT, c-Abl, p53, MAPK/JNK/ERK/p38 and related pathways respond to presence of DNA lesions [31, 33]. AKT molecule as most important Ser/Thr protein kinase in cell survival protects cells from damage induced by different stimuli as well as cisplatin [44]. Cisplatin downregulated XIAP protein level and promoted AKT cleavage resulting in apoptosis in chemosensitive but not in resistant ovarian cancer cells [45, 46]. Recently published data about synergistic effect of XIAP, c-FLIP, or NFkB inhibition with cisplatin are mainly mediated by AKT pathway [47].

Protein marked as the most important in signaling of the DNA damage is c-Abl which belongs to SRC family of non-receptor tyrosine kinases [31, 33]. This molecule acts as transmitter of DNA damage triggered by cisplatin from nucleus

to cytoplasm [48]. Moreover, sensitivity to cisplatin induced apoptosis is directly related with c-Abl content and could be blocked by c-Abl overexpression [33]. Key role of c-Abl in propagation of cisplatin signals is confirmed in experiments with ABL deficient cells [49]. It was found that cisplatin failed to activate p38 and JNK in the absence of c-Abl. Homology of this kinases with HMGB indicated the possibility that c-Abl recognized and interact with cisplatin DNA lesions like HMGB1 protein [31].

1.5. The Role of the Functional p53 Protein. Evaluation of a 60 cell line conducted by the National Cancer Institute revealed that functional p53 protein is very important for successful response to cisplatin treatment [33]. This tumor suppressor is crucial for many cellular processes and determined the balance between cell cycle arrest as a chance for repair and induction of apoptotic cell death [33]. However, despite extensive NCI study, there are controversial data about correlation between cisplatin sensitivity and p53. For example, it was found that functional p53 was associated with amplified cisplatin sensitivity in SaOS-2 osteosarcoma cells in high serum growth conditions while the opposite relation was observed upon starvation [33]. This phenomenon could be connected to autophagic process triggered in serum deficient conditions, which in turn downregulate cisplatin promoted apoptosis [50]. In some other studies, the response to cisplatin was not influenced by p53. It is indicative that antitumor potential of cisplatin and its interaction with p53 is a question of multiple factors such as tumor cell type, specific signaling involved in cancerogenesis, as well as other genetic alterations. In addition, protein involved or influenced by p53 pathway such as Aurora kinase A, cyclin G, BRCA1 as well as proapoptotic or antiapoptotic mediators are also able to control cisplatin toxicity [33].

1.6. Relation between Cisplatin and Mitogen-Activated Protein (MAP) Kinases. Finally, signaling pathways mediated by mitogen-activated kinases are strongly influenced by cisplatin. These enzymes are highly important in definition of cellular response to applied treatment because they are the major regulators of cell proliferation, differentiation, and cell death. ERK (extracellular signal-related kinase) preferentially responds to growth factor and cytokines but also determines cell reaction to different stress conditions, particularly, oxidative [33]. Cisplatin treatment mainly activated ERK in a dose- and time-dependent manner [33, 51, 52]. However, like as previously described, changes in ERK activity upon the exposure to cisplatin varying from type to type of the malignant cell and is defined by their intrinsic features. Following this, in some circumstances ERK activation antagonized cisplatin toxicity. In cells with significant upregulation of ERK activity in response to cisplatin treatment, exposure to specific MEK1 inhibitor PD98052 abrogated its toxicity. Also, development of the resistance to the cisplatin in HeLa cells is connected with reduced ERK response to the treatment [52]. Moreover, combined treatment with some of the naturally occurring compounds such as aloe-emodin-neutralized cisplatin toxicity through inhibition of ERK, indicated possible negative outcome of combining of conventional and phytotherapy [53, 54].

Regardless of numerous evidences about its critical role in cisplatin-mediated cell death, ERK is not the only molecule from MAP family which responded to cisplatin. Several studies revealed JNK (c-Jun N-terminal kinase) activation upon the cisplatin addition [55, 56]. However, similarly to other molecules previously mentioned this signal is not the unidirectional and could be responsible for realization but also protection from death triggered by the cisplatin [57, 58]. Finally, there are numerous evidences about highly important role of third member of MAP kinases, p38, in response to cisplatin [59, 60]. Lack of p38 MAPK leads to appearance of resistant phenotype in human cells [55, 60]. Early and short p38 activation is principally described in cells unresponsive to cisplatin while long-term activation was found in sensitive clones. Moreover, in the light of the fact that this kinase has a role in modifying the chromatin environment of target genes, its involvement in cisplatin-induced phosphorilation of histon 3 was determined [61].

1.7. On the Mode of Cell Death Induced by Cisplatin. The net effect of intracellular interaction of cisplatin with DNA and non-DNA targets is the cell cycle arrest and subsequent death in sensitive clones. There are two type of death signals resulting from cellular intoxication by this drug (Figure 4). Fundamentally, the drug concentration presents the critical point for cell decision to undergo apoptotic or necrotic cell death [62]. Primary cultures of proximal tubular cells isolated from mouse died by necrosis if they were exposed to high doses of cisplatin just for a few hours while apoptotic cell death is often triggered by long-term exposure to significantly lower concentrations [63]. However, the presence of necrosis in parallel with apoptosis in tumor-cell population indicated that type of cell death is not just the question of dose but also is defined by cell intrinsic characteristics and energetic status of each cell at the moment of the treatment. In fact, it was considered that intracellular ATP level dictate cell decision to die by necrotic or apoptotic cell death [64, 65]. One of the signals which are provoked with DNA damage is PARP-1 activation and subsequent ATP depletion caused by PARP-1 mediated cleavage of NAD+. This event is a trigger for necrotic cell death. However, activated caspases cleaved the PARP-1, preventing necrotic signal and favor the execution of apoptotic process. On the other hand, the inhibition of caspases by intracellular inhibitors IAP together with continual PARP activity and ATP depletion resulted in necrosis [31]. As numerous biological phenomena, this one is not unidirectional. It was found that failure in PARP cleavage may also serve to apoptosis [66]. This paradox was ascribed to changes in pyridine nucleotide pool as well as in pool of ATP/ADP responsible for regulation of mitochondrial potential [67]. Atypical apoptosis was observed in L1210 leukemia cell line exposed to cisplatin. Different death profiles in cisplatin treated cells confirmed plasticity of signals involved in cell destruction and focus the attention to the molecules responsible for resistance to death as possible targets for the therapy. Having in mind that

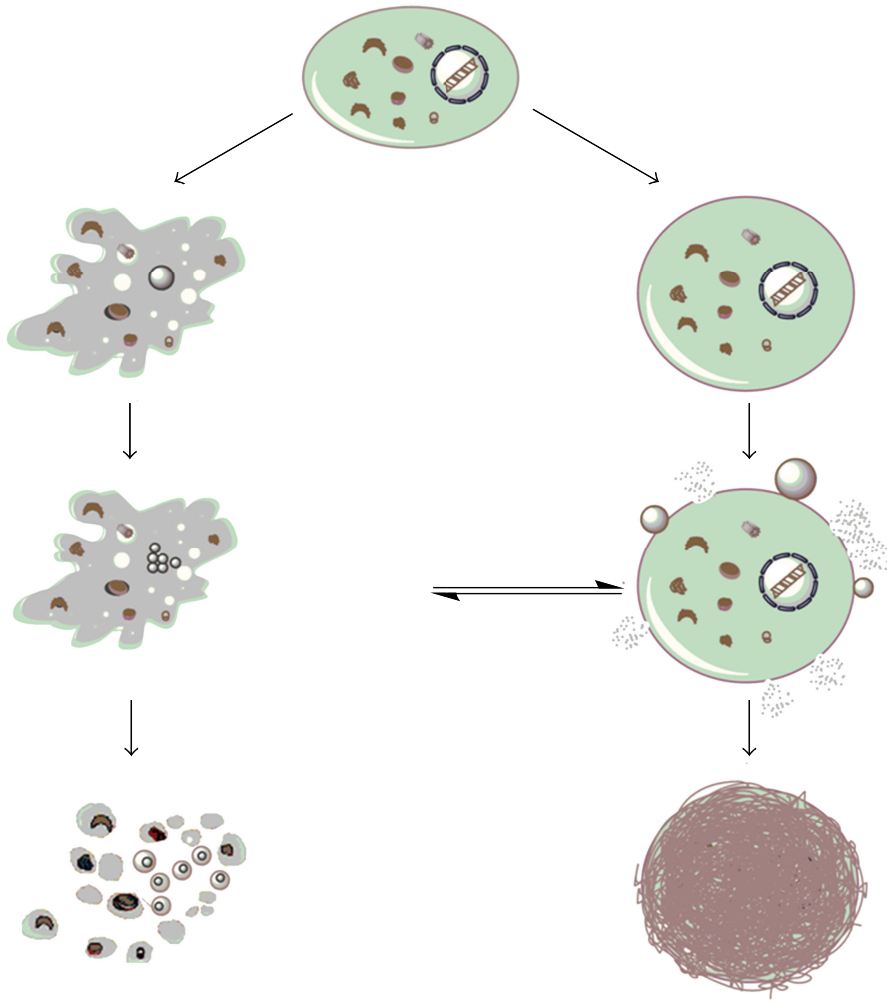

Figure 4: Mode of cell death induced by cisplatin: apoptosis (left) and necrosis (right).

cisplatin is toxic agent against whom the cell can activate autophagy as protective process; the specific inhibition of autophagy by certain type of molecules could amplify the effectiveness of cisplatin [50].

1.8. Cisplatin in Immune Senzitization. One of the rarely mentioned but very important aspects of antitumor activity of cisplatin is based on the experimental data about its potential to amplified the sensitivity of malignant cells to one or the most potent and selective antitumor immune response mediated by TNF-related apoptosis inducing ligand TRAIL [68, 69]. This molecule is produced by almost all immune cells involved in nonspecific as well as adoptive immune response. Unfortunately, in the moment when tumor is diagnosed, its sensitivity to natural immunity is debatable. In most of the situations, malignant cells became resistant to TRAIL-mediated cytotoxicity [70]. Moreover, it was confirmed that cisplatin promoted their sensitivity to TRAIL. Nature of its immune sensitizing potential is at least partly due to upregulation of expression of TRAIL receptors—DR4 and DR5 on the cellular membrane glioma, colon and prostate cell lines as well as downregulation of cellular form of caspase 8 inhibitor FLIP [68, 69]. In addition, presence of cysteine rich domen in the structure of TRAIL specific death receptors indicated possibility that cisplatin directly interact with them.

1.9. Resistance to Cisplatin and How to Surmount It. Resistance to cisplatin could be established at multiple levels, from cellular uptake of the drug through interaction with protein and DNA and finally activation of signals which lead the cell to death. Disturbed drug uptake, drug scavenging by cellular proteins, upregulation of prosurvival signals together with upregulated expression of antiapoptotic molecules such as Bcl-2 and BclXL, overexpressed natural inhibitors of caspases like FLIP and XIAP, diminished MAP signaling pathway or deficiency in proteins involved in signal transferring from damaged DNA to cytoplasm, enhanced activity of repair mechanisms and efficient redox system are features mainly responsible for unsuccessful treatment with cisplatin [33]. Well defined molecular background of the resistance to cisplatin point out the way on how to surmount it. It was

already known that some of combined treatments of cisplatin with other chemotherapeutics such as 5-fluorouracil improved therapeutic response rates in patients with head and neck cancer [71, 72]. Furthermore, inhibition of NER DNA repair system, cotreatment with histone deacetylase inhibitors (HDAC) such as trichostatin A (TSA) or suberoylanilide hydeoxamic (SAHA) [73], small molecules inhibitors of FLIP and XIAP as well as topoisomerase inhibitors strongly synergized with cisplatin, elevating its therapeutic potential.

2. Metallocenes in Anticancer Chemotherapy

Most of the metallodrugs used currently in chemotherapy treatment are based on platinum (cisplatin analogues), although as side effects are the weakest point in the use of cisplatin-based drugs in chemotherapy are the high number of side effects, many efforts are focused on the search of novel metal complexes with similar antineoplastic activity and less side effects as an alternative for platinum complexes. Transition-metal complexes have shown very useful properties in cancer treatment, and the most important work in chemotherapy with transition metals has been carried out with Group 4, 5, 6, 8, and 11 metal complexes.

From all the studied metal complexes, a wide variety of studies have been carried out for metallocenes which have become an alternative to platinum-based drugs.

According to the IUPAC classification metallocene contains a transition metal and two cyclopentadienyl ligands coordinated in a sandwich structure. These compounds have caused a great interest in chemistry due to their versatility which comes from their interesting physical properties, electronic structure, bonding, and their chemical and spectroscopical properties [74]. Academic and industrial research on metallocene chemistry has led to the utilization of these derivatives in many different applications such as olefin polymerization catalysis, asymmetric catalysis or organic syntheses, preparation of magnetic materials, use as nonlinear optics or molecular recognizers, flame retardants or in medicine [74].

Within medicine, metallocene complexes are being normally used as biosensors or as antitumor agents. Regarding their anticancer applicability, titanocene, vanadocene, molybdocene, and ferrocene have been traditionally used with very good results, however, recently also zirconocene derivatives have pointed towards a future potential applicability due to the increase of their cytotoxicity. All the other metallocene derivatives have been either not tested or have demonstrated no remarkable applicability in the fight against cancer.

In this part of the paper, we will briefly discuss separately the properties of metallocene derivatives of titanium, zirconium, vanadium, molybdenum, and iron.

2.1. Titanocene Derivatives. Titanocene derivatives are together with ferrocene complexes the most studied metallocenes in the fight against cancer. The pioneering work of Köpf and Köpf-Maier in the early 1980's showed the antiproliferative properties of titanocene dichloride, $[TiCp_2Cl_2]$ ($Cp = \eta^5\text{-}C_5H_5$, Figure 5(a)). This compound was studied in phase I clinical trials in 1993 [75–77] using water soluble formulations developed by Medac GmbH (Germany) [78].

Phase I clinical trials pointed towards a dose-limiting side effect associated to nephrotoxicity which together with hypoglycemia, nausea, reversible metallic taste immediately after administration, and pain during infusion, seemed to be the weakest part of the administration of titanocene dichloride in humans. On the other hand, the absence of any effect on proliferative activity of the bone marrow, one of the most common dose-limiting side-effect of nonmetallic drugs, was in interesting result that increased the potential applicability of this compound in humans.

Although phase I clinical trials were not as satisfactory as expected, some phase II clinical trials with patients with breast metastatic carcinoma [79] and advanced renal cell carcinoma [80] have been carried out observing a low activity which discouraged further studies.

However, after the recent work of many groups such as Tacke, Meléndez, McGowan, Baird, and Valentine the interest in this field has been renewed [81–85]. In this context a wide variety of titanocene derivatives with amino acids [86, 87], benzyl-substituted titanocene or *ansa*-titanocene derivatives [81], amide functionalized titanocenyls [88, 89], titanocene derivatives with alkylammonium substituents on the cyclopentadienyl rings [90–92], steroid-functionalized titanocenes [93], and alkenyl-substituted titanocene or *ansa*-titanocene derivatives (Figure 5) [94–96], have been reported with very interesting cytotoxic properties which enhance their applicability in humans. In particular, $[Ti\{\eta^5\text{-}C_5H_4(CH_2C_6H_4OCH_3)\}_2Cl_2]$ (titanocene Y, Figure 5(b)) and its family, reported by Tacke and coworkers, have demonstrated to have extremely interesting anticancer properties which need to be highlighted.

In general, the cytotoxic activity of titanocene complexes has been correlated to their structure, however, there are still several questions regarding the anticancer mechanism of titanocene(IV) complexes. According to the reported studies in the topic, it seems clear titanium ions reach cells assisted by the major iron transport protein "transferrin" [97–100], and the nucleus in an active transport facilitated probably by ATP. In a final step, binding of titanium ion to DNA leads to cell death (Figure 6) [101, 102]. However, recent experiments have shown interactions of a ligand-bound Ti(IV) complex to other proteins or enzymes [103–105], indicating alternatives in cell death mechanisms, which is currently leading to intensive studies by several research groups.

2.2. Zirconocene Derivatives. An alternative to titanium complexes may be zirconium(IV) derivatives which are in a very early stage of preclinical experiments. Already in the 1980's Köpf and Köpf-Maier showed the potential of zirconocene derivatives as anticancer agents and very recently, two different studies on zirconocene anticancer chemistry have been reported [106, 107]. These studies by Allen et al. [106] and Wallis et al. [107]have described the cytotoxic activity of different functionalized zirconocene complexes, observing an irregular behavior in the anticancer tests, from which only the complexes $[Zr\{\eta^5\text{-}C_5H_4(CH_2)_2N(CH_2)_5\}_2Cl_2\cdot 2HCl]$

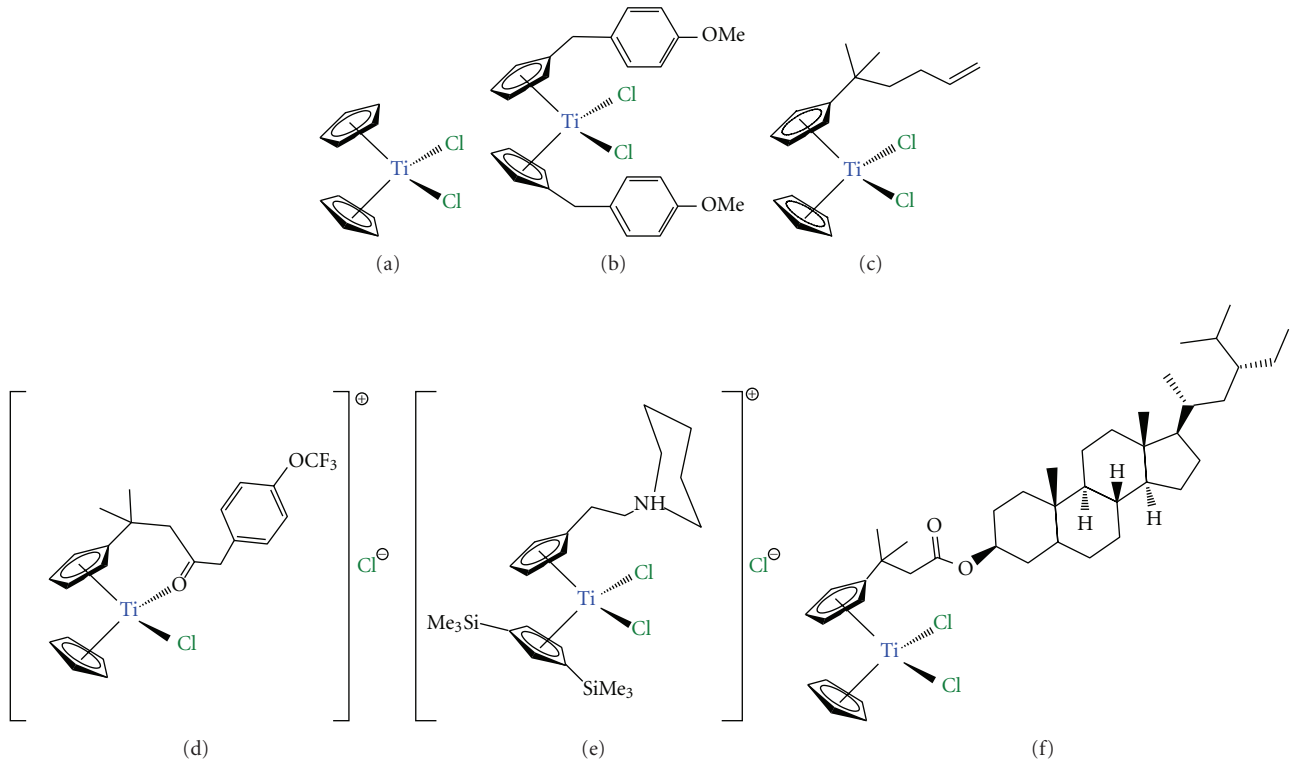

Figure 5: Titanocene derivatives used in preclinical and clinical trials: (a) titanocene dichloride; (b) titanocene-Y; (c) alkenyl-substituted titanocene derivative; (d) titanocenyl complex; (e) titanocene derivative with alkylammonium substituents; (f) steroid-functionalized titanocene derivative.

(Figure 7(a)) and $[Zr\{\eta^5\text{-}C_5H_4(CH_2C_6H_4OCH_3)\}_2Cl_2]$ (zirconocene Y, Figure 7(b)) have shown promising activity that needs to be improved in order to apply them in anticancer chemotherapy.

In parallel, our research group reported the synthesis, structural characterization, catalytic behavior in the polymerization of ethylene and copolymerization of ethylene and 1-octene and the cytotoxic activity on different human cancer cell lines of a novel alkenyl substituted silicon-bridged *ansa*-zirconocene complex (Figure 7(c)) which proved to be the most active zirconocene complex on human A2780 ovarian cancer cells, reported to date [108].

There is still hard work to do in this field to find a suitable zirconocene complex with increased cytotoxic activity and good applicability in humans.

2.3. Vanadocene Derivatives. Vanadocene dichloride, $[VCp_2Cl_2]$ (Cp = η^5-C_5H_5), was extensively studied in preclinical testing against both animal and human cancer cell lines, observing a higher *in vitro* activity of vanadocene(IV) dichloride on direct comparison with titanocene(IV) dichloride [109–111].

These results encouraged further preclinical studies which were restarted around eight years ago [112–114], and have been recently extended [115–118] with the study of the cytotoxic properties of vanadocene Y (Figure 8(a)) and similar derivatives. In addition, a comprehensive study of the cytotoxic activity of methyl- and methoxy-substituted vanadocene(IV) dichloride toward T-lymphocytic leukemia cells MOLT-4 has also been recently reported [119]. In most cases, vanadocene derivatives are more active than their corresponding titanocene analogues, however, the paramagnetic nature of the vanadium center, which precludes the use of classical NMR tools, makes the characterization of these compounds and their biologically active species more difficult. The need of the use of X-ray crystallography and other methods such as electron-spin resonance (ESR) spectroscopy slows down their analysis and the advances in this topic.

2.4. Molybdocene Derivatives. After the work of Köpf and Köpf-Maier there were some evidences of the potential properties as anticancer agents of molybdocene dichloride derivatives. In recent years, the extensive work carried out by many different research groups confirmed the anticancer properties of molybdocene [120–124]. But not only the cytotoxic properties of these compounds have been reported, the hydrolysis chemistry of $[MoCp_2Cl_2]$ has been intensively studied [125–127]. In the case of molybdocene derivatives the stability of the Cp ligands at physiological pH has led to the study of many different biological experiments with results which show new insights on the mechanism of antitumor action of $[MoCp_2Cl_2]$ and some analogous carboxylate derivatives (Figure 8(b)) [117, 128–130].

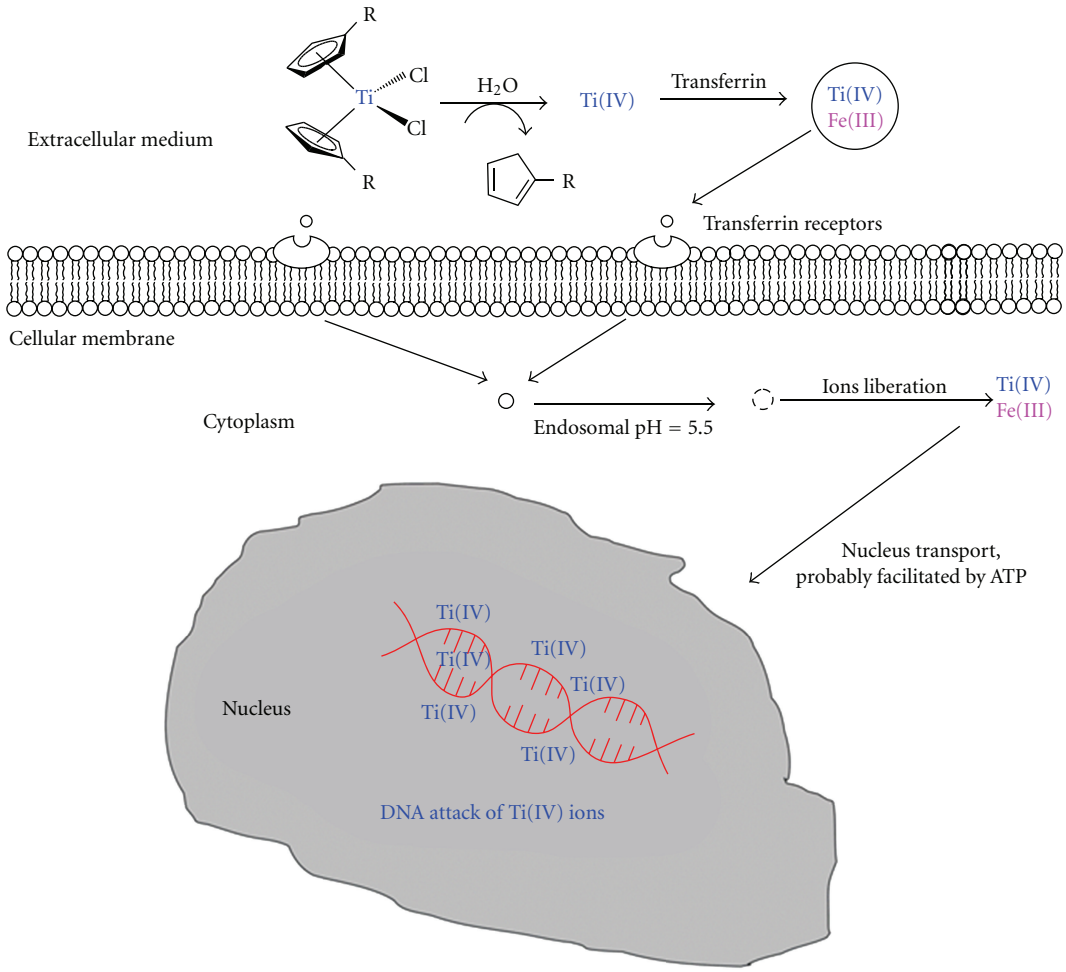

Figure 6: Proposed mechanism of action of titanocene derivatives (adapted from Abeysinghe and Harding, Dalton Trans. 32 (2007) 3474).

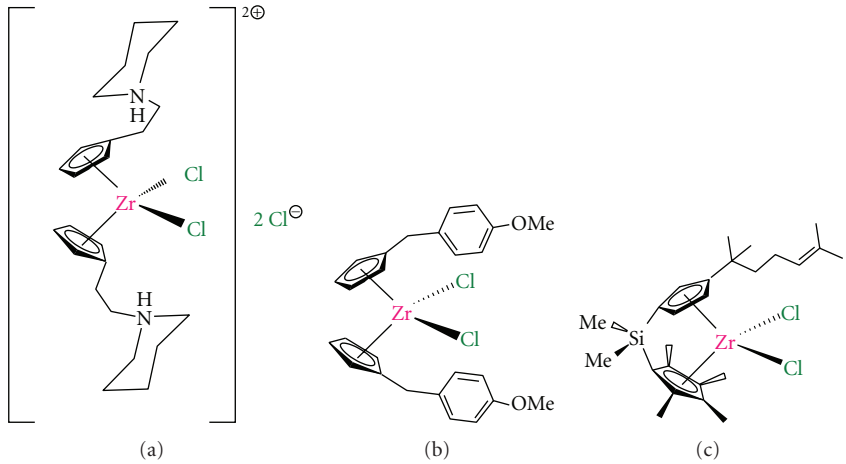

Figure 7: Zirconocene derivatives with anticancer activity: (a) zirconocene derivative with alkylammonium substituents; (b) zirconocene-Y; (c) alkenyl-substituted *ansa*-zirconocene complex.

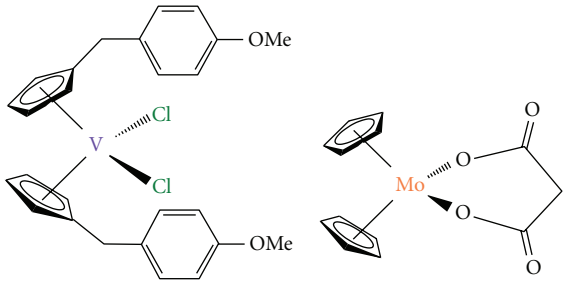

Figure 8: (a) Vanadocene-Y; (b) molybdocene carboxylate derivative.

2.5. Ferrocene Derivatives. The discovery of the cytotoxic properties of ferricinium salts on Ehrlich ascite tumors by Köpf and Köpf-Maier [131, 132] were an early breakthrough for the subsequent development of novel preparations of this class of anticancer agents.

There are different groups working in this field, however, to date, the most interesting work in the field of anticancer applications of ferrocene derivatives is being carried out by Jaouen and coworkers.

This group has published several reports on the synthesis of novel functionalized ferrocene derivatives "hydoxyferrocifens" which consist of the linking of the active metabolite of tamoxifen and ferrocene moieties (Figure 9(a)) [133, 134]. This novel class of compounds are able to combine the antioestrogenic properties of tamoxifen with the cytotoxic effects of ferrocene [135–137]. From all these complexes, the outstanding cytotoxicity of a ferrocene complex with a [3] ferrocenophane moiety conjugated to the phenol group (Figure 9(b)) is important to be remarked [138].

In addition, ferrocene-functionalized complexes with steroids or nonsteroidal antiandrogens have also been reported to be very effective to target prostate cancer cells [139].

But not only the design and synthesis of novel ferrocene derivatives with different ligands and cytotoxic properties have been studied, several investigations on the cell death induced mechanism of these anticancer drugs have been reported. Thus, two different action mechanisms have been proposed for ferrocene derivatives, production of electrophilic species, and/or production of ROS species [140].

2.6. Future Tendencies in the Use of Metallocenes in Anticancer Chemotherapy. Almost all metallocene derivatives which have been studied either in preclinical or clinical trials are extremely hydrophobic to be intravenously administered, thus limiting their bioavailability for clinical applications.

Novel formulations of metallocene derivatives in macromolecular systems such as cucurbit(n)urils [140] or cyclodextrins [141] leading to a presumably higher applicability in humans.

In addition, using a different approach, but with the same goal of circumventing the solubility problems of metallocenes in biological media, several metallocene-functionalized MCM-41 or SBA-15 starting from different

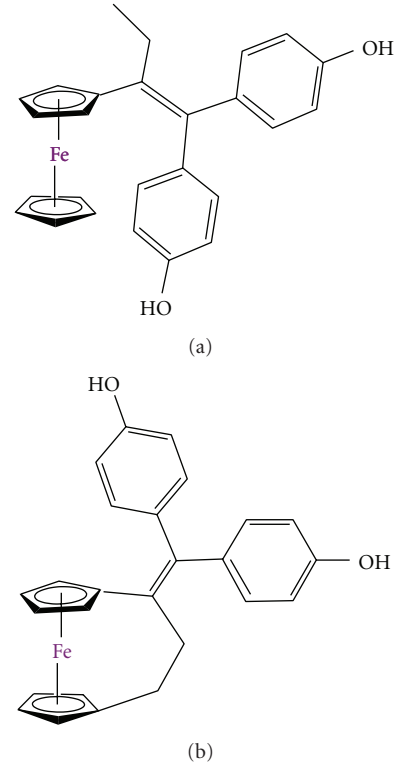

Figure 9: Ferrocene derivatives used in preclinical trials: (a) hydroxyferrocifens; (b) ferrocene complex with a [3] ferrocenophane moiety.

titanocene dichloride derivatives with anticancer activity have been reported and may be a good starting point for the development of novel metallocene-based drugs for the treatment of bone tumors [142–145].

3. Conclusions

One of the most potent antitumoral drugs cisplatin deserves special attention as exceptional of few with healing effect. Important role in the action of cisplatin is interaction with nuclear DNA and unfeasibility of the cell response to repair DNA strain containing covalently bonded diammineplatinum(II) moiety (nucleotide excision repair mechanism). Beside DNA, cisplatin might interact with other biomolecules (thioproteins, RNA) and in that way could be deactivated or even may possibly tune different signaling pathways involved in mediation of cell death, which is cell type specific. Namely, cisplatin has intense effects on signaling pathways facilitated by MAPs (e.g., ERK, JNK, p38). In recent years information on the cellular processing of cisplatin has essentially arisen. Knowledge collected from studies about biological effects of cisplatin and development of cisplatin resistant phenotype afford important clues for the design of more efficient and less toxic platinum and nonplatinum metal based drugs in cancer therapy. It is to be expected that nonplatinum metal compounds may

demonstrate anticancer activity and toxic side effects noticeably different from that of platinum based drugs. Thus titanocene, vanadocene, molybdocene, ferrocene, and zirconocene revealed encouraging results in *in vitro* studies. These compounds might enter by different transport mechanism through cell membrane and distinctly interact with biomolecules than cisplatin. Notwithstanding the extensive applications of cisplatin in the new investigations will provide us with powerful facts for finding a novel efficient and nontoxic metallotherapeutics in anticancer treatment.

Acknowledgments

The authors would like to acknowledge financial support from Alexander von Humboldt Foundation (GNK, SGR), from the Ministerio de Educación y Ciencia, Spain (Grant no. CTQ2011-24346), and from the Ministry of Science and Technological Development of the Republic of Serbia (Grant no. 173013 DMI, SI).

References

[1] F. Arnesano and G. Natile, "Mechanistic insight into the cellular uptake and processing of cisplatin 30 years after its approval by FDA," *Coordination Chemistry Reviews*, vol. 253, no. 15-16, pp. 2070–2081, 2009.

[2] D. J. Higby, H. J. Wallace, D. J. Albert, and J. F. Holland, "Diaminodichloroplatinum: a phase I study showing responses in testicular and other tumors," *Cancer*, vol. 33, no. 5, pp. 1219–1225, 1974.

[3] T. W. Hambley, "Developing new metal-based therapeutics: challenges and opportunities," *Dalton Transactions*, vol. 21, no. 43, pp. 4929–4937, 2007.

[4] E. R. Jamieson and S. J. Lippard, "Structure, recognition, and processing of cisplatin-DNA adducts," *Chemical Reviews*, vol. 99, no. 9, pp. 2467–2498, 1999.

[5] G. Giaccone, "Clinical perspectives on platinum resistance," *Drugs*, vol. 59, no. 4, pp. 9–17, 2000, discussion 37-38.

[6] M. A. Fuertes, C. Alonso, and J. M. Pérez, "Biochemical modulation of cisplatin mechanisms of action: enhancement of antitumor activity and circumvention of drug resistance," *Chemical Reviews*, vol. 103, no. 3, pp. 645–662, 2003.

[7] B. Köberle, J. R. W. Masters, J. A. Hartley, and R. D. Wood, "Defective repair of cisplatin-induced DNA damage caused by reduced XPA protein in testicular germ cell tumours," *Current Biology*, vol. 9, no. 5, pp. 273–276, 1999.

[8] E. L. Mamenta, E. E. Poma, W. K. Kaufmann, D. A. Delmastro, H. L. Grady, and S. G. Chaney, "Enhanced replicative bypass of platinum-DNA adducts in cisplatin-resistant human ovarian carcinoma cell lines," *Cancer Research*, vol. 54, no. 13, pp. 3500–3505, 1994.

[9] A. G. Eliopoulos, D. J. Kerr, J. Herod et al., "The control of apoptosis and drug resistance in ovarian cancer: influence of p53 and Bcl-2," *Oncogene*, vol. 11, no. 7, pp. 1217–1228, 1995.

[10] A. I. Ivanov, J. Christodoulou, J. A. Parkinson et al., "Cisplatin binding sites on human albumin," *The Journal of Biological Chemistry*, vol. 273, no. 24, pp. 14721–14730, 1998.

[11] R. C. DeConti, B. R. Toftness, R. C. Lange, and W. A. Creasey, "Clinical and pharmacological studies with cis diamminedichloroplatinum(II)," *Cancer Research*, vol. 33, no. 6, pp. 1310–1315, 1973.

[12] D. P. Gately and S. B. Howell, "Cellular accumulation of the anticancer agent cisplatin: a review," *British Journal of Cancer*, vol. 67, no. 6, pp. 1171–1176, 1993.

[13] S. Ishida, J. Lee, D. J. Thiele, and I. Herskowitz, "Uptake of the anticancer drug cisplatin mediated by the copper transporter Ctr1 in yeast and mammals," *Proceedings of the National Academy of Sciences of the United States of America*, vol. 99, no. 22, pp. 14298–14302, 2002.

[14] R. A. Alderden, M. D. Hall, and T. W. Hambley, "The discovery and development of cisplatin," *Journal of Chemical Education*, vol. 83, no. 5, pp. 728–734, 2006.

[15] A. R. Timerbaev, C. G. Hartinger, S. S. Aleksenko, and B. K. Keppler, "Interactions of antitumor metallodrugs with serum proteins: advances in characterization using modern analytical methodology," *Chemical Reviews*, vol. 106, no. 6, pp. 2224–2248, 2006.

[16] E. Volckova, F. Evanics, W. W. Yang, and R. N. Bose, "Unwinding of DNA polymerases by the antitumor drug, cis-diamminedichloroplatinum(II)," *Chemical Communications*, vol. 9, no. 10, pp. 1128–1129, 2003.

[17] S. Ahmad, "Platinum-DNA interactions and subsequent cellular processes controlling sensitivity to anticancer platinum complexes," *Chemistry and Biodiversity*, vol. 7, no. 3, pp. 543–566, 2010.

[18] R. J. Knox, F. Friedlos, D. A. Lydall, and J. J. Roberts, "Mechanism of cytotoxicity of anticancer platinum drugs: evidence that cis-diamminedichloroplatinum(II) and cis-diammine-(1,1-cyclobutanedicarboxylato)platinum(II) differ only in the kinetics of their interaction with DNA," *Cancer Research*, vol. 46, no. 4, pp. 1972–1979, 1986.

[19] L. L. Munchausen and R. O. Rahn, "Physical studies on the binding of cis dichlorodiamine platinum(II) to DNA and homopolynucleotides," *Biochimica et Biophysica Acta*, vol. 414, no. 3, pp. 242–255, 1975.

[20] A. Eastman, "Characterization of the adducts produced in DNA by cis-diamminedichloroplatinum(II) and cis-dichloro(ethylenediamine)platinum(II)," *Biochemistry*, vol. 22, no. 16, pp. 3927–3933, 1983.

[21] A. C. M. Plooy, A. M. J. Fichtinger-Schepman, and H. H. Schutte, "The quantitative detection of various Pt-DNA-adducts in Chinese hamster ovary cells treated with cisplatin: application of immunochemical techniques," *Carcinogenesis*, vol. 6, no. 4, pp. 561–566, 1985.

[22] A. E. Egger, C. G. Hartinger, H. B. Hamidane, Y. O. Tsybin, B. K. Keppler, and P. J. Dyson, "High resolution mass spectrometry for studying the interactions of cisplatin with oligonucleotides," *Inorganic Chemistry*, vol. 47, no. 22, pp. 10626–10633, 2008.

[23] D. B. Zamble, D. Mu, J. T. Reardon, A. Sancar, and S. J. Lippard, "Repair of cisplatin-DNA adducts by the mammalian excision nuclease," *Biochemistry*, vol. 35, no. 31, pp. 10004–10013, 1996.

[24] J. T. Reardon, A. Vaisman, S. G. Chaney, and A. Sancar, "Efficient nucleotide excision repair of cisplatin, oxaliplatin, and bis- acetoammine-dichloro-cyclohexylamine-platinum(IV) (JM216) platinum intrastrand DNA diadducts," *Cancer Research*, vol. 59, no. 16, pp. 3968–3971, 1999.

[25] S. W. Johnson, R. P. Perez, A. K. Godwin et al., "Role of platinum-DNA adduct formation and removal in cisplatin resistance in human ovarian cancer cell lines," *Biochemical Pharmacology*, vol. 47, no. 4, pp. 689–697, 1994.

[26] K. V. Ferry, T. C. Hamilton, and S. W. Johnson, "Increased nucleotide excision repair in cisplatin-resistant ovarian

cancer cells: role of ERCC1-XPF," *Biochemical Pharmacology*, vol. 60, no. 9, pp. 1305–1313, 2000.

[27] D. Fink, H. Zheng, S. Nebel et al., "In vitro and in vivo resistance to cisplatin in cells that have lost DNA mismatch repair," *Cancer Research*, vol. 57, no. 10, pp. 1841–1845, 1997.

[28] E. D. Scheeff, J. M. Briggs, and S. B. Howell, "Molecular modeling of the intrastrand guanine-guanine DNA adducts produced by cisplatin and oxaliplatin," *Molecular Pharmacology*, vol. 56, no. 3, pp. 633–643, 1999.

[29] A. Vaisman, M. Varchenko, A. Umar et al., "The role of hMLH1, hMSH3, and hMSH6 defects in cisplatin and oxaliplatin resistance: correlation with replicative bypass of platinum-DNA adducts," *Cancer Research*, vol. 58, no. 16, pp. 3579–3585, 1998.

[30] S. G. Chaney, S. L. Campbell, E. Bassett, and Y. Wu, "Recognition and processing of cisplatin- and oxaliplatin-DNA adducts," *Critical Reviews in Oncology/Hematology*, vol. 53, no. 1, pp. 3–11, 2005.

[31] V. Cepeda, M. A. Fuertes, J. Castilla, C. Alonso, C. Quevedo, and J. M. Pérez, "Biochemical mechanisms of cisplatin cytotoxicity," *Anti-Cancer Agents in Medicinal Chemistry*, vol. 7, no. 1, pp. 3–18, 2007.

[32] K. M. Henkels and J. J. Turchi, "Induction of apoptosis in cisplatin-sensitive and -resistant human ovarian cancer cell lines," *Cancer Research*, vol. 57, no. 20, pp. 4488–4492, 1997.

[33] D. Wang and S. J. Lippard, "Cellular processing of platinum anticancer drugs," *Nature Reviews Drug Discovery*, vol. 4, no. 4, pp. 307–320, 2005.

[34] Z. S. Juo, T. K. Chiu, P. M. Leiberman, I. Baikalov, A. J. Berk, and R. E. Dickerson, "How proteins recognize the TATA box," *Journal of Molecular Biology*, vol. 261, no. 2, pp. 239–254, 1996.

[35] J. Yaneva, S. H. Leuba, K. Van Holde, and J. Zlatanova, "The major chromatin protein his tone H1 binds preferentially to cis-platinum-damaged DNA," *Proceedings of the National Academy of Sciences of the United States of America*, vol. 94, no. 25, pp. 13448–13451, 1997.

[36] M. Kartalou, L. D. Samson, and J. M. Essigmann, "Cisplatin adducts inhibit 1,N6-ethenoadenine repair by interacting with the human 3-methyladenine DNA glycosylase," *Biochemistry*, vol. 39, no. 27, pp. 8032–8038, 2000.

[37] C. Söti, A. Rácz, and P. Csermely, "A nucleotide-dependent molecular switch controls ATP binding at the C-terminal domain of Hsp90. N-terminal nucleotide binding unmasks a C-terminal binding pocket," *The Journal of Biological Chemistry*, vol. 277, no. 9, pp. 7066–7075, 2002.

[38] T. Peleg-Shulman and D. Gibson, "Cisplatin-protein adducts are efficiently removed by glutathione but not by 5′-guanosine monophosphate," *Journal of the American Chemical Society*, vol. 123, no. 13, pp. 3171–3172, 2001.

[39] H. Daino, I. Matsumura, K. Takada et al., "Induction of apoptosis by extracellular ubiquitin in human hematopoietic cells: possible involvement of STAT3 degradation by proteasome pathway in interleukin 6-dependent hematopoietic cells," *Blood*, vol. 95, no. 8, pp. 2577–2585, 2000.

[40] P. A. Nguewa, M. A. Fuertes, V. Cepeda et al., "Pentamidine is an antiparasitic and apoptotic drug that selectively modifies ubiquitin," *Chemistry and Biodiversity*, vol. 2, no. 10, pp. 1387–1400, 2005.

[41] D. Maksimovic-Ivanic, S. Mijatovic, D. Miljkovic et al., "The antitumor properties of a nontoxic, nitric oxide-modified version of saquinavir are independent of Akt," *Molecular Cancer Therapeutics*, vol. 8, no. 5, pp. 1169–1178, 2009.

[42] A. Casini, C. Gabbiani, G. Mastrobuoni et al., "Insights into the molecular mechanisms of protein platination from a case study: the reaction of anticancer platinum(II) iminoethers with horse heart cytochrome C," *Biochemistry*, vol. 46, no. 43, pp. 12220–12230, 2007.

[43] F. Arnesano and G. Natile, ""Platinum on the road": interactions of antitumoral cisplatin with proteins," *Pure and Applied Chemistry*, vol. 80, no. 12, pp. 2715–2725, 2008.

[44] S. R. Datta, A. Brunet, and M. E. Greenberg, "Cellular survival: a play in three akts," *Genes and Development*, vol. 13, no. 22, pp. 2905–2927, 1999.

[45] M. Fraser, B. M. Leung, X. Yan, H. C. Dan, J. Q. Cheng, and B. K. Tsang, "p53 is a determinant of X-linked inhibitor of apoptosis protein/Akt-mediated chemoresistance in human ovarian cancer cells," *Cancer Research*, vol. 63, no. 21, pp. 7081–7088, 2003.

[46] H. C. Dan, M. Sun, S. Kaneko et al., "Akt phosphorylation and stabilization of X-linked inhibitor of apoptosis protein (XIAP)," *The Journal of Biological Chemistry*, vol. 279, no. 7, pp. 5405–5412, 2004.

[47] J. G. Viniegra, J. H. Losa, V. J. Sánchez-Arévalo et al., "Modulation of PI3K/Akt pathway by E1a mediates sensitivity to cisplatin," *Oncogene*, vol. 21, no. 46, pp. 7131–7136, 2002.

[48] Y. Shaul, "c-Abl: activation and nuclear targets," *Cell Death and Differentiation*, vol. 7, no. 1, pp. 10–16, 2000.

[49] J. Gong, A. Costanzo, H. Q. Yang et al., "The tyrosine kinase c-Abl regulates p73 in apoptotic response to cisplatin-induced DNA damage," *Nature*, vol. 399, no. 6738, pp. 806–809, 1999.

[50] L. Harhaji-Trajkovic, U. Vilimanovich, T. Kravic-Stevovic, V. Bumbasirevic, and V. Trajkovic, "AMPK-mediated autophagy inhibits apoptosis in cisplatin-treated tumour cells," *Journal of Cellular and Molecular Medicine*, vol. 13, no. 9, pp. 3644–3654, 2009.

[51] X. Wang, J. L. Martindale, and N. J. Holbrook, "Requirement for ERK activation in cisplatin-induced apoptosis," *The Journal of Biological Chemistry*, vol. 275, no. 50, pp. 39435–39443, 2000.

[52] W. Cui, E. M. Yazlovitskaya, M. S. Mayo et al., "Cisplatin-induced response of c-jun N-terminal kinase 1 and extracellular signal—regulated protein kinases 1 and 2 in a series of cisplatin-resistant ovarian carcinoma cell lines," *Molecular Carcinogenesis*, vol. 29, pp. 219–228, 2000.

[53] S. Mijatovic, D. Maksimovic-Ivanic, J. Radovic et al., "Aloe emodin decreases the ERK-dependent anticancer activity of cisplatin," *Cellular and Molecular Life Sciences*, vol. 62, no. 11, pp. 1275–1282, 2005.

[54] S. Mijatovic, D. Maksimovic-Ivanic, J. Radovic et al., "Anti-glioma action of aloe emodin: the role of ERK inhibition," *Cellular and Molecular Life Sciences*, vol. 62, no. 5, pp. 589–598, 2005.

[55] A. Mansouri, L. D. Ridgway, A. L. Korapati et al., "Sustained activation of JNK/p38 MAPK pathways in response to cisplatin leads to Fas ligand induction and cell death in ovarian carcinoma cells," *The Journal of Biological Chemistry*, vol. 278, no. 21, pp. 19245–19256, 2003.

[56] I. Sánchez-Perez, J. R. Murguía, and R. Perona, "Cisplatin induces a persistent activation of JNK that is related to cell death," *Oncogene*, vol. 16, no. 4, pp. 533–540, 1998.

[57] J. Hayakawa, M. Ohmichi, H. Kurachi et al., "Inhibition of extracellular signal-regulated protein kinase or c-Jun N-terminal protein kinase cascade, differentially activated by

cisplatin, sensitizes human ovarian cancer cell line," *The Journal of Biological Chemistry*, vol. 274, no. 44, pp. 31648–31654, 1999.

[58] R. J. Davis, "Signal transduction by the JNK group of MAP kinases," *Cell*, vol. 103, no. 2, pp. 239–252, 2000.

[59] P. Pandey, J. Raingeaud, M. Kaneki et al., "Activation of p38 mitogen-activated protein kinase by c-Abl-dependent and -independent mechanisms," *The Journal of Biological Chemistry*, vol. 271, no. 39, pp. 23775–23779, 1996.

[60] J. Hernández Losa, C. Parada Cobo, J. Guinea Viniegra, V. J. Sánchez-Arevalo Lobo, S. Ramón y Cajal, and R. Sánchez-Prieto, "Role of the p38 MAPK pathway in cisplatin-based therapy," *Oncogene*, vol. 22, no. 26, pp. 3998–4006, 2003.

[61] D. Wang and S. J. Lippard, "Cisplatin-induced post-translational modification of histones H3 and H4," *The Journal of Biological Chemistry*, vol. 279, no. 20, pp. 20622–20625, 2004.

[62] V. M. Gonzalez, M. A. Fuertes, C. Alonso, and J. M. Perez, "Is cisplatin-induced cell death always produced by apoptosis?" *Molecular Pharmacology*, vol. 59, no. 4, pp. 657–663, 2001.

[63] W. Lieberthal, V. Triaca, and J. Levine, "Mechanisms of death induced by cisplatin in proximal tubular epithelial cells: apoptosis vs. necrosis," *American Journal of Physiology*, vol. 270, no. 4, pp. F700–F708, 1996.

[64] Y. Eguchi, S. Shimizu, and Y. Tsujimoto, "Intracellular ATP levels determine cell death fate by apoptosis or necrosis," *Cancer Research*, vol. 57, no. 10, pp. 1835–1840, 1997.

[65] R. Zhou, M. G. Vander Heiden, and C. M. Rudin, "Genotoxic exposure is associated with alterations in glucose uptake and metabolism," *Cancer Research*, vol. 62, no. 12, pp. 3515–3520, 2002.

[66] Z. Herceg and Z. Q. Wang, "Failure of poly(ADP-ribose) polymerase cleavage by caspases leads to induction of necrosis and enhanced apoptosis," *Molecular and Cellular Biology*, vol. 19, no. 7, pp. 5124–5133, 1999.

[67] T. Hirsch, P. Marchetti, S. A. Susin et al., "The apoptosis-necrosis paradox. Apoptogenic proteases activated after mitochondrial permeability transition determine the mode of cell death," *Oncogene*, vol. 15, no. 13, pp. 1573–1581, 1997.

[68] L. Ding, C. Yuan, F. Wei et al., "Cisplatin restores TRAIL apoptotic pathway in glioblastoma-derived stem cells through up-regulation of DR5 and down-regulation of c-FLIP," *Cancer Investigation*, vol. 29, pp. 511–520, 2011.

[69] O. Vondálová Blanárová, I. Jelínková, A. Szöor et al., "Cisplatin and a potent platinum(IV) complex-mediated enhancement of TRAIL-induced cancer cells killing is associated with modulation of upstream events in the extrinsic apoptotic pathway," *Carcinogenesis*, vol. 32, no. 1, pp. 42–51, 2011.

[70] D. Maksimovic-Ivanic, S. Stosic-Grujicic, F. Nicoletti, and S. Mijatovic, "Resistance to TRAIl and how to surmount it," *Immunology Research*, vol. 52, no. 1-2, pp. 157–168, 2012.

[71] M. P. Decatris, S. Sundar, and K. J. O'Byrne, "Platinum-based chemotherapy in metastatic breast cancer: current status," *Cancer Treatment Reviews*, vol. 30, no. 1, pp. 53–81, 2004.

[72] M. D. Shelley, K. Burgon, and M. D. Mason, "Treatment of testicular germ-cell cancer: a cochrane evidence-based systematic review," *Cancer Treatment Reviews*, vol. 28, no. 5, pp. 237–253, 2002.

[73] M. S. Kim, M. Blake, J. H. Baek, G. Kohlhagen, Y. Pommier, and F. Carrier, "Inhibition of histone deacetylase increases cytotoxicity to anticancer drugs targeting DNA," *Cancer Research*, vol. 63, no. 21, pp. 7291–7300, 2003.

[74] N. J. Long, *Metallocenes*, Blackwell Science, Oxford, UK, 1998.

[75] A. Korfel, M. E. Scheulen, H. J. Schmoll et al., "Phase I clinical and pharmacokinetic study of titanocene dichloride in adults with advanced solid tumors," *Clinical Cancer Research*, vol. 4, no. 11, pp. 2701–2708, 1998.

[76] C. V. Christodoulou, D. R. Ferry, D. W. Fyfe et al., "Phase I trial of weekly scheduling and pharmacokinetics of titanocene dichloride in patients with advanced cancer," *Journal of Clinical Oncology*, vol. 16, no. 8, pp. 2761–2769, 1998.

[77] K. Mross, P. Robben-Bathe, L. Edler et al., "Phase I clinical trial of a day-1, -3, -5 every 3 weeks schedule with titanocene dichloride (MKT 5) in patients with advanced cancer: a study of the phase I study group of the association for medical oncology (AIO) of the German Cancer Society," *Onkologie*, vol. 23, no. 6, pp. 576–579, 2000.

[78] B. W. Müller, R. Müller, S. Lucks, and W. Mohr, "Medac Gesellschaft fur Klinische Spzeilpräparate GmbH," US Patent 5, 296, 237, 1994.

[79] N. Kröger, U. R. Kleeberg, K. Mross, L. Edler, G. Saß, and D. K. Hossfeld, "Phase II clinical trial of titanocene dichloride in patients with metastatic breast cancer," *Onkologie*, vol. 23, no. 1, pp. 60–62, 2000.

[80] G. Lümmen, H. Sperling, H. Luboldt, T. Otto, and H. Rübben, "Phase II trial of titanocene dichloride in advanced renal-cell carcinoma," *Cancer Chemotherapy and Pharmacology*, vol. 42, no. 5, pp. 415–417, 1998.

[81] E. Meléndez, "Titanium complexes in cancer treatment," *Critical Reviews in Oncology/Hematology*, vol. 42, no. 3, pp. 309–315, 2002.

[82] F. Caruso and M. Rossi, "Antitumor titanium compounds and related metallocenes," in *Metal Ions in Biological System*, A. Sigel and H. Sigel, Eds., vol. 42 of *Metal Complexes in Tumor Diagnostics and as Anticancer Agents*, Marcel Dekker, New York, NY, USA, 2004.

[83] J. C. Dabrowiak, *Metals in Medicine*, John Wiley & Sons, West Sussex, UK, 2009.

[84] U. Olszewski and G. Hamilton, "Mechanisms of cytotoxicity of anticancer titanocenes," *Anti-Cancer Agents in Medicinal Chemistry*, vol. 10, no. 4, pp. 302–311, 2010.

[85] K. Strohfeldt and M. Tacke, "Bioorganometallic fulvene-derived titanocene anti-cancer drugs," *Chemical Society Reviews*, vol. 37, no. 6, pp. 1174–1187, 2008.

[86] R. Hernández, J. Lamboy, L. M. Gao, J. Matta, F. R. Román, and E. Meléndez, "Structure-activity studies of Ti(IV) complexes: aqueous stability and cytotoxic properties in colon cancer HT-29 cells," *Journal of Biological Inorganic Chemistry*, vol. 13, no. 5, pp. 685–692, 2008.

[87] R. Hernández, J. Méndez, J. Lamboy, M. Torres, F. R. Román, and E. Meléndez, "Titanium(IV) complexes: cytotoxicity and cellular uptake of titanium(IV) complexes on caco-2 cell line," *Toxicology in Vitro*, vol. 24, no. 1, pp. 178–183, 2010.

[88] L. M. Gao, J. Matta, A. L. Rheingold, and E. Meléndez, "Synthesis, structure and biological activity of amide-functionalized titanocenyls: improving their cytotoxic properties," *Journal of Organometallic Chemistry*, vol. 694, no. 26, pp. 4134–4139, 2009.

[89] A. Gansäuer, I. Winkler, D. Worgull et al., "Carbonyl-substituted titanocenes: a novel class of cytostatic compounds with high antitumor and antileukemic activity," *Chemistry*, vol. 14, no. 14, pp. 4160–4163, 2008.

[90] O. R. Allen, L. Croll, A. L. Gott, R. J. Knox, and P. C. McGowan, "Functionalized cyclopentadienyl titanium organometallic compounds as new antitumor drugs," *Organometallics*, vol. 23, no. 2, pp. 288–292, 2004.

[91] O. R. Allen, A. L. Gott, J. A. Hartley, J. M. Hartley, R. J. Knox, and P. C. McGowan, "Functionalised cyclopentadienyl titanium compounds as potential anticancer drugs," *Dalton Transactions*, no. 43, pp. 5082–5090, 2007.

[92] G. D. Potter, M. C. Baird, and S. P. C. Cole, "A new series of titanocene dichloride derivatives bearing chiral alkylammonium groups; Assessment of their cytotoxic properties," *Inorganica Chimica Acta*, vol. 364, no. 1, pp. 16–22, 2010.

[93] L. M. Gao, J. L. Vera, J. Matta, and E. Meléndez, "Synthesis and cytotoxicity studies of steroid-functionalized titanocenes as potential anticancer drugs: sex steroids as potential vectors for titanocenes," *Journal of Biological Inorganic Chemistry*, vol. 15, no. 6, pp. 851–859, 2010.

[94] S. Gómez-Ruiz, G. N. Kaluđerović, S. Prashar et al., "Cytotoxic studies of substituted titanocene and ansa-titanocene anticancer drugs," *Journal of Inorganic Biochemistry*, vol. 102, no. 8, pp. 1558–1570, 2008.

[95] S. Gómez-Ruiz, G. N. Kaluđerović, Ž. Žižak et al., "Anticancer drugs based on alkenyl and boryl substituted titanocene complexes," *Journal of Organometallic Chemistry*, vol. 694, no. 13, pp. 1981–1987, 2009.

[96] G. N. Kaluđerović, V. Tayurskaya, R. Paschke, S. Prashar, M. Fajardo, and S. Gómez-Ruiz, "Synthesis, characterization and biological studies of alkenyl-substituted titanocene(IV) carboxylate complexes," *Applied Organometallic Chemistry*, vol. 24, no. 9, pp. 656–662, 2010.

[97] H. Sun, H. Li, R. A. Weir, and P. J. Sadler, "You have full text access to this content the first specific Ti^{IV}-protein complex: potential relevance to anticancer activity of titanocenes," *Angewandte Chemie International Edition*, vol. 37, no. 11, pp. 1577–1579, 1998.

[98] M. Guo and P. J. Sadler, "Competitive binding of the anticancer drug titanocene dichloride to N,N′-ethylenebis(o-hydroxyphenylglycine) and adenosine triphosphate: a model for Ti^{IV} uptake and release by transferrin," *Journal of the Chemical Society, Dalton Transactions*, vol. 1, pp. 7–9, 2000.

[99] M. Guo, H. Sun, S. Bihari et al., "Stereoselective formation of seven-coordinate titanium(IV) monomer and dimer complexes of ethylenebis(o-hydroxyphenyl)glycine," *Inorganic Chemistry*, vol. 39, no. 2, pp. 206–215, 2000.

[100] M. Guo, H. Sun, H. J. McArdle, L. Gambling, and P. J. Sadler, "Ti(IV) uptake and release by human serum transferrin and recognition of Ti(IV)-transferrin by cancer cells: understanding the mechanism of action of the anticancer drug titanocene dichloride," *Biochemistry*, vol. 39, no. 33, pp. 10023–10033, 2000.

[101] P. Köpf-Maier and D. Krahl, "Tumor inhibition by metallogenes: ultrastructural localization of titanium and vanadium in treated tumor cells by electron energy loss spectroscopy," *Chemico-Biological Interactions*, vol. 44, no. 3, pp. 317–328, 1983.

[102] P. Köpf-Maier, "Intracellular localization of titanium within xenografted sensitive human tumors after treatment with the antitumor agent titanocene dichloride," *Journal of Structural Biology*, vol. 105, no. 1–3, pp. 35–45, 1990.

[103] A. D. Tinoco, C. D. Incarvito, and A. M. Valentine, "Calorimetric, spectroscopic, and model studies provide insight into the transport of Ti(IV) by human serum transferrin," *Journal of the American Chemical Society*, vol. 129, no. 11, pp. 3444–3454, 2007.

[104] A. D. Tinoco, E. V. Eames, and A. M. Valentine, "Reconsideration of serum Ti(IV) transport: albumin and transferrin trafficking of Ti(IV) and its complexes," *Journal of the American Chemical Society*, vol. 130, no. 7, pp. 2262–2270, 2008.

[105] M. Pavlaki, K. Debeli, I. E. Triantaphyllidou, N. Klouras, E. Giannopoulou, and A. J. Aletras, "A proposed mechanism for the inhibitory effect of the anticancer agent titanocene dichloride on tumour gelatinases and other proteolytic enzymes," *Journal of Biological Inorganic Chemistry*, vol. 14, no. 6, pp. 947–957, 2009.

[106] O. R. Allen, R. J. Knox, and P. C. McGowan, "Functionalised cyclopentadienyl zirconium compounds as potential anticancer drugs," *Dalton Transactions*, no. 39, pp. 5293–5295, 2008.

[107] D. Wallis, J. Claffey, B. Gleeson, M. Hogan, H. Müller-Bunz, and M. Tacke, "Novel zirconocene anticancer drugs?" *Journal of Organometallic Chemistry*, vol. 694, no. 6, pp. 828–833, 2009.

[108] S. Gómez-Ruiz, G. N. Kaluderović, D. Polo-Cerón et al., "A novel alkenyl-substituted ansa-zirconocene complex with dual application as olefin polymerization catalyst and anticancer drug," *Journal of Organometallic Chemistry*, vol. 694, no. 18, pp. 3032–3038, 2009.

[109] P. Köpf-Maier, "Antitumor bis(cyclopentadienyl) metal complexes," in *Metal Complexes in Cancer Chemotherapy*, B. K. Keppler, Ed., pp. 259–296, VCH Verlagsgesellschaft, Weinheim, Germany, 1993.

[110] C. S. Navara, A. Benyumov, A. Vassilev, R. K. Narla, P. Ghosh, and F. M. Uckun, "Vanadocenes as potent anti-proliferative agents disrupting mitotic spindle formation in cancer cells," *Anti-Cancer Drugs*, vol. 12, no. 4, pp. 369–376, 2001.

[111] P. Ghosh, O. J. D'Cruz, R. K. Narla, and F. M. Uckun, "Apoptosis-inducing vanadocene compounds against human testicular cancer," *Clinical Cancer Research*, vol. 6, no. 4, pp. 1536–1545, 2000.

[112] H. Paláčková, J. Vinklárek, J. Holubová, I. Císařová, and M. Erben, "The interaction of antitumor active vanadocene dichloride with sulfur-containing amino acids," *Journal of Organometallic Chemistry*, vol. 692, no. 17, pp. 3758–3764, 2007.

[113] J. Vinklárek, J. Honzíček, and J. Holubová, "Interaction of the antitumor agent vanadocene dichloride with phosphate buffered saline," *Inorganica Chimica Acta*, vol. 357, no. 12, pp. 3765–3769, 2004.

[114] J. Vinklárek, H. Paláčková, J. Honzíček, J. Holubová, M. Holčapek, and I. Císařová, "Investigation of vanadocene(IV) α-amino acid complexes: synthesis, structure, and behavior in physiological solutions, human plasma, and blood," *Inorganic Chemistry*, vol. 45, no. 5, pp. 2156–2162, 2006.

[115] B. Gleeson, J. Claffey, A. Deally et al., "Synthesis and cytotoxicity studies of fluorinated derivatives of vanadocene Y," *European Journal of Inorganic Chemistry*, no. 19, pp. 2804–2810, 2009.

[116] B. Gleeson, J. Claffey, M. Hogan, H. Müller-Bunz, D. Wallis, and M. Tacke, "Novel benzyl-substituted vanadocene anticancer drugs," *Journal of Organometallic Chemistry*, vol. 694, no. 9-10, pp. 1369–1374, 2009.

[117] B. Gleeson, J. Claffey, A. Deally et al., "Novel benzyl-substituted molybdocene anticancer drugs," *Inorganica Chimica Acta*, vol. 363, no. 8, pp. 1831–1836, 2010.

[118] B. Gleeson, M. Hogan, H. Müller-Bunz, and M. Tacke, "Synthesis and preliminary cytotoxicity studies of indole-substituted vanadocenes," *Transition Metal Chemistry*, vol. 35, no. 8, pp. 973–983, 2010.

[119] J. Honzíček, I. Klepalová, J. Vinklárek et al., "Synthesis, characterization and cytotoxic effect of ring-substituted and ansa-bridged vanadocene complexes," *Inorganica Chimica Acta*, vol. 373, no. 1, pp. 1–7, 2011.

[120] J. B. Waern and M. M. Harding, "Bioorganometallic chemistry of molybdocene dichloride," *Journal of Organometallic Chemistry*, vol. 689, no. 25, pp. 4655–4668, 2004.

[121] J. B. Waern, C. T. Dillon, and M. M. Harding, "Organometallic anticancer agents: cellular uptake and cytotoxicity studies on thiol derivatives of the antitumor agent molybdocene dichloride," *Journal of Medicinal Chemistry*, vol. 48, no. 6, pp. 2093–2099, 2005.

[122] J. B. Waern, H. H. Harris, B. Lai, Z. Cai, M. M. Harding, and C. T. Dillon, "Intracellular mapping of the distribution of metals derived from the antitumor metallocenes," *Journal of Biological Inorganic Chemistry*, vol. 10, no. 5, pp. 443–452, 2005.

[123] J. B. Waern, P. Turner, and M. M. Harding, "Synthesis and hydrolysis of thiol derivatives of molybdocene dichloride incorporating electron-withdrawing substituents," *Organometallics*, vol. 25, no. 14, pp. 3417–3421, 2006.

[124] K. S. Campbell, A. J. Foster, C. T. Dillon, and M. M. Harding, "Genotoxicity and transmission electron microscopy studies of molybdocene dichloride," *Journal of Inorganic Biochemistry*, vol. 100, no. 7, pp. 1194–1198, 2006.

[125] J. H. Toney and T. J. Marks, "Hydrolysis chemistry of the metallocene dichlorides $M(\eta^5\text{-}C_5H_5)_2Cl_2$, M = Ti, V, Zr. Aqueous kinetics, equilibria, and mechanistic implications for a new class of antitumor agents," *Journal of the American Chemical Society*, vol. 107, no. 4, pp. 947–953, 1985.

[126] C. Balzarek, T. J. R. Weakley, L. Y. Kuo, and D. R. Tyler, "Investigation of the monomer-dimer equilibria of molybdocenes in water," *Organometallics*, vol. 19, no. 15, pp. 2927–2931, 2000.

[127] L. Y. Kuo, M. G. Kanatzidis, M. Sabat, A. L. Tipton, and T. J. Marks, "Metallocene antitumor agents. Solution and solid-state molybdenocene coordination chemistry of DNA constituents," *Journal of the American Chemical Society*, vol. 113, no. 24, pp. 9027–9045, 1991.

[128] P. M. Abeysinghe and M. M. Harding, "Antitumour bis(cyclopentadienyl) metal complexes: titanocene and molybdocene dichloride and derivatives," *Dalton Transactions*, no. 32, pp. 3474–3482, 2007.

[129] M. M. Harding and G. Mokdsi, "Antitumour metallocenes: structure-activity studies and interactions with biomolecules," *Current Medicinal Chemistry*, vol. 7, no. 12, pp. 1289–1303, 2000.

[130] K. S. Campbell, C. T. Dillon, S. V. Smith, and M. M. Harding, "Radiotracer studies of the antitumor metallocene molybdocene dichloride with biomolecules," *Polyhedron*, vol. 26, no. 2, pp. 456–459, 2007.

[131] P. Köpf-Maier, H. Köpf, and E. W. Neuse, "Ferrocenium salts—the first antineoplastic iron compounds," *Angewandte Chemie—International Edition in English*, vol. 23, no. 6, pp. 456–457, 1984.

[132] P. Köpf-Maier, H. Kopf, and E. W. Neuse, "Ferricenium complexes: a new type of water-soluble antitumor agent," *Journal of Cancer Research and Clinical Oncology*, vol. 108, no. 3, pp. 336–340, 1984.

[133] S. Top, J. Tang, A. Vessières, D. Carrez, C. Provot, and G. Jaouen, "Ferrocenyl hydroxytamoxifen: a prototype for a new range of oestradiol receptor site-directed cytotoxics," *Chemical Communications*, vol. 8, pp. 955–956, 1996.

[134] S. Top, B. Dauer, J. Vaissermann, and G. Jaouen, "Facile route to ferrocifen, 1-[4-(2-dimethylaminoethoxy)]-1-(phenyl-2-ferrocenyl-but-1-ene), first organometallic analogue of tamoxifen, by the McMurry reaction," *Journal of Organometallic Chemistry*, vol. 541, no. 1-2, pp. 355–361, 1997.

[135] S. Top, A. Vessières, C. Cabestaing et al., "Studies on organometallic selective estrogen receptor modulators. (SERMs) Dual activity in the hydroxy-ferrocifen series," *Journal of Organometallic Chemistry*, vol. 637–639, no. 1, pp. 500–506, 2001.

[136] S. Top, A. Vessières, G. Leclercq et al., "Synthesis, biochemical properties and molecular modelling studies of organometallic Specific Estrogen Receptor Modulators (SERMs), the ferrocifens and hydroxyferrocifens: evidence for an antiproliferative effect of hydroxyferrocifens on both hormone-dependent and hormone-independent breast cancer cell lines," *Chemistry*, vol. 9, no. 21, pp. 5223–5236, 2003.

[137] G. Jaouen, S. Top, A. Vessières, G. Leclercq, and M. J. McGlinchey, "The first organometallic selective estrogen receptor modulators (SERMs) and their relevance to breast cancer," *Current Medicinal Chemistry*, vol. 11, no. 18, pp. 2505–2517, 2004.

[138] D. Plazuk, A. Vessières, E. A. Hillard et al., "A [3]ferrocenophane polyphenol showing a remarkable antiproliferative activity on breast and prostate cancer cell lines," *Journal of Medicinal Chemistry*, vol. 52, no. 15, pp. 4964–4967, 2009.

[139] E. A. Hillard, A. Vessières, and G. Jaouen, "Ferrocene functionalized endocrine modulators as anticancer agents," *Topics in Organometallic Chemistry*, vol. 32, pp. 81–117, 2010.

[140] D. P. Buck, P. M. Abeysinghe, C. Cullinane, A. I. Day, J. G. Collins, and M. M. Harding, "Inclusion complexes of the antitumour metallocenes Cp_2MCl_2 (M = Mo, Ti) with cucurbit[n]urils," *Dalton Transactions*, no. 17, pp. 2328–2334, 2008.

[141] C. C. L. Pereira, C. V. Diogo, A. Burgeiro et al., "Complex formation between heptakis(2,6-di-O-methyl)-β-cyclodextrin and cyclopentadienyl molybdenum(II) dicarbonyl complexes: structural studies and cytotoxicity evaluations," *Organometallics*, vol. 27, no. 19, pp. 4948–4956, 2008.

[142] D. Pérez-Quintanilla, S. Gomez-Ruiz, Ž. Žižak et al., "A new generation of anticancer drugs: mesoporous materials modified with titanocene complexes," *Chemistry*, vol. 15, no. 22, pp. 5588–5597, 2009.

[143] G. N. Kaluđerović, D. Pérez-Quintanilla, I. Sierra et al., "Study of the influence of the metal complex on the cytotoxic activity of titanocene-functionalized mesoporous materials," *Journal of Materials Chemistry*, vol. 20, no. 4, pp. 806–814, 2010.

[144] G. N. Kaluđerović, D. Pérez-Quintanilla, Ž. Žižak, Z. D. Juranić, and S. Gómez-Ruiz, "Improvement of cytotoxicity of titanocene-functionalized mesoporous materials by the increase of the titanium content," *Dalton Transactions*, vol. 39, no. 10, pp. 2597–2608, 2010.

[145] A. García-Peñas, S. Gómez-Ruiz, D. Pérez-Quintanilla et al., "Study of the cytotoxicity and particle action in human cancer cells of titanocene-functionalized materials," *Journal of Inorganic Biochemistry*, vol. 106, no. 2, pp. 100–110, 2012.

Hindawi Publishing Corporation
Bioinorganic Chemistry and Applications
Volume 2012, Article ID 210682, 8 pages
doi:10.1155/2012/210682

Research Article

Pharmacokinetic Study of Di-Phenyl-Di-(2,4-Difluobenzohydroxamato)Tin(IV): Novel Metal-Based Complex with Promising Antitumor Potential

Yunlan Li, Zhuyan Gao, Pu Guo, and Qingshan Li

School of Pharmaceutical Science, Shanxi Medical University, Taiyuan 030001, China

Correspondence should be addressed to Qingshan Li, qingshanl@yahoo.com

Received 31 August 2011; Revised 31 October 2011; Accepted 17 November 2011

Academic Editor: Sanja Mijatović

Di-phenyl-di-(2,4-difluobenzohydroxamato)tin(IV)(DPDFT), a new metal-based arylhydroxamate antitumor complex, showed high *in vivo* and *in vitro* antitumor activity with relative low toxicity, but no data was reported regarding its pharmacokinetics and dependent toxicity. In this paper, a rapid, sensitive, and reproducible HPLC method *in vivo* using Diamonsil ODS column with a mixture of methanol and phosphoric acid in water (30 : 70, V/V, pH 3.0) as mobile phase was developed and validated for the determination of DPDFT. The plasma was deproteinized with methanol that contained acetanilide as the internal standard (I.S.). The photodiode array detector was set at a wavelength of 228 nm at room temperature and a linear curve over the concentration range $0.1 \sim 25\,\mu g \cdot mL^{-1}$ ($r = 0.9993$) was obtained. The method was used to determine the concentration-time profiles for DPDFT in the plasma after single intravenous administration with doses of 5, 10, $15\,mg \cdot kg^{-1}$ to rats. The pharmacokinetics parameter calculations and modeling were carried out using the 3p97 software. The results showed that the concentration-time curves of DPDFT in rat plasma could be fitted to two-compartment model.

1. Introduction

Metals offer potential advantages over the more common organic-based drugs, including a wide range of coordination numbers and geometries, accessible redox states, "tuneability" of the kinetics of ligand substitution, as well as a wide structural diversity. Medicinal inorganic chemistry is a thriving area of research [1, 2], initially fueled by the discovery of cisplatin, a metal-based antitumor drug about 40 years ago. Since the discovery of cisplatin and its introduction in the clinics, metal compounds have been intensely investigated in view of their possible application in cancer therapy. Platinum anticancer agents, such as cisplatin, have been highly successful but there are several disadvantages associated with their clinical use. What needs to be recognized is that there are many other nonplatin metal-based antitumor drugs in the periodic table with therapeutic potential. Diorganotin(IV) complexes are potential antitumor agents mainly active against P388 lymphocytic leukemia and other tumors [3–5]. Lately, these antitumor agents are actually being studied widely. Among diorganotin(IV) compounds, dibutyltin(IV) derivatives of hydroxamic acid have received more attention due to their structural and biological importance [6–8].

Recently, we reported a series of diorganotin(IV) arylhydroxamates which exhibit *in vitro* antitumor activities (against a series of human tumor cell lines) which, in some case, are identical to, or even higher than, that of *cisplatin* [3, 5]. Di-phenyl-di-(2,4- difluobenzohydroxamato)tin(IV) (DPDFT, its structure was shown in Figure 1), a kind of efficient diorganotin(IV) patent compound (number: ZL01135148 and 102826Z) with lower toxicity, is a potential antitumor candidate for the clinical application due to its high *in vivo and in vitro* activity mainly against hepatoma, gastric cancer, nasopharyngeal carcinoma and other tumors (data not shown here). However, its antitumor molecular action mechanism is still unclear. In order to study the precise action mechanism and toxicity of this metal-based antitumor diorganotin(IV) compound, its fate should be

first elucidated *in vivo*, including their absorption, distribution, metabolism, and elimination. However, nothing is known about the pharmacokinetic behavior of DPDFT in body. Therefore, it is essential to establish a rapid, sensitive, and accurate method to determine the pharmacokinetic of organotin compound DPDFT in a body.

For medical care, practical, robust, simple, and efficient analytical methods are needed. Several methods have been reported for the determination of organotin compounds, including HPLC-MS [9, 10], HPLC-ICP-MS [10, 11], GC [12], GC-MIP AED [12–14], GC-MS [15–17], GC-ICP MS [18, 19], and so on. However, these methods have obvious disadvantages. For examples, GC methods have complicated pretreatments for the samples and seem to be unsuitable for quantitative determination in rat plasma because only a small amount of blood is normally used in pharmacokinetic studies. HPLC-MS is superior method and should be used whenever is possible. MS methods were used for mentioned analysis in order to increase selectivity of detection of DPDFT from complex matrixes. However, in this study, the HPLC-MS method was not used because the mass spectrometry conditions were still not ripe for DPDFT detection, and the high analysis cost and the expensive apparatus required were other considerations. So far, to the best of our knowledge, no method has been reported for determination of the diorganotin(IV) patent compound DPDFT by HPLC method with UV detection in the pharmacokinetic studies in rat plasma. Therefore, in this research, we chose DPDFT as a typical antitumor diorganotin(IV) arylhydroxamate to develop a simple, sensitive, and specific HPLC assay for its quantitative determination in rat plasma and to investigate its preliminary pharmacokinetic properties.

2. Experimental

2.1. Materials and Reagents. DPDFT used in analysis was synthesized by the same method as described in [20]. Its purity was 99.9%. Acetanilide used as an internal standard (I.S.) was purchased from Sigma Laboratories (St. Louis, MO). The chromatographic solvents and reagents such as methanol and phosphoric acid were obtained from the National Institute for the Control of Pharmaceutical and Biologic Products (Beijing, China). All substances were of chromatographic grade. Deionized water was prepared using a Milli-Q water purifying system from Millipore Corp. (Bedford, MA).

2.2. Animal Treatment. Laboratory bred adult Wistar albino rats (200–250 g), which were supplied by the Animal Research Center at Shanxi Medical University (Taiyuan, Shanxi Province, China), were housed at 25±2°C in a well-ventilated animal house under 12 : 12 h light dark cycle. The animals drank sterilized drinking water, and standard chow diet was supplied *ad libitum* to each cage. The animal experiments were performed in accordance with the ARVO Statement for the Use of Animals in Ophthalmic and Vision Research and were approved by the Animal Ethics Committee of Shanxi Medical University.

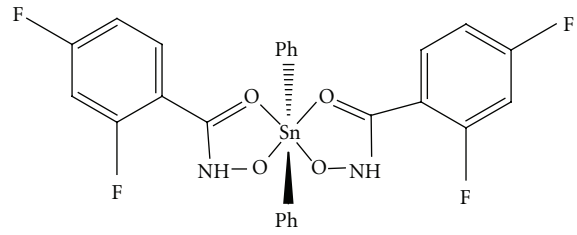

Figure 1: Chemical structure of DPDFT.

2.3. Instrumentation and Chromatographic Conditions. HPLC analysis was carried out using a Waters 2695 HPLC system (Waters Associates, Milford, MA) which consisted of a photodiode array detector, an autosampler, and a degasser. The apparatus was interfaced to a DELL PC compatible computer using Empower Pro software for data acquisition. The sensitivity was 0.2 AUFS. The autosampler was cooled to 10°C. The column was maintained at room temperature. Chromatographic separation of DPDFT and the I.S. was achieved on a Diamonsil C_{18} column (250 mm × 4.6 mm, 5 μm) from Dikma Technologies (Beijing, China) protected by a SHIMADZU LC guard column at 25°C. The mobile phase for HPLC analysis consisted of phosphoric acid in water (solvent A)/methanol (solvent B) (30 : 70, V/V, pH 3.0) with a flow rate of 0.8 mL·min^{-1}. A sample volume of 20 μL was injected. Prior to use, the mobile phase was filtered through a 0.45 μm hydrophilic membrane filter. The photodiode array detector was set at a wavelength of 228 nm at room temperature. Under the chromatographic condition mentioned above, DPDFT and the I.S. acetanilide could be separated completely in the chromatograms ($R > 1.5$), and there was no endogenous interference with the chromatographic peak of DPDFT and the I.S.acetanilide. Besides, the retention time of acetanilide (t_R = 15.67 min) was very suitable as the I.S. compared to that of DPDFT (t_R = 8.34 min).

2.4. Preparation of Plasma Samples. Blood samples collected from rat blood plasma were immediately transferred to 1.5 mL heparinized microcentrifuge tubes from fossa orbitalis of rats, and then processed for plasma by centrifugation. The supernatant plasma (0.2 mL) was then vortex-mixed with methanol (0.4 mL) containing acetanilide (0.2 mL, 50.0 μg·mL^{-1}) as internal standard (I.S.) for 30 s. After vortex-mixing, the mixture was centrifuged at 13000 rpm for 10 min 4°C to separate precipitated proteins. The supernatant solution of methanol layer was filtered through a 0.45 μm membrane filter. Twenty microliters of filtrate were injected into the chromatography. The same sample processing was also applied to the recovery and to the precision study in plasma. All harvested samples stored at −4°C were brought to room temperature before use and analyzed within one week. No significant differences were found between the samples stored at −4°C and those stored at −20°C (data not shown).

2.5. Bioanalytical Method Validation

2.5.1. Preparation of Stocks, Calibration Standards, and Quality Control Samples. A stock solution of DPDFT was prepared in methanol at the concentration of 100 $mg \cdot mL^{-1}$ and was further diluted in HPLC mobile phase to make working standards. The I.S. stock solution was prepared and diluted to 50.0 $\mu g \cdot mL^{-1}$ working solution with HPLC mobile phase. All the stock solutions were maintained at 4°C until use.

The linearity of HPLC method for the determination of DPDFT was evaluated by a calibration curve in the range of 0.1~25 $\mu g \cdot mL^{-1}$. Calibration standard samples were prepared by adding different concentrations of the standards of DPDFT and 0.2 mL of the I.S. working solution to the blank plasma. The final concentrations of DPDFT standard samples of plasma (0.1, 0.5, 1.0, 2.5, 5.0, 10.0, and 25.0 $\mu g \cdot mL^{-1}$, resp.) were prepared by spiking control rat plasma with appropriate amounts of the standard stock solution prepared above. The I.S. was added to each standard sample immediately before sample processing. For the evaluation of the linearity of the standard calibration curve, the analyses of DPDFT in plasma samples were performed on three independent days using fresh preparations. Each calibration curve consisted of a double blank sample (without internal standard), a blank sample (with internal standard), and seven calibrator concentrations. Each calibration curve was constructed by plotting the analyte to internal standard peak area ratio (y) against analyte concentrations (x). The calibration curves were fitted using a least-square linear regression model $y = ax + b$. The resulting a, b parameters were used to determine back-calculated concentrations, which were then statistically evaluated. All calibration curves of DPDFT were constructed before the experiments with correlation coefficient (r^2) of 0.99 or better.

2.5.2. Bioanalytical Method Validation. The specificity was defined as non-interference when DPDFT was being retained from the endogenous plasma components, and no crossinterference between DPDFT and the I.S. using the proposed extraction procedure. Six different lots of blank (DPDFT-free plasma) were evaluated both with and without internal standard to assess the specificity of the method.

Quality control (QC) samples were used to determine the accuracy and precision of method and were independently prepared at low (0.8 $\mu g \cdot mL^{-1}$), medium (4 $\mu g \cdot mL^{-1}$), and high (20 $\mu g \cdot mL^{-1}$) concentrations. To evaluate the accuracy and precision, we used at least five QC samples of three different concentrations of DPDFT. The intraday and interday accuracies were expressed as the percentage difference between the measured concentration and the nominal concentration in rat plasma. The intraday precision and accuracy were calculated using replicate ($n = 6$) determinations for each concentration of the spiked plasma sample during a single analytical run. The interassay precision and accuracy were calculated using replicate ($n = 6$) determinations of each concentration made on three separate days. The variability of determination was expressed as the relative standard deviation (RSD) which should be ≤15%, covering the range of actual experimental concentrations.

The extraction efficiency of DPDFT was determined by analyzing replicate sets ($n = 6$) of QC samples: 0.4, 8, 20 $\mu g \cdot mL^{-1}$ for rat plasma, representing low, medium, and high QCs, respectively. The recoveries were calculated by comparing the peak areas of DPDFT added into blank samples and extracted using the protein precipitation procedure, with those obtained from DPDFT spiked directly into postprotein precipitation solvent at three QC concentration levels.

The stability of DPDFT in rat plasma was assessed by analyzing replicates ($n = 6$) of QC samples at concentrations of 0.8, 4, 20 $\mu g \cdot mL^{-1}$, respectively. The investigation covered the expected conditions during all of the sample storage and process periods, which included the stability data from freeze/thaw cycle and long-term stability tests. The concentrations obtained from stability studies were compared with the freshly prepared QC samples, and the percentage concentration deviation was calculated. In each freeze–thaw cycle, the samples were frozen and stored at −20°C for 10 days, then thawed at room temperature. The stability of the fresh plasma samples was tested after keeping the samples at −4, −20°C and room temperature for 72 h. The stability of deproteinized samples at 10°C in the autosampler was evaluated up to 24 h.

To determine the limit and quantification of detection, we prepared the dilutions of 1, 2.5, 5, 10, 15, 20, and 30 $ng \cdot mL^{-1}$ DPDFT in plasma. The results were evaluated by analyzing each plasma sample spiked with the analyte at a final concentration at which the signal-to-noise ratio (S/N) was 10 and 3.

2.5.3. Pharmacokinetic Study. To evaluate the suitability of the assay for pharmacokinetic studies, 7.5, 15, and 30 $mg \cdot kg^{-1}$ of DPDFT were intravenously administered to rats (half males and half females, resp.). Six animals were used in each dosage by direct injection into a lateral tail vein, with a duration of infusion less than 1 min. Heparinized blood samples (0.5 mL) were collected at 0, 1, 3, 5, 10, 30, 60, and 120 min after injection. Eighteen rats were used for each time point. After each sampling, the removed volume of blood was supplemented with an equal volume of sodium chloride. The blood samples were immediately centrifuged and the resulting plasma was prepared according to the procedure given for the calibrators. Pharmacokinetic calculations were performed using the observed data. Pharmacokinetic analysis of DPDFT concentrations in plasma was performed using two-compartment model methods via the 3p97 software package (Chinese Pharmacology Society). All values obtained were expressed in mean ± standard deviation.

3. Results and Discussion

A deproteinized method to detect DPDFT, an typical antitumor diorganotin(IV) compound in plasma, was first developed in this paper. Diverse proportional solvents (methanol and acidified water) were selected in the deproteinizing process. The plasma deproteinized with double volume of

methanol could produce the minimal dilution, optimum peak shape, and an increase of detector sensitivity along with the satisfactory recovery.

3.1. Wavelength Selection Results. The Waters 2695 HPLC–DAD measurement was performed under the chromatographic condition mentioned above. Chromatographic separation of DPDFT was achieved on a Diamonsil C_{18} column (250 mm × 4.6 mm, 5 μm) protected by a SHIMADZU guard column at 25°C. The mobile phase for HPLC analysis consisted of phosphoric acid in water (solvent A)/methanol (solvent B) (30 : 70, V/V, pH 3.0) with a flow rate of 0.8 mL·min^{-1}. A sample volume of 20 μL was injected. The DAD wavelength range was set on 190~400 nm with a slid width of 1 nm and a response time of 2.0 s at room temperature. As shown in Figures 2(a), 2(b), and 2(c), the peaks were detected with good baseline separation. Peak identification was confirmed by comparison of UV spectra. The maximum absorption wavelength of DPDFT was 228 nm, and there was no endogenous interference with the chromatographic peak of DPDFT.

3.2. Validation Data of Bioanalytical Method. The method was validated using the criteria described above. The data were found to be linear over a concentration range of 0.1~25 μg·mL^{-1} in blood samples. The regression equation was $y = 32.001x + 0.31$, with the correlation coefficient $r = 0.9993$ ($n = 7$), where y represented the peak-area ratio of DPDFT to the I.S. in rat plasma and x was the concentration of DPDFT. The limit of quantitation (LOQ) was 10 ng, which can be determined with a relative error (RE) and precision (RSD) of <15% at a signal to-noise ratio of 10. The limits of detection (LOD) were 3.5 ng, based on a signal-to-noise ratio of 3.

Under the chromatographic condition, the number of theoretical plates was 5000. The degree of interference by endogenous plasma with DPDFT and the I.S. was assessed by inspection of chromatograms derived from a processed blank plasma sample. The results show that there were no endogenous interfering peaks with the I.S. and DPDFT in the rat plasma. Typical chromatograms of blank plasma, blank plasma spiked with DPDFT QC sample (3 μg·mL^{-1}) and the I.S., and a rat plasma sample after dosing with 15 mg·kg^{-1} DPDFT are presented (Figure 3). DPDFT and the I.S. were eluted at 15.67 and 8.34 min, respectively. The total run time was less than 30 min. A good separation of the I.S. and DPDFT was obtained under the specified chromatographic conditions.

The recoveries of the assay were assessed by comparing the peak-area ratios (analyte/the I.S.) obtained from spiked plasma samples of three DPDFT standard concentrations (0.4, 8, 20 mg/mL) with the peak-area ratios (analyte/the I.S.) for the samples containing the equivalent analyte and the I.S. which were directly dissolved in methanol. The recoveries were approximately 90.0–97.0% in the rat plasma, as shown in Table 1, the mean extraction recovery and the coefficient of variation RSD of DPDFT at three various concentrations from the rat plasma were 94.2%± 10.3% and 10.9% ($n = 18$), respectively.

Table 1: Recoveries of the assay for determining DPDFT in rat plasma ($n = 6$).

Spiked concentration (μg/mL)	Recovery (%, mean ± SD)	RSD (%)
0.8	90.8 ± 7.0	7.7
4	95.7 ± 12.9	13.5
20	96.2 ± 10.8	11.3

The precision and accuracy of this method were evaluated by assaying each low, middle, and high concentration QC sample. The reproducibility of the method was assessed by examining both intraday and interday variance. Accuracy (%) = [(Cobs − Cnom)/Cnom] × 100. The precision (%RSD) was calculated from the observed concentrations as follows: RSD = [standard deviation (SD)/Cobs] ×100. As shown in Table 2, the data showed that the intraday and interday precisions (% RSD) of the three QC samples in rat plasma were <15%. The RSD values of the intraday and the interday for rat plasma samples ranged from 3.8% ~9.0% and 4.0% ~9.0%, respectively. These validations demonstrated the reliability of the assay.

Stability of DPDFT during storage and processing was checked using quality control samples. The DPDFT and I.S. stock solutions were stable for at least 2 months when stored at 4°C. The deviation of the mean test responses was within ±10% of appropriate controls in all stability tests of DPDFT in rat plasma. After three freeze-thaw cycles, the concentration changes of DPDFT were less than 7%. The analyte was stable in the matrices at 4, −20°C and room temperature for 72 h without significant degradation (<8%). The run-time stability study showed that DPDFT in deproteinized rat plasma was stable at 10°C for up to 24 h (<6%). These results suggested that the rat plasma samples containing DPDFT can be handled under normal laboratory conditions without significant loss of the compound. All stability results are summarized in Table 3.

3.3. Pharmacokinetic Applicability. The developed RP-HPLC analytical method has been successfully used for the pharmacokinetic study after a single intravenous administration of DPDFT within 120 min. The mean plasma concentration-time curves of DPDFT after administration of 7.5, 15, and 30 mg·kg^{-1} in rats are shown in Figure 4, the concentration-time data conformed to a two-compartment model and the major mean pharmacokinetic parameters (mean ± SD) are summarized in Table 4. The RP-HPLC method satisfied the requirement of this study and demonstrated its general suitability for pharmacokinetics studies of DPDFT in rats.

3.4. The Pharmacokinetics Features of DPDFT in Rat Plasma. HPLC analysis for amphoteric, polar substances with low wavelength ultraviolet absorption is always associated with some difficulties, especially when high sensitivity is required. The results showed that this classic liquid extraction HPLC

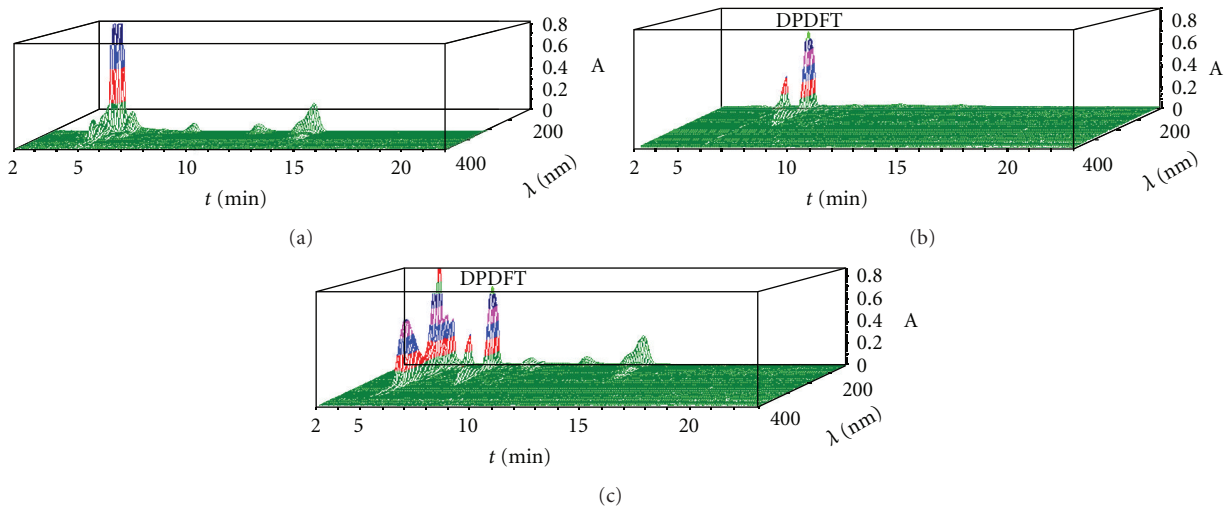

Figure 2: HPLC-DAD profiles of DPDFT in plasma sample. (a) Blank plasma; (b) DPDFT ($2\,\mu g \cdot mL^{-1}$) standard; (c) blood sample containing DPDFT ($2.4\,\mu g \cdot mL^{-1}$) collected at 3 min after administration of DPDFT ($15\,mg \cdot kg^{-1}$, i.v.).

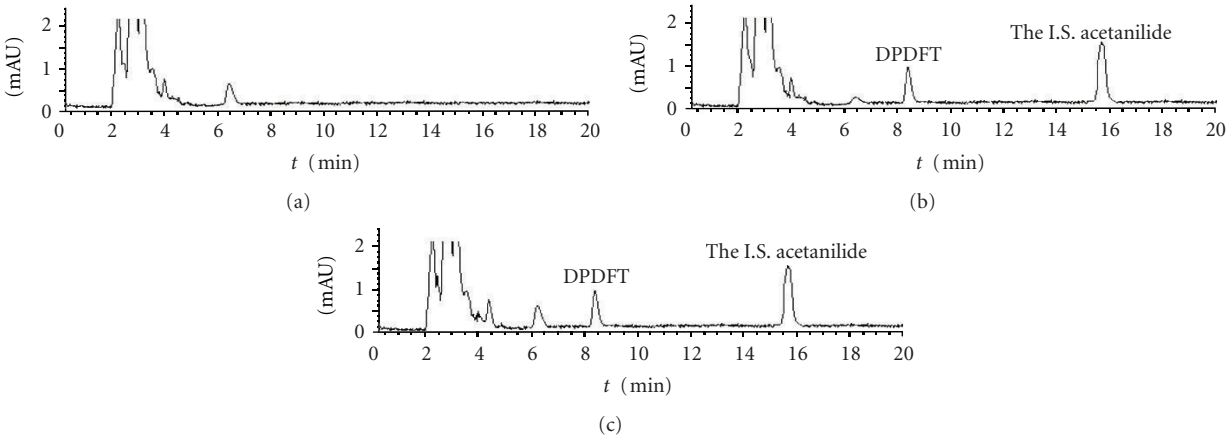

Figure 3: Chromatograms of DPDFT in plasma sample. Separation was performed using Waters 2695 HPLC system. The mobile phase consisted of phosphoric acid in water (solvent A)/methanol (solvent B) (30 : 70, V/V, pH 3.0) using Diamonsil C_{18} column at 25°C with a flow rate of $0.8\,mL \cdot min^{-1}$. (a) Blank plasma; (b) blank plasma spiked with DPDFT ($3\,\mu g \cdot mL^{-1}$) and the I.S. ($8\,\mu g \cdot mL^{-1}$); (c) blood sample containing DPDFT ($2.4\,\mu g \cdot mL^{-1}$) collected at 3 min after administration of DPDFT ($15\,mg \cdot kg^{-1}$, i.v.).

with UV detecting method was sensitive (the limit of detection was 3.5 ng) enough for pharmacokinetics studies of DPDFT in rats and did not require any forms of analyte derivatization or special columns or instruments. The most important factor for achievement of high sensitivity was the clean baseline owing to appropriate sample preparation on the chromatograms. Thus, a high signal/noise ratio was achieved, which constituted the base for the high sensitivity. The second factor was the high recovery of DPDFT from plasma during the extraction process. Methanol was used not only for deproteination, but also as extractive solvent for assay. So, the high recoveries of DFDPT (90.8, 95.7, and 96.2% for three determinations, resp.) were obtained. During the process of method development, it was discovered that DPDFT spiked with aqueous I.S. showed a symmetric single peak in the chromatograms at a pH around 3.0. With high sensitivity, small sample requirement, and simple sample treatment procedures, this method was successfully applied to the analysis of rat plasma samples and the pharmacokinetic study of DPDFT in rat.

The mean pharmacokinetic parameters (mean ± SD) are summarized in Table 4. There were no significant differences in all pharmacokinetic parameters between male and female rats at dose of 7.5, 15, and $30\,mg \cdot kg^{-1}$. The results showed that there was significant difference for AUC(0–t), they were calculated to be 7.56, 37.15, $81.25\,mg \cdot kg^{-1} \cdot min^{-1}$ at doses of 7.5, 15, and $30\,mg \cdot kg^{-1}$, respectively, and for the value of V_d after three dosages, 2.13, 1.13, $0.62\,L \cdot kg^{-1}$, respectively. These results suggested that the pharmacokinetics of the complex is a nonlinear process from 7.5 to 30 mg/kg. Otherwise, the distribution half-life $t_{1/2a}$ (1.04, 1.01, 1.12 min, resp.) and elimination half-life $t_{1/2\beta}$ (17.68,

Table 2: Intra- and interday precision and accuracy for DPDFT in rat plasma ($n = 6$).

Matrix	Nominal concentration ($\mu g \cdot mL^{-1}$)	Observed concentration ($\mu g \cdot mL^{-1}$) ± SD	Precision (%RSD)	Accuracy (%)
Intra-day	0.8	0.73 ± 0.05	6.8	−8.75
	4	3.73 ± 0.14	3.8	−6.75
	20	19.21 ± 1.02	5.3	−3.95
Inter-day	0.8	0.69 ± 0.06	8.7	−13.75
	4	3.80 ± 0.15	4.0	−5.00
	20	19.02 ± 1.11	5.9	−4.90

Notes: accuracy (%) = [(Cobs − Cnom)/Cnom] × 100, RSD = [standard deviation (SD)/Cobs] × 100.

Table 3: Stability results of DPDFT at different conditions in rat plasma ($n = 6$).

Storage period and storage condition	Nominal concentration ($\mu g \cdot mL^{-1}$)	Observed concentration ($\mu g \cdot mL^{-1}$) ± SD	Accuracy (%)	RSD (%)
Concentration of fresh preparation	0.8	0.85 ± 0.07	6.25	8.2
	4	3.91 ± 0.12	−2.25	3.1
	20	21.06 ± 1.33	5.30	6.3
Three freeze and thaw cycles	0.8	0.76 ± 0.05	−5.00	6.6
	4	3.79 ± 0.13	−5.25	3.5
	20	18.97 ± 1.17	−5.15	6.2
Stability for 72 h at 4°C	0.8	0.87 ± 0.04	8.75	4.6
	4	3.70 ± 0.16	−7.50	4.3
	20	21.14 ± 1.27	5.70	6.0
Stability for 72 h at −20°C	0.8	0.74 ± 0.05	−7.50	6.8
	4	4.22 ± 0.12	5.50	2.9
	20	19.13 ± 1.53	−4.35	7.9
Stability for 72 h at room temperature	0.8	0.78 ± 0.05	−2.50	6.4
	4	3.87 ± 0.19	−3.25	4.9
	20	19.46 ± 1.19	−2.75	6.1
Autosampler stability for 24 h at 10°C	0.8	0.83 ± 0.04	3.75	4.8
	4	3.83 ± 0.18	−4.25	4.7
	20	19.19 ± 1.08	−4.05	5.6

Notes: accuracy (%) = [(Cobs − Cnom)/Cnom] × 100, RSD = [standard deviation (SD)/Cobs] × 100.

Table 4: Mean pharmacokinetic parameters in rats after intravenous administration of 7.5, 15, and 30 $mg \cdot kg^{-1}$ of DPDFT (mean ± SD, $n = 6$).

Parameter (unit)	Dosage/mg kg^{-1}		
	7.5 (low)	15 (middle)	30 (high)
A/min^{-1}	2.21 ± 0.03	7.94 ± 3.12	22.36 ± 8.12
$B/mg \cdot kg^{-1}$	0.15 ± 0.04	0.92 ± 0.04	1.85 ± 0.44
β/min^{-1}	0.04 ± 0.003	0.04 ± 0.003	0.04 ± 0.003
$V_d/L \cdot kg^{-1}$	2.13 ± 0.07	1.13 ± 0.08	0.62 ± 0.08
$t_{1/2a}/min$	1.04 ± 0.01	1.01 ± 0.01	1.12 ± 0.1
$t_{1/2\beta}/min$	17.68 ± 2.6	19.38 ± 3.6	16.81 ± 3.6
K_{21}/min^{-1}	0.08 ± 0.004	0.11 ± 0.01	0.09 ± 0.01
K_{10}/min^{-1}	0.32 ± 0.05	0.24 ± 0.08	0.30 ± 0.18
K_{12}/min^{-1}	0.26 ± 0.04	0.38 ± 0.01	0.28 ± 0.11
AUC/$mg \cdot kg^{-1}$ min^{-1}	7.56 ± 1.02	37.15 ± 3.06	81.25 ± 15.3
CL(s)/$mg \cdot mL^{-1}$, mg kg^{-1}	0.66 ± 0.05	0.27 ± 0.02	0.018 ± 0.02

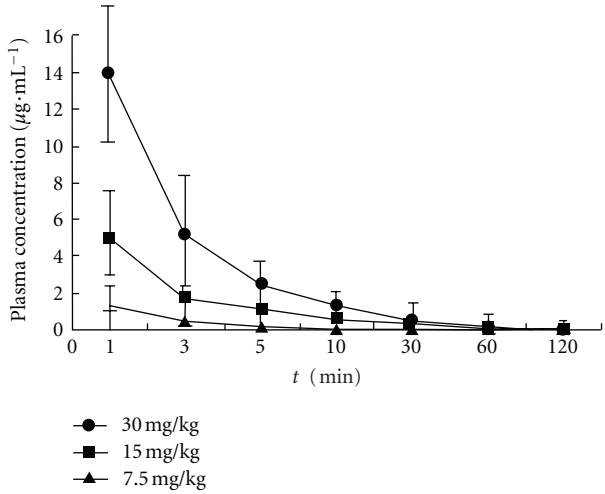

Figure 4: Mean plasma concentration-time profiles of DPDFT in rats after intravenous administration of 7.5, 15, and 30 mg·kg^{-1}. Each point represents the mean concentration of six rats.

19.38, 16.81 min, resp.) have no significant difference when the administration dosage of DPDFT was increased from 7.5 to 30 mg/kg, indicating that DPDFT distributed and eliminated very quickly.

4. Conclusions

In this paper, a simple, economical, sensitive, and specific method for the determination of DPDFT, a typical antitumor diorganotin(IV) compound in rat plasma, was first reported. The assay was validated for linearity, specificity, accuracy, precision, recovery, and stability, and good results were obtained. The results of preliminary pharmacokinetic studies indicated that DPDFT showed nonlinear pharmacokinetics in the studied dose ranges in rats and the concentration-time curves of DPDFT in rat plasma could be fitted to two-compartment model. These results hinted that DPDFT might accumulate in certain organs, thus produce the toxicity or could be quickly metabolized in the plasma into active constituent for antitumor. In order to study the precise toxicity mechanism of this metal-based antitumor diorganotin(IV) compounds, we should further elucidate their *in vivo* absorption, distribution, metabolism, and elimination. Meanwhile, based on the structure of DPDFT as a lead compound, structure reconstitution and optimization should be carried out to explore the better antitumor diorganotin(IV) compounds with higher activity, relative lower toxicity, and good pharmacokinetics features in the future.

Abbreviations

DPDFT: Di-phenyl-di-(2,4-difluobenzohydroxamato)tin(IV)
I.S.: Internal standard
HPLC: High performance liquid chromatography
QC: Quality control
S/N: The signal-to-noise ratio
LOQ: The limit of quantitation
LOD: The limits of detection
RE: Relative error
Cobs: Observed concentration
Cnom: Nominal concentration
SD: Standard deviation
RSD: Relative standard deviation
$t_{1/2a}$: Distribution half-life
$t_{1/2\beta}$: Elimination half-life
AUC: Area under the plasma concentration-time curve
K_{21}: First order transfer from compartment 2 to compartment 1
K_{10}: First order elimination from compartment 1
K_{12}: First order transfer from compartment 1 to compartment 2
Cl: Clearance.

Acknowledgments

Financial supports from the support of the State "Innovative Drug Development" Key Science and Technology Projects of China (no. 2009ZX09103-104), the National Natural Science Foundation of China (nos. 30973603 and 30772682), the Shanxi Foundation for overseas returned (no. 2010-54), the Program for the Top Young and Middle-aged Innovative Talents of Higher Learning Institutions of Shanxi Province and by Shanxi Province Foundation Science for Youths, the Foundation for the Younth Doctor from Shanxi Medical University in 2008, and Program for the Top Science and Technology Innovation Teams of Higher Learning Institutions of Shanxi province (2011) are gratefully acknowledged.

References

[1] T. W. Hambley, "Chemistry: metal-based therapeutics," *Science*, vol. 318, no. 5855, pp. 1392–1393, 2007.

[2] T. Storr, K. H. Thompson, and C. Orvig, "Design of targeting ligands in medicinal inorganic chemistry," *Chemical Society Reviews*, vol. 35, no. 6, pp. 534–544, 2006.

[3] L. Yunlan, L. Jinjie, and L. Qingshan, "Mechanisms by which the antitumor compound di-n-butyl-di-(4- chlorobenzohydroxamato)tin(IV) induces apoptosis and the mitochondrial-mediated signaling pathway in human cancer SGC-7901 cells," *Molecular Carcinogenesis*, vol. 49, no. 6, pp. 566–581, 2010.

[4] Q. Li, M. F. C. Guedes Da Silva, and A. J. L. Pombeiro, "Diorganotin(IV) derivatives of substituted benzohydroxamic acids with high antitumor activity," *Chemistry—A European Journal*, vol. 10, no. 6, pp. 1456–1462, 2004.

[5] L. Yunlan, L. Yang, N. Xiaoqiang et al., "Synthesis and antitumor activity of a new mixed-ligand complex di-n-butyl-(4-chlorobenzohydroxamato)tin(IV) chloride," *Journal of Inorganic Biochemistry*, vol. 102, no. 9, pp. 1731–1735, 2008.

[6] L. Pellerito, C. Prinzivalli, G. Casella et al., "Diorganotin(IV) N-acetyl-l-cysteinate complexes: synthesis, solid state, solution phase, DFT and biological investigations," *Journal of Inorganic Biochemistry*, vol. 104, no. 7, pp. 750–758, 2010.

[7] T. S. Basu Baul, A. Paul, L. Pellerito et al., "Dibutyltin(IV) complexes containing arylazobenzoate ligands: chemistry, in vitro cytotoxic effects on human tumor cell lines and mode of interaction with some enzymes," *Investigational New Drugs*, vol. 29, no. 2, pp. 285–289, 2011.

[8] W. Li, Z. W. Zhang, S. M. Ren, Y. Sibiril, D. Parent Massin, and T. Jiang, "Synthesis and antitumor activity of novel dibutyltin carboxylates of aminoglucosyl derivatives," *Chemical Biology and Drug Design*, vol. 73, no. 6, pp. 682–686, 2009.

[9] Y. Suzuki, Y. Endo, M. Ogawa, Y. Kim, N. Onda, and K. Yamanaka, "Development of an analytical method to confirm toxic trimethylated tin in human urine," *Journal of Chromatography B*, vol. 868, no. 1-2, pp. 116–119, 2008.

[10] Z. H. Yu, M. Jing, X. R. Wang, D. Y. Chen, and Y. L. Huang, "Simultaneous determination of multi-organotin compounds in seawater by liquid-liquid extraction-high performance liquid chromatography-inductively coupled plasma mass spectrometry," *Guang Pu Xue Yu Guang Pu Fen Xi*, vol. 29, no. 10, pp. 2855–2859, 2009.

[11] G. Zhai, J. Liu, L. Li et al., "Rapid and direct speciation of methyltins in seawater by an on-line coupled high performance liquid chromatography-hydride generation-ICP/MS system," *Talanta*, vol. 77, no. 4, pp. 1273–1278, 2009.

[12] G. A. Zachariadis and E. Rosenberg, "Speciation of organotin compounds in urine by GC-MIP-AED and GC-MS after ethylation and liquid-liquid extraction," *Journal of Chromatography B*, vol. 877, no. 11-12, pp. 1140–1144, 2009.

[13] D. Sakati and T. Teddy, "Seperation of organotin and organolead conpounds in drinking water by GC-MIP ADE," *Chemosphere*, vol. 32, no. 10, pp. 1983–1992, 1996.

[14] J. Carpinteiro, I. Rodríguez, and R. Cela, "Applicability of solid-phase microextraction combined with gas chromatography atomic emission detection (GC-MIP AED) for the determination of butyltin compounds in sediment samples," *Analytical and Bioanalytical Chemistry*, vol. 380, no. 5-6, pp. 853–857, 2004.

[15] Y. Li, Y. Hu, J. Liu, Y. Guo, and G. Wang, "Determination of organotin compounds in textile auxiliaries by gas chromatography-mass spectrometry," *Se Pu*, vol. 29, no. 4, pp. 353–357, 2011.

[16] K. Inagaki, A. Takatsu, T. Watanabe et al., "Certification of butyltins and phenyltins in marine sediment certified reference material by species-specific isotope-dilution mass spectrometric analysis using synthesized 118Sn-enriched organotin compounds," *Analytical and Bioanalytical Chemistry*, vol. 387, no. 7, pp. 2325–2334, 2007.

[17] R. B. Rajendran, H. Tao, T. Nakazato, and A. Miyazaki, "A quantitative extraction method for the determination of trace amounts of both butyl- and phenyltin compounds in sediments by gas chromatography-inductively coupled plasma mass spectrometry," *The Analyst*, vol. 125, no. 10, pp. 1757–1763, 2000.

[18] H. Nsengimana, E. M. Cukrowska, A. Dinsmore, E. Tessier, and D. Amouroux, "*In situ* ethylation of organolead, organotin and organomercury species by bromomagnesium tetraethylborate prior to GC-ICP-MS analysis," *Journal of Separation Science*, vol. 32, no. 14, pp. 2426–2433, 2009.

[19] M. Vahčič, R. Milačič, and J. Ščančar, "Development of analytical procedure for the determination of methyltin, butyltin, phenyltin and octyltin compounds in landfill leachates by gas chromatography-inductively coupled plasma mass spectrometry," *Analytica Chimica Acta*, vol. 694, no. 1-2, pp. 21–30, 2011.

[20] S. Xianmen, C. Jingrong, and L. Qingshan, "The preliminary structure-activity relationship of aromatic hydroxamic acid organotin compounds," *Science China Chemistry Series B*, vol. 38, no. 5, pp. 429–440, 2008.

Hindawi Publishing Corporation
Bioinorganic Chemistry and Applications
Volume 2012, Article ID 795812, 6 pages
doi:10.1155/2012/795812

Research Article

Antifungal and Antioxidant Activities of Pyrrolidone Thiosemicarbazone Complexes

Ahmed A. Al-Amiery,[1,2] Abdul Amir H. Kadhum,[1] and Abu Bakar Mohamad[1]

[1] *Department of Chemical and Process Engineering, Faculty of Engineering and Built Environment, University of Kebangsaan Malaysia, 43600 Bangi, Selangor, Malaysia*
[2] *Biotechnology Division, Applied Science Department, University of Technology, Baghdad 10066, Iraq*

Correspondence should be addressed to Ahmed A. Al-Amiery, dr.ahmed1975@gmail.com

Received 14 September 2011; Revised 3 October 2011; Accepted 18 October 2011

Academic Editor: Danijela Maksimović-Ivanić

Metal complexes of (Z)-2-(pyrrolidin-2-ylidene)hydrazinecarbothioamide (L) with Cu(II), Co(II), and Ni(II) chlorides were tested against selected types of fungi and were found to have significant antifungal activities. The free-radical-scavenging ability of the metal complexes was determined by their interaction with the stable free radical 2,2′′-diphenyl-1-picrylhydrazyl, and all the compounds showed encouraging antioxidant activities. DFT calculations of the Cu complex were performed using molecular structures with optimized geometries. Molecular orbital calculations provide a detailed description of the orbitals, including spatial characteristics, nodal patterns, and the contributions of individual atoms.

1. Introduction

Schiff bases have often been used as chelating ligands in the field of coordination chemistry, and their metal complexes have been of great interest to researchers for many years. It is well known that N and S atoms play a key role in the coordination of metals at the active sites of many metallobiomolecules [1]. The importance of metal ions in biological systems is well established. One of the most interesting features of metal-coordinated systems is the concerted spatial arrangement of the ligands around the metal ion. Among metal ions of biological importance, the Cu(II) ion involved in a large number of distorted complexes [2]. Over the past two decades, considerable attention has been paid to metal complexes of Schiff bases containing nitrogen and other donor atoms [3, 4]. Bioorganometallic chemistry is dedicated to the study of metallic complexes and their biological applications [5], including the design of new drugs that are more effective than those already known. The development of the field of bioinorganic chemistry has increased the interest in Schiff base complexes, because it has been recognized that many of these complexes may serve as models for biologically important species [6–9]. Antioxidants are extensively studied for their capacity to protect organisms and cells from damage induced by oxidative stress. Scientists in various disciplines have become more interested in new compounds, either synthesized or obtained from natural sources, that could provide active components to prevent or reduce the impact of oxidative stress on cells [10].

Thiosemicarbazones are well established as an important class of sulfur-donor Schiff base ligands that are particularly useful for transition metal ions. This is due to the remarkable biological activities observed for these compounds, which have been shown to be related to their metal-complexing ability. Thiosemicarbazone Schiff bases are an important class of compounds in the medicinal and pharmaceutical fields [11].

The work discussed herein describes the *in vitro* antioxidant and antifungal activities for metal complexes derived from (Z)-2-(pyrrolidin-2-ylidene)hydrazinecarbothioamide (L) [12].

2. Experimental

2.1. General. All chemicals used in this study were of reagent grade (supplied either by Sigma-Aldrich or Fluka) and used without further purification.

The FTIR spectra were recorded in the 4.000–200 cm^{-1} range on cesium iodide windows using a Shimadzu FTIR 8300 spectrophotometer. Proton NMR spectra were recorded on a Bruker-DPX 300 MHz spectrometer using TMS as an internal standard. The UV-VIS spectra were measured in ethanol using the Shimadzu UV-VIS -160A spectrophotometer in the range 200–1.000 nm. Magnetic susceptibility measurements for the complexes were obtained at room temperature using a Magnetic Susceptibility Balance Model MSB-MKI. Flame atomic absorption spectra from the Shimadzu AA-670 elemental analyzer were used for metal determination. Elemental microanalysis was performed using a CHN elemental analyzer model 5500-Carlo Erba. A Gallenkamp M.F.B.600.010 F melting point apparatus was used to measure the melting points of all the synthesized compounds.

2.2. Chemistry. The ligand and metal complexes were synthesized according to reference [12], and the structures of the compounds were confirmed with elemental analyses, spectral analyses (IR, UV-VIS, ^{1}H-NMR), conductance experiments, and magnetic measurements.

2.2.1. DFT. The molecular sketches of the reference compounds were plotted using Visualization Materials Studio 5.5 software. All quantum chemical calculations were performed using density functional theory (DFT) methodology. The DMol3 model was employed to obtain quantum chemical parameters and optimization of the molecular geometry. Molecular atomic charges were calculated by Mulliken population analysis [13].

2.3. Pharmacology

2.3.1. Evaluation of Antifungal Assay. All tests with the microorganisms (*Aspergillus niger* and *Candida albicans*) were obtained from the Biotechnology Division, Department of Applied Science, University of Technology.

Antifungal activity [14–16] was determined based on the growth inhibition rates of the mycelia of *Aspergillus niger* and *Candida albicans* strains grown in potato dextrose broth medium (PDB). Under aseptic conditions, one mL of spore suspension (5×10^6 cfu/mL) of the fungus being tested was added to 50 mL of PDB medium in a 100 mL Erlenmeyer flask. Appropriate volumes of tested metal complexes were added to produce concentrations ranging from 10 to 100 $\mu g\,mL^{-1}$. The flasks were incubated at 27 ± 1°C in the dark for 5 days, at which time the mycelia were collected on filter papers. The filter papers were dried to a constant weight, and the level of inhibition relative to the control flasks was calculated from the following formula:

$$\text{percentage of inhibition} = \frac{C - T}{C} \times 100, \quad (1)$$

where T is the weight of mycelia from the test flasks and C represents the weight of mycelia from the control flasks.

A note on statistical analysis is that significant differences between values were determined by a multiple-range test ($P < 0.05$) following one-way ANOVA.

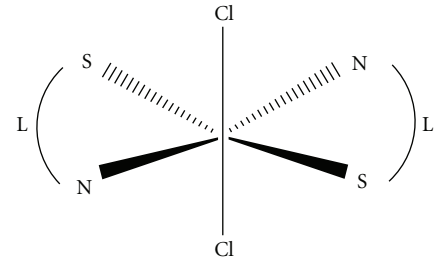

M = Co, Ni and Cu

Scheme 1: Proposed structure of the complexes.

2.3.2. Evaluation of Antioxidant Activity. A stock solution (1 mg/mL) was diluted to final concentrations of 20–100 μg/mL. An ethanolic DPPH solution (1 mL, 0.3 mmol) was added to sample solutions in DMSO (3 mL) at various concentrations (50–300 μg/mL) [17]. The mixture was shaken vigorously and allowed to stand at room temperature for 30 min. The absorbance was then measured at 517 nm using the UV-VIS. spectrophotometer. Less absorbance by the reaction mixture indicates higher free-radical-scavenging activity. Ethanol was used as the solvent and ascorbic acid as the standard. The DPPH radical scavenger effect was calculated using the following equation:

$$\text{scavenging effect (\%)} = \frac{A_0 - A_1}{A_0} \times 100, \quad (2)$$

where A_0 is the absorbance of the control reaction and A_1 is the absorbance in the presence of the samples or standards.

3. Results and Discussion

3.1. Chemistry. The ligand was synthesized according to [12]. Reaction could be explained by a Schiff base mechanism.

The complexes (Scheme 1) were then synthesized by the reactions of hot ethanolic solutions of the ligand (L) with the metal ions. The ligand behaves as a bidentate ligand *via* both the thione sulfur and the azomethine nitrogen [12].

3.1.1. Density Functional Theory (DFT). DFT calculations were performed for L and CuL_2Cl_2. The optimized molecular structure of the most stable form for the Cu complex is shown in Figure 1. Orbital calculations provide a detailed description of the orbitals, including spatial characteristics, nodal patterns, and individual atomic contributions. Contour plots of the frontier orbitals for the ground state of the ligand are shown in Figure 2, including the highest occupied molecular orbital (HOMO) and the lowest unoccupied molecular orbital (LUMO) [18]. It is interesting that both orbitals are substantially distributed over the plane of conjugation. It can be seen from Figure 2 that HOMO orbitals are located on the substituted molecule whereas the LUMO orbitals resemble those obtained for the unsubstituted molecule. Therefore, the substitution has an

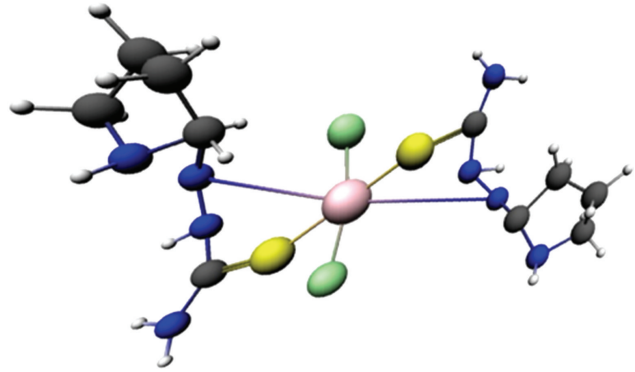

Figure 1: Optimized 3D structure of CuL_2Cl_2.

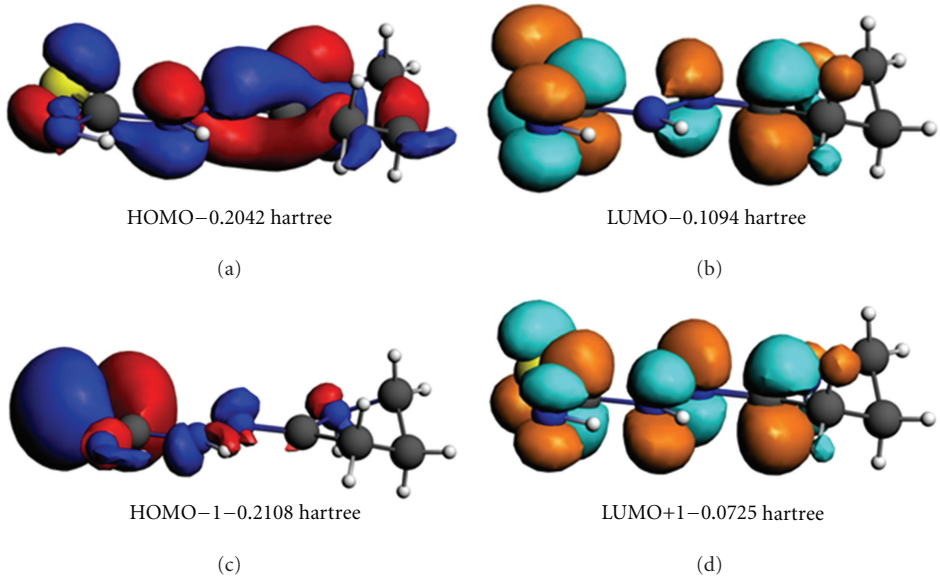

Figure 2: HOMO-LUMO energies for ligand (the energy in hartrees).

influence on the electron donation ability but only a small impact on the electron acceptance ability. The orbital energy levels of the HOMO and LUMO for the ligand are listed. It can be seen that the energy gap between the HOMO and LUMO is 0.0984 Hartrees for the ligand. The low value for the HOMO-LUMO energy gap explains the eventual charge transfer interaction taking place within these molecules.

3.1.2. Stereochemistry of the Metal Complexes. A thiosemicarbazone was first used in this study with the expectation that it would bind to the metal ion as a bidentate N,S-donor. From the preliminary characterization data, it was evident that the thiosemicarbazone ligand does indeed serve as a bidentate ligand, but the coordination mode of the ligand was not clear. The two ligands that are in the coordination sphere around the metal are significantly distorted from the ideal octahedral geometry [19]. To determine the coordination mode of the thiosemicarbazone ligand in these complexes, the structure shows that the thiosemicarbazone ligand is again coordinated to the metal in the same fashion as before. Due to the restricted rotation around the C=N bond, the ligand may exist as two different geometric isomers. The structural determination of one representative ligand (Scheme 2) shows that the free ligand exists in the thione form.

The absence of a thiol group in both the IR and NMR spectra indicates that the ligand exists predominantly as the thione tautomeric form in solution, as shown in Scheme 2. None of the synthesized ligands or metal complexes have any bands between 2,000 and 2,500 cm^{-1}, suggesting that the ligand and metal complexes in the solid state are not in the thiol form, as shown in Scheme 2.

3.2. Pharmacology

3.2.1. Antifungal Activities. Metal ions are adsorbed on the cell walls of the microorganisms, disturbing the respiration processes of the cells and thus blocking the protein synthesis that is required for further growth of the organisms. Hence, metal ions are essential for the growth-inhibitory effects [20]. According to Overtone's concept of cell permeability, the

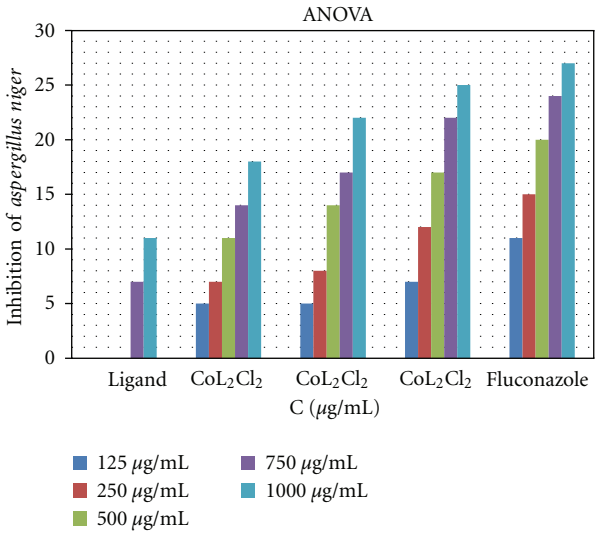

Figure 3: Effect of the metal complexes on *Aspergillus niger*, $^*P < 0.05$, one way Ligand (L) = $C_5H_{10}N_4S$; CoL_2Cl_2= $Co(C_5H_{10}N_4S)_2Cl_2$; NiL_2Cl_2= $Ni(C_5H_{10}N_4S)_2Cl_2$; CuL_2Cl_2= $Cu(C_5H_{10}N_4S)_2Cl_2$.

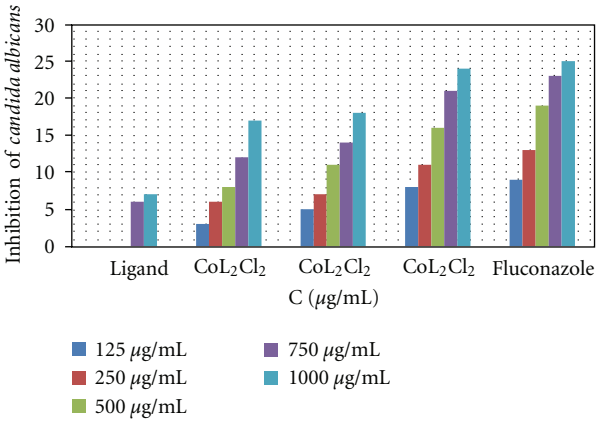

Figure 4: Effect of the metal complexes on *Candida albicans*, $^*P < 0.05$, one-way ANOVA.

lipid membrane that surrounds the cell favors the passage of only lipid-soluble materials, so lipophilicity is an important factor controlling the antifungal activity. Upon chelation, the polarity of the metal ion will be reduced due to the overlap of the ligand orbitals and partial sharing of the positive charge of the metal ion with donor groups. In addition, chelation allows for the delocalization of π-electrons over the entire chelate ring and enhances the lipophilicity of the complexes. This increased lipophilicity facilitates the penetration of the complexes into lipid membranes, further restricting proliferation of the microorganisms. The variation in the effectiveness of different compounds against different organisms depends either on the impermeability of the microbial cells or on differences in the ribosomes of the cells [21]. All of the metal complexes possess higher antifungal activity than the ligand [22, 23]. Although the exact biochemical mechanism is not completely understood,

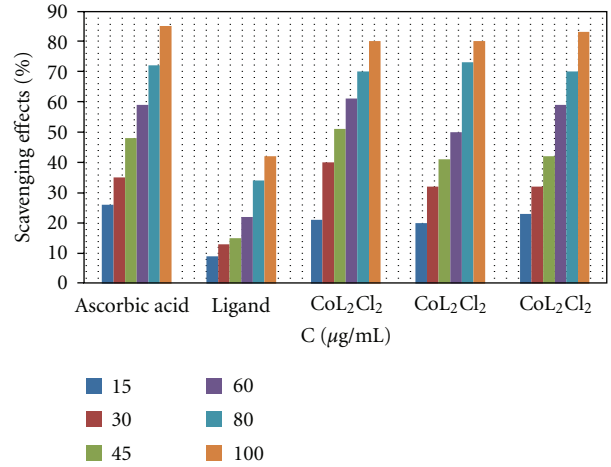

Figure 5: Scavenging effect of metal complexes and ascorbic acid at various concentrations, using the DPPH method.

the mode of action of antimicrobials may involve various targets in the microorganisms.

These targets include the following.

(i) The higher activity of the metal complexes may be due to the different properties of the metal ions upon chelation. The polarity of the metal ions will be reduced due to the overlap of the ligand orbitals and partial sharing of the positive charge of the metal ion with donor groups. Thus, chelation enhances the penetration of the complexes into lipid membranes and the blockage of metal binding sites in the enzymes of the microorganisms [24].

(ii) Tweedy's chelation theory predicts that chelation reduces the polarity of the metal atom mainly because of partial sharing of its positive charge with donor groups and possible electron delocalization over the entire ring. This consequently increases the lipophilic character of the chelates, favoring their permeation through the lipid layers of the bacterial membrane [25].

(iii) Interference with the synthesis of cellular walls, causing damage that can lead to altered cell permeability characteristics or disorganized lipoprotein arrangements, ultimately resulting in cell death.

(iv) Deactivation of various cellular enzymes that play a vital role in the metabolic pathways of these microorganisms.

(v) Denaturation of one or more cellular proteins, causing the normal cellular processes to be impaired.

(vi) Formation of a hydrogen bond through the azomethine group with the active centers of various cellular constituents, resulting in interference with normal cellular processes [26].

In vitro antifungal effects of the investigated compounds were tested against two fungal species (*Aspergillus niger* and *Candida albicans*). The results showed that the ligand itself

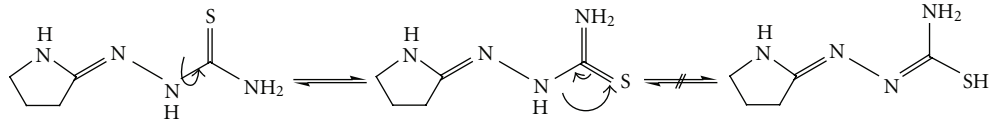

Scheme 2

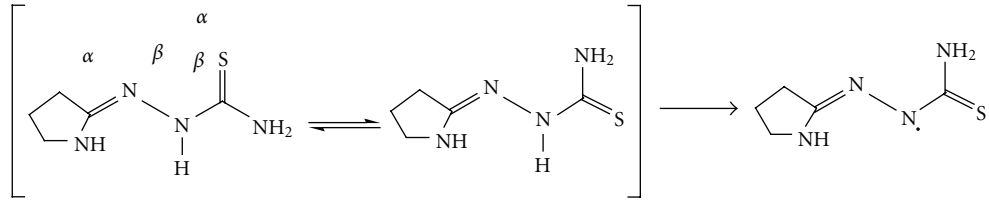

Scheme 3: Suggested mechanism for the antioxidant activity of the ligand.

does not exhibit any antifungal activity, but all metal-ligand complexes exhibit good activities. The CuL_2Cl_2 shows more activity than NiL_2Cl_2 and CoL_2Cl_2 which may be due to the higher stability of the CuL_2Cl_2 complex (DFT studies, [12], Figures 3 and 4).

The mode of action of the compounds may involve formation of a hydrogen bond through the azomethine group (>C=N–) with the active centers of various cellular constituents, resulting in interference with normal cellular processes [27, 28].

3.2.2. Radical-Scavenging Activity. DPPH is a stable free radical that is often used for detection of the radical-scavenging activity in chemical analysis [29, 30]. The reduction capability of DPPH radicals was determined by the decrease in its absorbance at 517 nm which can be induced by antioxidants. [31]. A graph may be plotted with percentage scavenging effects on the y-axis and concentration (μg/mL.) on the x-axis. The metal complexes used in the study showed good activities as a radical scavenger compared to the scavenging ability of ascorbic acid, which was used as a standard (Figure 5). These results were in agreement with previous studies of metallic complexes [32, 33] in which the ligand has antioxidant activity and it is expected that the metal moiety will increase its activity.

A postulated mechanism for the antioxidant ability of the ligand is shown in Scheme 3. The mechanism depends on the hydrogen atom of the secondary amine, which is influenced by both the allylic double bond and inductive effects. The allylic stabilization facilitates the release of hydrogen as a free radical, whereas the inductive effect from sulfur and nitrogen pushes electron density toward the free radical, resulting in a relatively stable molecule.

4. Conclusions

In this study, a ligand and its metal complexes were tested for antioxidant and antifungal activities. Of the complexes studied, CuL_2Cl_2 showed significant antifungal activities compared to either CoL_2Cl_2 or NiL_2Cl_2. In addition, all complexes were found to be superior antioxidants compared to ascorbic acid. The synthesized compounds were studied theoretically, and the atomic charges, heat of formation, and stereochemistry were estimated. Furthermore, it was found that the compounds are not planar.

References

[1] K. Singh, M. S. Barwa, and P. Tyagi, "Synthesis, characterization and biological studies of Co(II), Ni(II), Cu(II) and Zn(II) complexes with bidentate Schiff bases derived by heterocyclic ketone," *European Journal of Medicinal Chemistry*, vol. 41, no. 1, pp. 147–153, 2006.

[2] J. A. Obaleye, J. F. Adediji, and M. A. Adebayo, "Synthesis and biological activities on metal complexes of 2,5-diamino-1,3,4-thiadiazole derived from semicarbazide hydrochloride," *Molecules*, vol. 16, no. 7, pp. 5861–5874, 2011.

[3] X. Tai, X. Yin, Q. Chen, and M. Tan, "Synthesis of some transition metal complexes of a novel Schiff base ligand derived from 2,2′-bis(p-methoxyphenylamine) and salicylicaldehyde," *Molecules*, vol. 8, no. 5, pp. 439–443, 2003.

[4] A. A. H. Kadhum, A. B. Mohamad, A. A. Al-Amiery, and M. S. Takriff, "Antimicrobial and antioxidant activities of new metal complexes derived from 3-aminocoumarin," *Molecules*, vol. 16, no. 8, pp. 6969–6984, 2011.

[5] A. Corona-Bustamante, J. M. Viveros-Paredes, A. Flores-Parra et al., "Antioxidant activity of butyl- and phenylstannoxanes derived from 2-, 3- and 4-pyridinecarboxylic acids," *Molecules*, vol. 15, no. 8, pp. 5445–5459, 2010.

[6] N. H. Al-Sha'alan, "Antimicrobial activity and spectral, magnetic and thermal studies of some transition metal complexes of a Schiff base hydrazone containing a quinoline moiety," *Molecules*, vol. 12, no. 5, pp. 1080–1091, 2007.

[7] S. Chandra, D. Jain, A. K. Sharma, and P. Sharma, "Coordination modes of a Schiff base pentadentate derivative of 4-aminoantipyrine with cobalt(II), nickel(II) and copper(II) metal ions: synthesis, spectroscopic and antimicrobial studies," *Molecules*, vol. 14, no. 1, pp. 174–190, 2009.

[8] K. S. Prasad, L. S. Kumar, M. Prasad, and H. D. Revanasiddappa, "Novel organotin(IV)-Schiff base complexes: synthesis, characterization, antimicrobial activity, and DNA interaction studies," *Bioinorganic Chemistry and Applications*, vol. 2010, Article ID 854514, 9 pages, 2010.

[9] H. L. Singh and A. K. Varshney, "Synthetic, structural, and biochemical studies of organotin(IV) with Schiff bases having nitrogen and sulphur donor ligands," *Bioinorganic Chemistry and Applications*, vol. 2006, Article ID 23245, 7 pages, 2006.

[10] M. Alkan, H. Yüksek, Ö. Gürsoy-Kol, and M. Calapoğlu, "Synthesis, acidity and antioxidant properties of some novel 3,4-disubstituted-4,5-dihydro-1H-1,2,4-triazol-5-one derivatives," *Molecules*, vol. 13, no. 1, pp. 107–121, 2008.

[11] K. S. Abou-Melha and H. Faruk, "Bimetallic complexes of schiff base bis-[4-hydroxycuomarin-3-yl]- 1N,5N-thiocarbohydrazone as a potentially dibasic pentadentate ligand. Synthesis, spectral, and antimicrobial properties," *Journal of the Iranian Chemical Society*, vol. 5, no. 1, pp. 122–134, 2008.

[12] A. A. Al-Amiery, Y. K. Al-Majedy, H. Abdulreazak, and H. Abood, "Synthesis, characterization, theoretical crystal structure, and antibacterial activities of some transition metal complexes of the thiosemicarbazone (Z)-2-(pyrrolidin-2-ylidene)hydrazinecarbothioamide," *Bioinorganic Chemistry and Applications*, vol. 2011, Article ID 483101, 6 pages, 2011.

[13] A. A. H. Kadhum, A. A. Al-Amiery, A. Y. Musa, and A. B. Mohamad, "The antioxidant activity of new coumarin derivatives," *International Journal of Molecular Sciences*, vol. 12, no. 9, pp. 5747–5761, 2011.

[14] Z. Y. Daw, G. S. EL-Baroty, and A. E. Mahmoud, "Inhibition of *Aspergillus parasiticus* growth and aflatoxin production by some essential oils," *Chemie, Mikrobiologie, Technologie der Lebensmittel*, vol. 16, pp. 129–135, 1994.

[15] S. Myiut, W. R. W. Daud, A. B. Mohamed, and A. A. H. Kadhum, "Gas chromatographic determination of eugenol in ethanolextract of cloves," *Journal of Chromatography B*, vol. 76, pp. 193–195, 1996.

[16] A. A. Al-Amiery, "Antimicrobial and antioxidant activities of new metal complexes derived from (E)-3-((5-phenyl-1,3,4-oxadiazol-2-ylimino)methyl)naphthalen-2-ol," *Medicinal Chemistry Research*. In press.

[17] Y. Chen, M. Wang, R. T. Rosen, and C. T. Ho, "2,2-Diphenyl-1-picrylhydrazyl radical-scavenging active components from Polygonum multiflorum Thunb," *Journal of Agricultural and Food Chemistry*, vol. 47, no. 6, pp. 2226–2228, 1999.

[18] A. A. Al-Amiery, R. I. Al-Bayati, K. Y. Saour, and M. F. Radi, "Cytotoxicity, antioxidant and antimicrobial activitiesof novel 2-quinolone derivatives derived from coumarin," *Research on Chemical Intermediates*. In press.

[19] A. B. P. Lever, *Lever, Inorganic Electronic Spectroscopy*, Elsevier, New York, NY, USA, 1984.

[20] I. Pal, F. Basuli, and S. Bhattacharya, "Thiosemicarbazone complexes of the platinum metals. A story of variable coordination modes," *Proceedings of the Indian Academy of Sciences: Chemical Sciences*, vol. 114, no. 4, pp. 255–268, 2002.

[21] Y. Anjaneyula and R. P. Rao, "Preparation, characterization and antimicrobial activity studies on some ternary complexes of Cu(II) with acetylacetone and various salicylic acids," *Synthesis and Reactivity in Inorganic and Metal-Organic Chemistry*, vol. 16, pp. 257–272, 1986.

[22] Z. H. Chohan, M. Arif, M. A. Akhtar, and C. T. Supuran, "Metal-based antibacterial and antifungal agents: synthesis, characterization, and in vitro biological evaluation of Co(II), Cu(II), Ni(II), and Zn(II) complexes with amino acid-derived compounds," *Bioinorganic Chemistry and Applications*, vol. 2006, Article ID 83131, 13 pages, 2006.

[23] Z. H. Chohan, A. Scozzafava, and C. T. Supuran, "Zinc complexes of benzothiazole-derived Schiff bases with antibacterial activity," *Journal of Enzyme Inhibition and Medicinal Chemistry*, vol. 18, no. 3, pp. 259–263, 2003.

[24] K. S. Prasad, L. S. Kumar, S. C. Shekar, M. Prasad, and H. D. Revanasiddappa, "Oxovanadium complexes with bidentate N, O ligands: synthesis, characterization, DNA binding, nuclease activity and antimicrobial studies," *Chemical Sciences Journal*, vol. 12, pp. 1–10, 2011.

[25] T. D. Thangadurai and K. Natarajan, "Mixed ligand complexes of ruthenium(II) containing α,β-unsaturated-β-ketoamines and their antibacterial activity," *Transition Metal Chemistry*, vol. 26, no. 4-5, pp. 500–504, 2001.

[26] N. Dharmaraj, P. Viswanathamurthi, and K. Natarajan, "Ruthenium(II) complexes containing bidentate Schiff bases and their antifungal activity," *Transition Metal Chemistry*, vol. 26, no. 1-2, pp. 105–109, 2001.

[27] R. Joseyphus and M. Nair, "Antibacterial and antifungal studies on some schiff base complexes of zinc(II)," *Mycobiology*, vol. 36, pp. 93–98, 2008.

[28] L. Malhota, S. Kumar, K. S. Dhindsa et al., "Synthesis, characterization and microbial activity of Co(II), Ni(II), Cu(II) and Zn(II) complexes of aryloxyacetic acid and hydrazides," *Indian Journal of Chemistry Section A*, vol. 32, pp. 457–459, 1993.

[29] J. R. Soares, T. C. P. Dinis, A. P. Cunha, and L. M. Almeida, "Antioxidant activities of some extracts of Thymus zygis," *Free Radical Research*, vol. 26, no. 5, pp. 469–478, 1997.

[30] P. D. Duh, Y. Y. Tu, and G. C. Yen, "Antioxidant activity of water extract of Harng Jyur (Chyrsanthemum morifolium Ramat)," *Lebensmittel-Wissenschaft und-Technologie*, vol. 32, no. 5, pp. 269–277, 1999.

[31] B. Matthäus, "Antioxidant activity of extracts obtained from residues of different oilseeds," *Journal of Agricultural and Food Chemistry*, vol. 50, no. 12, pp. 3444–3452, 2002.

[32] S. B. Bukhari, S. Memon, M. Mahroof-Tahir, and M. I. Bhanger, "Synthesis, characterization and antioxidant activity copper-quercetin complex," *Spectrochimica Acta Part A*, vol. 71, no. 5, pp. 1901–1906, 2009.

[33] J. Gabrielska, M. Soczyńska-Kordala, J. Hładyszowski, R. Zyłka, J. Miśkiewicz, and S. Przestalski, "Antioxidative effect of quercetin and its equimolar mixtures with phenyltin compounds on liposome membranes," *Journal of Agricultural and Food Chemistry*, vol. 54, no. 20, pp. 7735–7746, 2006.

Hindawi Publishing Corporation
Bioinorganic Chemistry and Applications
Volume 2012, Article ID 850390, 5 pages
doi:10.1155/2012/850390

Research Article

Analysis of the Release Characteristics of Cu-Treated Antimicrobial Implant Surfaces Using Atomic Absorption Spectrometry

Carmen Zietz,[1] Andreas Fritsche,[1] Birgit Finke,[2] Vitezslav Stranak,[3] Maximilian Haenle,[1] Rainer Hippler,[3] Wolfram Mittelmeier,[1] and Rainer Bader[1]

[1] *Biomechanics and Implant Technology Research Laboratory, Department of Orhtopeadics, University of Rostock, Doberaner Straße 142, 18057 Rostock, Germany*
[2] *Leibniz Institute for Plasma Science and Technology (INP e.V. Greifswald), Felix-Hausdorff-Straße 2, 17489 Greifswald, Germany*
[3] *Institute of Physics, Ernst-Moritz-Arndt University of Greifswald, Felix-Hausdorff-Straße 6, 17487 Greifswald, Germany*

Correspondence should be addressed to Carmen Zietz, carmen.zietz@med.uni-rostock.de

Received 1 September 2011; Accepted 24 October 2011

Academic Editor: Reinhard Paschke

New developments of antimicrobial implant surfaces doped with copper (Cu) ions may minimize the risk of implant-associated infections. However, experimental evaluation of the Cu release is influenced by various test parameters. The aim of our study was to evaluate the Cu release characteristics *in vitro* according to the storage fluid and surface roughness. Plasma immersion ion implantation of Cu (Cu-PIII) and pulsed magnetron sputtering process of a titanium copper film (Ti-Cu) were applied to titanium alloy (Ti6Al4V) samples with different surface finishing of the implant material (polished, hydroxyapatite and corundum blasted). The samples were submersed into either double-distilled water, human serum, or cell culture medium. Subsequently, the Cu concentration in the supernatant was measured using atomic absorption spectrometry. The test fluid as well as the surface roughness can alter the Cu release significantly, whereby the highest Cu release was determined for samples with corundum-blasted surfaces stored in cell medium.

1. Introduction

Total joint replacement (TJR) meets high quality and safety standards and has become a frequent surgical procedure in order to restore joint function [1]. However, implant revision remains a relevant problem in clinical use. Failure of TJR is mainly due to aseptic loosening caused by inflammatory reactions due to wear particles [2]. Postoperative implant-associated infections are rare but considered devastating complications after TJR. Although surgical techniques and environmental conditions during the surgical intervention have improved over the years, infections occur with a frequency of 0.5–2% with incisive consequences for the patients and medical costs [3]. Most implant-associated infections are caused by *Staphylococcus aureus* and *Staphylococcus epidermidis* [4, 5].

Immediately after implantation bacteria, and human host cells compete for the implant surface in the so-called "race for the surface" [6]. If bacteria adhere to the implant surface prior to human bone cells, biofilm formation might occur and osseous integration of the implant is precarious. In terms of biofilms, the treatment of implant-associated infections can be further hindered by the thus increased bacterial resistance against antibiotics [7]. Novel developments of ion-based antimicrobial implant surfaces such as silver (Ag) [8] or copper (Cu) [9] might offer a possible solution to this problem. Various *in vitro* and *in vivo* studies confirm the antibacterial properties and cytocompatibility of Cu [10–13]. Other alternative antibacterial materials and agents are in development or already in use to prevent or treat implant-associated infections [14–18]. *In vitro* investigations of the antibacterial effects are usually performed on simplified samples and under simplified testing conditions, whereas *in vivo* tests are usually closer to the final application. *In vitro* conditions are often adjusted according to the respective test, that is, cell biological and microbiological tests are performed

with regard to their specific test protocols. Test fluids, storage times and fluid volume are essential parameters to characterise the antibacterial behaviour as well as the cytocompatibility and release kinetics of the antibacterial agents. Furthermore, the surface characteristics, such as the surface roughness, are an important aspect for coated surfaces with regard to the ion release properties [19]. Moreover, the ion release of ion-based antimicrobial coatings is of essential interest for the bactericidal activity and the cyto-compatibility of the coating.

The aim of the present study was to evaluate the Cu release characteristics of two different plasma surface treatments doped with Cu according to the storage fluid and surface roughness of the samples in order to provide an approach for possible standardised investigations in the future.

2. Materials and Methods

Titanium alloy (Ti6Al4V) discs (11 mm in diameter, 2 mm in height) were used as specimens for the investigation of ion release characteristics of Cu-doped plasma implant treatments. Two different plasma processes applying Cu were used: a plasma immersion ion implantation process (Cu-PIII) [20] and a pulsed magnetron sputtering process of a Ti-Cu film [21].

To analyse the influence of the composition of the test fluid on the Cu release, the Cu-PIII, and Ti-Cu-coated test samples were placed in 24-well plates and covered with 700 μL test fluid. Additionally, uncoated Ti6Al4V test samples were submersed as a reference. The following test fluids were used: double-distilled water (TKA Wasseraufbereitungssysteme GmbH, Niederelbert, Germany), human serum (invitrogen, Darmstadt, Germany), and Dulbecco's Modified Eagle's medium (DMEM, Invitrogen, Carlsbad, USA) with 10% fetal calf serum (FCS Gold, PAA Laboratories GmbH, Pasching, Austria) as well as 1% gentamicin (Ratiopharm GmbH, Ulm, Germany). Subsequently, the samples were incubated at 37°C in a humidified atmosphere with 5% CO_2 for 24 h to simulate physiological conditions. All samples were corundum-blasted before plasma treating and exhibited a surface roughness after plasma treatment of Ra = 3.76 ± 0.7 μm and 2.02 ± 0.1 μm for the Cu-PIII and Ti-Cu coatings, respectively. Three samples of each coating were submersed for each test fluid configuration.

In addition, to evaluate a possible influence on the Cu release due to surface topology and roughness, three different surface treatments of the Ti6Al4V samples were performed before Cu-PIII plasma treatment: polishing (Ra = 0.09 ± 0.09 μm), hydroxyapatite (HA) blasting (Ra = 1.17 ± 0.2 μm), and corundum blasting (Ra = 4.44 ± 0.5 μm). Subsequently three Cu-PIII treated samples of each surface roughness, were immersed in double-distilled water for 5 days. Furthermore, roughness was investigated after storage in DMEM for 24 hours.

After the lapse of submersion time, the supernatants were removed from the samples and 1% nitric acid (HNO_3) was added to stabilize the released Cu ions. In addition, the supernatants were diluted for the following atomic absorption spectrometry (AAS) analysis. By means of an AAS with electrothermal atomization (ZEEnit 650, Analytik Jena AG, Jena, Germany), the concentration of Cu ions released into the supernatants from the Cu plasma treatments was determined.

Thereby, the solutions of the different samples were evaporated in a three-step process (90°C for 20 s, 105°C for 20 s, 110°C for 10 s) followed by a pyrolysis phase at 850°C (10 s) in a platform tube. The pyrolysis phase eliminates residual organic material and combusts solid particles from the solution into ash. Using a rapid heat increase (1500°C/s), the tube was heated to 2000°C for 4 s to vaporize and convert solid particles into free atoms. This step also included the element analysis using a hollow cathode lamp with a Cu cathode radiating at 324.8 nm. Parts of the total emitted intensity were absorbed by the Cu atoms present in the tube from the diluted solution samples of the release experiments. The measured intensity was compared with the intensity of a standard Cu reference allowing the determination of the Cu concentration in the supernatants. In a final step the platform tube was cleaned by heating up to 2300°C for 4 s.

All data were stored and analyzed using the SPSS statistical package 15.0 (SPSS Inc. Chicago, Ill, USA). Descriptive statistics were computed for continuous and categorical variables [22]. The statistical data included mean and standard deviations of continuous variables, frequencies, and relative frequencies of categorical factors. Comparisons within the independent groups were achieved using the ANOVA test (Post Hoc LSD). All P values resulted from two-sided statistical tests, and values of $P < 0.05$ were considered to be significant.

3. Results

The uncoated Ti6Al4V control test samples showed no traces of copper in the supernatant. However, specific release characteristics were found for the analysed Cu-doped Ti6Al4V samples in different supernatants (Figure 1). Hereby, DMEM provoked the highest Cu ion release with a significant increase compared to double-distilled water ($P \leq 0.001$), but no statistical significance was observed when compared to human serum ($P \geq 0.068$). Higher Cu concentrations were released from the Ti-Cu films than from the Cu-PIII-treated surfaces in human serum (4.96 ± 0.22 mmol/l versus 1.25 ± 0.01 mmol/l) and in DMEM (5.27 ± 0.90 mmol/l versus 2.00 ± 0.63 mmol/l), respectively. Using double-distilled water, the observed concentration of released Cu was significantly lower ($P \leq 0.019$) compared to human serum and DMEM and approximately the same for all samples with different Cu treatments (Ti-Cu: 0.20 ± 0.01 mmol/l, Cu-PIII: 0.25 ± 0.02 mmol/l).

The surface roughness did not reveal a significant influence on the Cu release in double-distilled water (Figure 2). Polished surfaces resulted in a Cu concentration in the supernatant of 0.23 ± 0.01 mmol/l. For the HA and corundum-blasted surfaces the Cu concentration is in the same dimension at 0.16 ± 0.01 mmol/l and 0.20 ± 0.01 mmol/l, respectively. In comparison to DMEM, the Cu concentrations were significantly lower ($P \leq 0.007$) for all

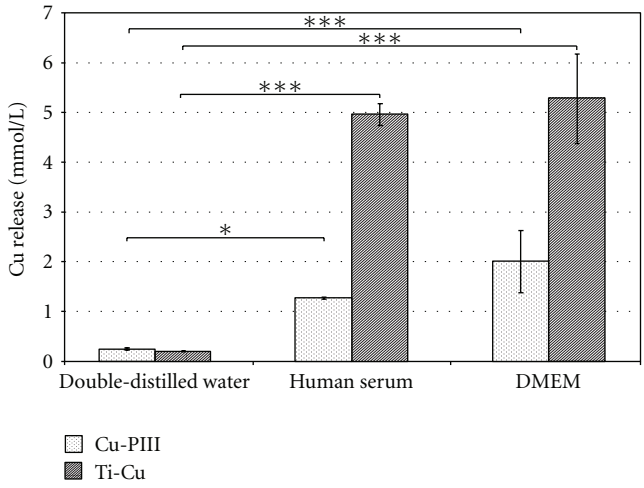

Figure 1: Copper concentration of Cu-PIII- and Ti-Cu-coated corundum-blasted Ti6Al4V surfaces submersed in 700 μL of different supernatants (human serum, double-distilled water, and DMEM) for 24 h at 37°C and 5% CO_2; ANOVA (Post Hoc LSD) test, $^*P < 0.05$, $^{***}P \leq 0.001$.

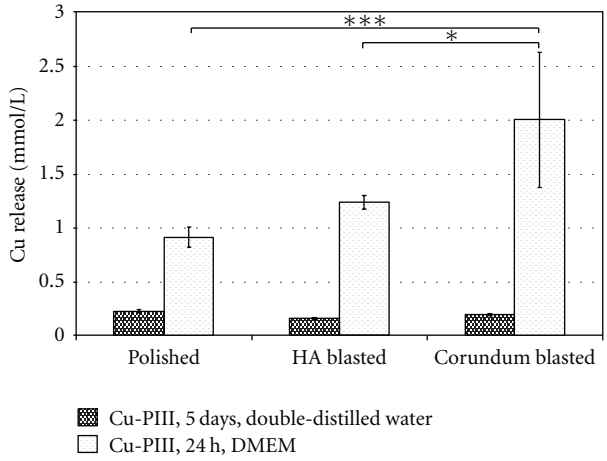

Figure 2: Copper concentration of Cu-PIII-treated Ti6Al4V samples with varying substrate surface roughness (polished, HA blasted, corundum blasted), submersed for 5 days in double-distilled water and 24 h in DMEM at 37°C and 5% CO_2. ANOVA (Post Hoc LSD) test, $^*P < 0.05$, $^{***}P \leq 0.001$.

surface topologies using double-distilled water. Corundum-blasted samples submersed in DMEM showed the highest Cu levels in the supernatant (2.00 ± 0.63 mmol/l, $P \leq 0.004$). A decrease in Cu concentration was observed for the polished samples in comparison to the HA-blasted ($P = 0.156$) and corundum-blasted ($P \leq 0.004$) samples.

4. Discussion

In order to enhance implant survival, bioactive coatings have moved into the focus of research and development. Due to the increasing risk of implant infections from multiresistant bacteria such as MRSA (multiresistant *Staphylococcus aureus*) [10, 11, 23] or ESBL (enterobacteria producing extended spectrum beta-lactamases) [24], different antimicrobial coatings [17, 25–28] are being developed. However, the mechanical, biological and chemical properties of such innovative coatings have to be investigated thoroughly. Cu ions can be an effective antimicrobial agent to inhibit bacterial growth and biofilm formation on endoprosthetic surfaces [10, 29]. Analyses of the ion release are strictly necessary for the determination of relevant Cu concentrations required in order to regulate both antimicrobial effects and compatibility to human cells. Furthermore, the release kinetics of copper-doped surfaces needs to be investigated in standardised tests in order to ensure effective and valid ion concentrations. In this context, however, standardised test conditions have not been established so far.

The AAS is a suitable device to measure Cu concentrations in supernatants. Uncoated samples did not show any Cu in any of the analysed supernatants, whereas the Cu-treated samples revealed differences in Cu concentration. Nevertheless, using an AAS, both Cu^+ and Cu^{2+} ions are assessed at the same time without any distinction. However, only Cu^{2+} ions cause an antimicrobial effect [30]. Hence, the concentration alone is not enough to predict the effectiveness of the coating and should be supported by microbiological tests.

Investigations of the ion release of an antimicrobial coating should coincide with cell biological tests using human cells to study biocompatibility of the coating. Furthermore, test fluid volumes should be the same for all studies, ensuring similar Cu concentrations. A test fluid volume of 700 μL was chosen to represent *in vivo* conditions. After conventional implantation technique, Wu et al. [31] observed that 40% of an uncemented femoral stem showed no bone contact with an average gap width between the bone and the femoral stem of 0.77 mm. In relation to the test samples deployed in this study, a volume of approximately 200 μL would be adequate to simulate the gap volume at the uncemented stem. However, 200 μL is not enough to cover the test samples completely, which would make *in vitro* testing impossible. Therefore, a volume of 700 μL was chosen as a compromise, which was the smallest possible volume that assured proper cell and bacterial growth in the supernatant.

The results of this study show that the amount of Cu ions released into the supernatant depends on various factors. The supernatant and its properties to dissolve Cu ions plays an important role. Surprisingly, the Cu concentration in double-distilled water for the Cu-PIII coating after 24 hours did not differ from the Cu concentration after 5 days. Therefore, double-distilled water showed an early Cu saturation for both tested coatings, whereas human serum and DMEM revealed a much higher Cu concentration in the supernatant. In fact, the highest concentration was obtained in DMEM for the Ti-Cu coating. The presence of serum proteins increases the solubility of Cu in the supernatants significantly compared to the double-distilled water because of the complex compounds between copper and amino groups found in the proteins in human serum and DMEM. Wu et al. [32] showed a higher concentration of Ag^+ ions after 24 h in cell culture medium as in simulated body

fluid, which coincides with the Cu concentrations found in our present study. However, based on the current results, it is not possible to appoint a Cu ion saturation level for neither human serum nor DMEM. Repeated and cumulative investigations at different time periods need to be carried out and could provide a precise saturation level.

Surface roughness increases the surface area in contact with the supernatant. With rising surface roughness, an increase of the Cu concentration in the supernatant was observed. Compared to a polished surface, the corundum-blasted surface released approximately three times as many Cu ions within 24 h. In double-distilled water, the Cu concentration levels remained constant after 5 days regardless of the surface roughness, since the Cu saturation has set in within the first 24 h.

Temperature may also influence the ion release characteristic of an implant material. Therefore, the release studies should be carried out at 37°C body temperature. A time-dependant Cu release behaviour, cumulative and non cumulative, of the analysed coatings is currently under investigation. First results show that most of the Cu is released during the first 24 h, followed by a highly reduced release rate during the succeeding days. Furthermore, the effect of copper ions on human cells and tissue is currently under investigation provided by cell biological and microbiological tests as well as animal studies using an infection model.

5. Conclusion

When testing antimicrobial Cu-coated implant surfaces, it is important to apply appropriate test conditions regarding the ion release into the surrounding tissue. With respect to future clinical applications of the coated implants, a suitable test fluid such as human serum or DMEM should be used to coincide with cell biological and microbiological studies; otherwise, false conclusions may be drawn. Furthermore, it is important to use test samples with adequate surface properties close to those needed in the final application, since the surface roughness can affect the ion release dramatically.

Acknowledgments

This work was supported by the TEAM program of Mecklenburg-Vorpommern and the Helmholtz Association in Germany (UR 0402210, VH-MV1) and by the BMBF program Campus PlasmaMed (subproject PlasmaImp 13N9775, 13N11188). The authors thank Mr. U. Kellner, U. Lindemann (INP Greifswald), and L. Middelborg for the excellent technical assistance as well as Ms. A. Jonitz for the assistance in the statistical analysis.

References

[1] C. A. Jones, L. A. Beaupre, D. W. C. Johnston, and M. E. Suarez-Almazor, "Total joint arthroplasties: current concepts of patient outcomes after surgery," *Rheumatic Disease Clinics of North America*, vol. 33, no. 1, pp. 71–86, 2007.

[2] T. W. Bauer and J. Schils, "The pathology of total joint arthroplasty II. Mechanisms of implant failure," *Skeletal Radiology*, vol. 28, no. 9, pp. 483–497, 1999.

[3] W. Zimmerli, A. Trampuz, and P. E. Ochsner, "Current concepts: prosthetic-joint infections," *New England Journal of Medicine*, vol. 351, no. 16, pp. 1645–1654, 2004.

[4] A. Trampuz and W. Zimmerli, "Prosthetic joint infections: update in diagnosis and treatment," *Swiss Medical Weekly*, vol. 135, no. 17-18, pp. 243–251, 2005.

[5] D. Campoccia, L. Montanaro, P. Speziale, and C. R. Arciola, "Antibiotic-loaded biomaterials and the risks for the spread of antibiotic resistance following their prophylactic and therapeutic clinical use," *Biomaterials*, vol. 31, no. 25, pp. 6363–6377, 2010.

[6] A. Gristina, "Biomaterial-centered infection: microbial adhesion versus tissue integration. 1987," *Clinical Orthopaedics and Related Research*, no. 427, pp. 4–12, 2004.

[7] J. W. Costerton, P. S. Stewart, and E. P. Greenberg, "Bacterial biofilms: a common cause of persistent infections," *Science*, vol. 284, no. 5418, pp. 1318–1322, 1999.

[8] H. S. Ryu, I. H. Bae, and K. G. Lee, "Antibacterial effect of silver-platinumcoating for orthodontic appliances," *Angle Orthodontist*. In press.

[9] G. Borkow and J. Gabbay, "Copper as a biocidal tool," *Current Medicinal Chemistry*, vol. 12, no. 18, pp. 2163–2175, 2005.

[10] M. Haenle, A. Fritsche, C. Zietz et al., "An extended spectrum bactericidal titanium dioxide (TiO_2) coating for metallic implants: *in vitro* effectiveness against MRSA and mechanical properties," *Journal of Materials Science: Materials in Medicine*, vol. 22, no. 2, pp. 381–387, 2010.

[11] L. Weaver, J. O. Noyce, H. T. Michels, and C. W. Keevil, "Potential action of copper surfaces on meticillin-resistant Staphylococcus aureus," *Journal of Applied Microbiology*, vol. 109, no. 6, pp. 2200–2205, 2010.

[12] M. Yasuyuki, K. Kunihiro, S. Kurissery, N. Kanavillil, Y. Sato, and Y. Kikuchi, "Antibacterial properties of nine pure metals: a laboratory study using Staphylococcus aureus and Escherichia coli," *Biofouling*, vol. 26, no. 7, pp. 851–858, 2010.

[13] R. Sharan, S. Chhibber, and R. H. Reed, "A murine model to study the antibacterial effect of copper on infectivity of Salmonella enterica serovar Typhimurium," *International Journal of Environmental Research and Public Health*, vol. 8, no. 1, pp. 21–36, 2011.

[14] D. Neut, R. J.B. Dijkstra, J. I. Thompson, H. C. van der Mei, and H. J. Busscher, "Antibacterial efficacy of a new gentamicin-coating for cementless prostheses compared to gentamicin-loaded bone cement," *Journal of Orthopaedic Research*, vol. 29, no. 11, pp. 1654–1661, 2011.

[15] L. Wang, U. J. Erasquin, M. Zhao et al., "Stability, antimicrobial activity, and cytotoxicity of poly(amidoamine) dendrimers on titanium substrates," *ACS Applied Materials & Interfaces*, vol. 3, no. 8, pp. 2885–2894, 2011.

[16] J. Holt, B. Hertzberg, P. Weinhold, W. Storm, M. Schoenfisch, and L. Dahners, "Decreasing bacterial colonization of external fixation pins through nitric oxide release coatings," *Journal of Orthopaedic Trauma*, vol. 25, no. 7, pp. 432–437, 2011.

[17] E. M. Hetrick and M. H. Schoenfisch, "Reducing implant-related infections: active release strategies," *Chemical Society Reviews*, vol. 35, no. 9, pp. 780–789, 2006.

[18] S. Chandra, S. Raizada, M. Tyagi, and A. Gautam, "Synthesis, spectroscopic, and antimicrobial studies on bivalent nickel and copper complexes of bis(thiosemicrbazone)," *Bioinorganic Chemistry and Applications*, vol. 2007, Article ID 51483, 7 page, 2007.

[19] G. D. Christensen, L. Baldassarri, and W. A. Simpson, "Methods for studying microbial colonization of plastics," *Methods in Enzymology*, vol. 253, pp. 477–500, 1995.

[20] K. Schröder, B. Finke, M. Polak et al., "Gas-discharge plasma-assisted functionalization of titanium implant surfaces," *Materials Science Forum*, vol. 638-642, pp. 700–705, 2010.

[21] V. Stranak, H. Wulff, H. Rebl et al., "Deposition of thin titanium-copper films with antimicrobial effect by advanced magnetron sputtering methods," *Materials Science and Engineering C*, vol. 31, no. 7, pp. 1512–1519, 2011.

[22] R. Marcus, E. Peritz, and K. R. Gabriel, "On closed testing procedures with special reference to ordered analysis of variance," *Biometrika*, vol. 63, no. 3, pp. 655–660, 1976.

[23] D. Ip, S. K. Yam, and C. K. Chen, "Implications of the changing pattern of bacterial infections following total joint replacements," *Journal of Orthopaedic Surgery*, vol. 13, no. 2, pp. 125–130, 2005.

[24] M. Haenle, A. Podbielski, M. Ellenrieder et al., "Periprosthetic infections following total hip replacement with ESBL-forming bacteria importance for clinical practice," *Orthopade*, vol. 40, no. 6, pp. 528–534, 2011.

[25] A. Ewald, S. K. Glückermann, R. Thull, and U. Gbureck, "Antimicrobial titanium/silver PVD coatings on titanium," *BioMedical Engineering Online*, vol. 5, article 22, 2006.

[26] G. Schmidmaier, M. Lucke, B. Wildemann, N. P. Haas, and M. Raschke, "Prophylaxis and treatment of implant-related infections by antibiotic-coated implants: a review," *Injury*, vol. 37, no. 2, pp. S105–S112, 2006.

[27] N. Y. Pfeufer, K. Hofmann-Peiker, M. Mühle, P. H. Warnke, M. C. Weigel, and M. Kleine, "Bioactive coating of titanium surfaces with recombinant human β-defensin-2 (rHuβD2) may prevent bacterial colonization in orthopaedic surgery," *Journal of Bone and Joint Surgery. Series A*, vol. 93, no. 9, pp. 840–846, 2011.

[28] A. Fritsche, F. Heidenau, H. G. Neumann, W. Mittelmeier, and R. Bader, "Mechanical properties of anti-infectious, bioactive and wear resistant ceramic implant surface coatings," *Key Engineering Materials*, vol. 396-398, pp. 357–360, 2009.

[29] F. Heidenau, W. Mittelmeier, R. Detsch et al., "A novel antibacterial titania coating: metal ion toxicity and *in vitro* surface colonization," *Journal of Materials Science: Materials in Medicine*, vol. 16, no. 10, pp. 883–888, 2005.

[30] I. Iakovidis, I. Delimaris, and S. M. Piperakis, "Copper and its complexes in medicine: a biochemical approach," *Molecular Biology International*, vol. 2011, Article ID 594529, 13 pages, 2011.

[31] L. D. Wu, H. J. Hahne, and J. Hassenpflug, "The dimensional accuracy of preparation of femoral cavity in cementless total hip arthroplasty," *Journal of Zhejiang University Science*, vol. 5, no. 10, pp. 1270–1278, 2004.

[32] X. Wu, J. Li, L. Wang, D. Huang, Y. Zuo, and Y. Li, "The release properties of silver ions from Ag-nHA/TiO_2/PA66 antimicrobial composite scaffolds," *Biomedical Materials*, vol. 5, no. 4, Article ID 044105, 2010.

Hindawi Publishing Corporation
Bioinorganic Chemistry and Applications
Volume 2012, Article ID 923914, 9 pages
doi:10.1155/2012/923914

Research Article

DNA-Platinum Thin Films for Use in Chemoradiation Therapy Studies

Mohammad Rezaee, Elahe Alizadeh, Darel Hunting, and Léon Sanche

Groupe en Sciences des Radiations, Département de Médecine Nucléaire et Radiobiologie, Faculté de Médecine et des Sciences de la Santé, Université de Sherbrooke, Sherbrooke, QC, Canada J1H5N4

Correspondence should be addressed to Mohammad Rezaee, mohammad.rezaee@usherbrooke.ca

Received 8 July 2011; Accepted 3 August 2011

Academic Editor: Goran N. Kaluderovic

Dry films of platinum chemotherapeutic drugs covalently bound to plasmid DNA (Pt-DNA) represent a useful experimental model to investigate direct effects of radiation on DNA in close proximity to platinum chemotherapeutic agents, a situation of considerable relevance to understand the mechanisms underlying concomitant chemoradiation therapy. In the present paper we determine the optimum conditions for preparation of Pt-DNA films for use in irradiation experiments. Incubation conditions for DNA platination reactions have a substantial effect on the structure of Pt-DNA in the films. The quantity of Pt bound to DNA as a function of incubation time and temperature is measured by inductively coupled plasma mass spectroscopy. Our experiments indicate that chemical instability and damage to DNA in Pt-DNA samples increase when DNA platination occurs at 37°C for 24 hours, the condition which has been extensively used for in vitro studies. Platination of DNA for the formation of Pt-DNA films is optimal at room temperature for reaction times less than 2 hours. By increasing the concentration of Pt compounds relative to DNA and thus accelerating the rate of their mutual binding, it is possible to prepare Pt-DNA samples containing known concentrations of Pt while reducing DNA degradation caused by more lengthy procedures.

1. Introduction

Clinical studies have shown that concomitant treatment with chemotherapeutic drugs and radiotherapy often leads to a higher rate of survival and local tumor control compared to nonsynchronous treatments [1, 2]. Platinum chemotherapeutic drugs are commonly used in concurrent chemoradiation therapy (CRT) for treatment of solid tumors [3]. Although it is clear that platinum drugs and radiation in CRT modalities increase tumor cell killing, improve locoregional control of tumors, and enhance patient survival [4, 5], the optimum schedule of the combination and the underlying mechanisms of their synergistic action have not been yet defined [6, 7]. Since DNA is the common target of both radiation and platinum chemotherapeutic agents, most studies have focused on the structural and functional alteration of DNA resulting from the combination [8, 9]. One possible mechanism responsible for the observed synergy is enhancement in immediate (secondary) species induced by primary radiation in the vicinity of the binding site of the platinum compounds (Pt compounds) to DNA [10, 11]. The most abundant of these secondary species are electrons with the most probable energy of 9-10 eV [12]. Studies on the interaction of secondary low energy electrons (LEEs) with DNA have elucidated some of the fundamental mechanisms leading to DNA damage [13]. However, owing to the short range (~10 nm) of LEE in biological matters, such studies must be performed on very thin DNA films of similar thickness. Pt-DNA thin films could provide an experimental approach to investigate the direct effects of the secondary electrons and other short-range particles (or secondary species) on DNA in the presence of Pt compounds. Such investigations could disclose mechanisms underlying the synergistic effect between the radiation and the drug, which may have implications for the optimization of protocols in CRT as well as in the design and development of new chemotherapeutic and radiosensitizing drugs [14].

Dry thin films of bacterial plasmid DNA in supercoiled conformation are widely used in low-energy irradiations with LEEs [15, 16], photons [17], and ions [18]. They provide a simple system to evaluate the direct interaction of short-range radiations with DNA, despite the complexity of the molecule. Although purified prokaryotic DNA differs from eukaryotic DNA in terms of supercoiling and the presence of N6-methyladenine [19, 20], supercoiled plasmid DNA offers the advantage of very high sensitivity for the detection of single- and double-strand breaks. One of the main concerns with plasmid DNA films is maintenance of the DNA integrity during film preparation [21]. When the irradiation target is supercoiled DNA, the proportion of the supercoiled configuration is often used as a measure of DNA integrity. The DNA molecule is very sensitive to conditions such as temperature, humidity, and pH, hence, the DNA films must be prepared under well-controlled conditions to minimize damage. The concentration of ions in the solution of DNA has also a considerable influence in maintaining the DNA during film preparation [21, 22]. Furthermore, the type of substrate on which DNA is deposited affects the integrity of the molecule. Among the various substrates tested including tantalum (Ta), gold and graphite, Ta induces the least damage to DNA [23].

Pt compounds such as cisplatin and carboplatin bind to the N7 atom of purine bases and produce the Pt-DNA adducts including mainly intrastrand cross-links, interstrand cross-links, and monofunctional binding to guanine [24]. The adducts distort the DNA conformation and reduce the structural stability of DNA [24, 25]. Moreover, DNA must tolerate the incubation conditions required to react with Pt compounds. In most in vitro studies, a DNA solution is mixed with a solution of the Pt compounds at 37°C for 24 or 48 hours [26–30]. These conditions affect the integrity of the DNA as a result of depurination and oxidation processes [31]. To maximize the amount of the Pt compounds bound to DNA while keeping the DNA intact, all parameters involved in the preparation of the films must be known and carefully controlled. In particular, experimental conditions for the reaction of Pt compounds with DNA must be determined as well as the effect of chemical binding of Pt compounds on the stability of DNA.

In the present study, we investigate the parameters of the Pt compounds and platination reactions on DNA integrity in the preparation of cisplatin/DNA and carboplatin/DNA films. Optimum experimental conditions are determined to retain a high proportion of the supercoiled form of plasmid DNA in Pt-DNA films.

2. Experimental Section

2.1. Preparation of Plasmid DNA. Plasmid DNA (pGEM-3Zf(-), 3197 base pairs, ca. 1968966 amu per plasmid) was extracted from Escherichia coli JM109 and purified with a HiSpeed plasmid Maxi kit (QIAGEN) [32]. The purified plasmid DNA consisted of 96% supercoiled, 2% cancatemeric, and 2% nicked circular forms. The concentration of DNA and the relative quantity of proteins in the plasmid DNA solution was then calculated by measuring the ratio of ultraviolet (UV) absorption of DNA and protein at 260 nm and 280 nm, respectively, with a Synergy HT-I spectrophotometer. The ratio was 1.98 which corresponds to a purity greater than 85% [33]. The TE buffer (Tris-EDTA: 10 mM–1 mM) was separated from DNA by gel filtration with a Sephadex G-50 medium [34]. Thus the final solution consisted of DNA and ddH_2O after the filtration. To evaluate the effect of Tris on the binding of Pt compounds to DNA, two different groups of the DNA solutions were prepared. In the first group, Tris buffer was added to the DNA solution at the ratio of the one tris molecule per nucleotide, and in the second group, the DNA solution was prepared with ddH_2O alone. The DNA concentration was the same in both groups. In each group, control samples were kept in the temperature of −20°C and quantified for the analysis of temperature effect on DNA.

2.2. Platination of Plasmid DNA. The Pt compounds, cisplatin [*cis*-diamminedichloroplatinum(II)] and carboplatin [*cis*-diammine(1,1-cyclobutanedicarboxylato)platinum(II)], were purchased from Sigma-Aldrich with a stated purity of 99.9% and ≥98%, respectively, and used without further purification. Their solutions were prepared in ddH_2O in different concentrations based on their molar solubility. Reactions of cisplatin and carboplatin with the DNA solutions were performed under diverse experimental conditions. These consisted of (1) two different incubation temperatures, that is, 37°C and 25°C, (2) incubation times varying from 40 minutes to 24 hours, and (3) molar ratios between Pt compounds and DNA varying from ratios 2 : 1 up to 200 : 1. DNA platination reactions were performed in the dark to inhibit photoaquation processes as aqueous solutions of cisplatin and carboplatin are degraded via illumination, especially at wavelengths below 500 nm [35, 36]. To terminate the reactions after a given incubation time, the solutions were passed through a gel filtration medium packed into a column. By the filtration, the unbound Pt compounds, tris molecules, and complexes of tris with Pt compounds were separated from the Pt-DNA solutions. The solutions passed through the homemade column packed with Sephadex-G50 gel on a glass bead bed. Sephadex G-50 is a suitable medium for separation of the molecules having a molecular weight larger than 3×10^4 g mol^{-1} from molecules with a molecular weight smaller than 1500 g mol^{-1}. Such filtration is expected to produce clean solutions of Pt-DNA in ddH_2O because the molecular weights of most undesired compounds and complexes found in the solutions during platination have the molecular weight smaller than 1500 g mol^{-1}.

2.3. Analysis of Platinum-DNA Binding. The concentration of platinum in the solutions was measured by Elan DRC II inductively coupled plasma mass spectroscopy (ICPMS, from Perkin Elmer) which has been used as a suitable method for measurement of platinum in many biomedical applications [37, 38]. Additionally, three control samples consisting of the Pt compounds dissolved in ddH_2O at known concentrations were also prepared to calibrate the ICPMS

measurements of Pt-DNA samples. The DNA concentration was measured by spectrophotometry. It was determined from the optical density of DNA in solution measured by UV absorption at a wavelength of 260 nm. The concentration of DNA was calculated from the reference optical density.

2.4. Preparation of Substrate, DNA, and Pt-DNA Films. The DNA and Pt-DNA samples were deposited on a Ta substrate. As shown in previous studies, the stability of supercoiled plasmid DNA on Ta substrate is acceptable for vacuum experiments on LEE-induced damage [23, 39]. The Ta substrates in the current work consist of a thin film of Ta of thickness 450 ± 50 nm evaporated onto a 0.4 mm thick silicon wafer. The surface of Ta was cleaned in pure ethanol and ddH_2O and dried with a flow of dry nitrogen. Before deposition of DNA and Pt-DNA samples onto the substrate, the TE buffer was added to the DNA and Pt-DNA solutions in the ratio of 3 : 1 (three organic ions per nucleotide). It has been shown that this ratio protects the supercoiled form of DNA during the process of DNA film preparation [22]. The volumes of 7 μL of the latter solutions of DNA and Pt-DNA consisting of 250 ng of each complex (DNA and TE molecules as well as Pt-DNA and TE molecules) were deposited onto the cleaned Ta surface. These quantities were calculated to allow formation of a five-monolayer film (about 10 nm thickness) on the Ta substrate. Such a thickness has been widely used in DNA-LEE experiments because it is smaller than the effective range of these electrons (12–14 nm) for damaging DNA [40]. After freezing at −65°C for 10 minutes in a glove box, the samples were lyophilized (freeze-dried) under a pressure of 7 mTorr by a hydrocarbon-free turbomolecular pump for 2 hours.

2.5. Quantification of the DNA and Pt-DNA Films. The DNA and Pt-DNA films were recovered from the Ta substrates with 10 μL of TE buffer. Comparison of the amount of recovered DNA with the original DNA solution used for deposition showed that approximately 98% of DNA was recovered by the TE buffer. Quantification of the different structural forms (e.g., supercoiled, nicked circular, linear, etc.) in the DNA and Pt-DNA samples was performed by agarose gel electrophoresis. The DNA samples and the agarose gels were stained with SYBR Green I in the concentration of 100x and 10000x, respectively. The samples were run on 1% agarose gel in 1x TAE buffer at 100 volts for 7 minutes following by 75 volts for 68 minutes (5 V cm^{-1}). The gels were then scanned by Typhoon-Trio laser scanner (from GE Healthcare) adjusted for the blue fluorescent mode at an excitation wavelength of 488 nm and filter type 520 nm-bandpass (520 BP 40) in the normal sensitivity mode. Various forms of the DNA such as supercoiled, nicked circular, etc. were analyzed by ImageQuant 5.0 (Molecular Dynamics) software. To accurately quantify, the binding efficiencies of SYBR Green I for the same amount (75 ng) of supercoiled and linear DNA were measured, and then the correction factor was determined. This factor arises from the weaker binding of SYBR Green I to supercoiled DNA than to the nicked circular and linear forms. A correction factor of 1.2 was obtained and applied to the quantification of plasmid DNA.

2.6. Statistical Analysis. OriginPro 8.1 SR1 (OriginLab Corporation) software was used for statistical and mathematical analysis. Paired t-test was the statistical test in which a probability of 0.05 (5%) has been considered significant.

3. Results and Discussion

3.1. Effects of Incubation Temperature on DNA and Pt-DNA Samples. Figure 1 (panels a and b) shows a comparison of the percentage of supercoiled and nicked circular forms of the DNA in the samples that had been incubated for 24 hours at three different temperatures: −20°C, 25°C, and 37°C. For each incubation temperature, DNA analysis was performed for two types of samples: (i) "DNA solutions", that is, samples obtained directly from the incubated solutions, and (ii) "DNA films", that is, samples that had, after incubation, been deposited and recovered from a Ta substrate. TE buffer was added to the samples at a concentration corresponding to three organic ions per nucleotide. Increasing the incubation temperature resulted in a reduction of the supercoiled form of DNA in both the solution and the film samples. The decrease is relatively small for the DNA solution samples; the samples incubated at 25°C and 37°C show a decrease of 3.8% and 9.5%, respectively, relative to that seen in the sample maintained at −20°C. At each temperature, the DNA samples recovered from Ta show a greater loss of supercoiled DNA than do the samples analyzed directly from solution. A fraction of the supercoiled loss in the film samples is related to the damages which were induced during the incubation in solution. Consequently, for DNA recovered from Ta, a decrease in the supercoiled form with increasing temperature is also observed, and the decrease is very large for the samples incubated at 37°C. The decreases in the supercoiled form are not statistically significant among the DNA solution samples with different incubation temperatures (P value: 0.314, 0.106). However, the difference is statistically significant between the DNA film samples incubated at 37°C and the DNA films from samples incubated at 25°C and −20°C (P value: 0.012 and 0.009). Additionally, there is no significant difference between the DNA films incubated at 25°C and −20°C (P value: 0.136).

As expected, there are enhancements in the formation of the nicked circular form with increasing incubation temperature. The increase is small except for the DNA film samples which were incubated at 37°C. In these samples the nicked circular form increases by factors of 3.7 and 3.4 compared to those kept at −20°C and 25°C, respectively. These differences are statistically significant (P value: 0.02 and 0.011). The high proportion of the nicked circular form in the DNA recovered from films introduces considerable inaccuracy in the evaluation of radiation-induced DNA damage.

In vitro studies have shown that heat can induce various types of DNA damage such as depurination and guanine

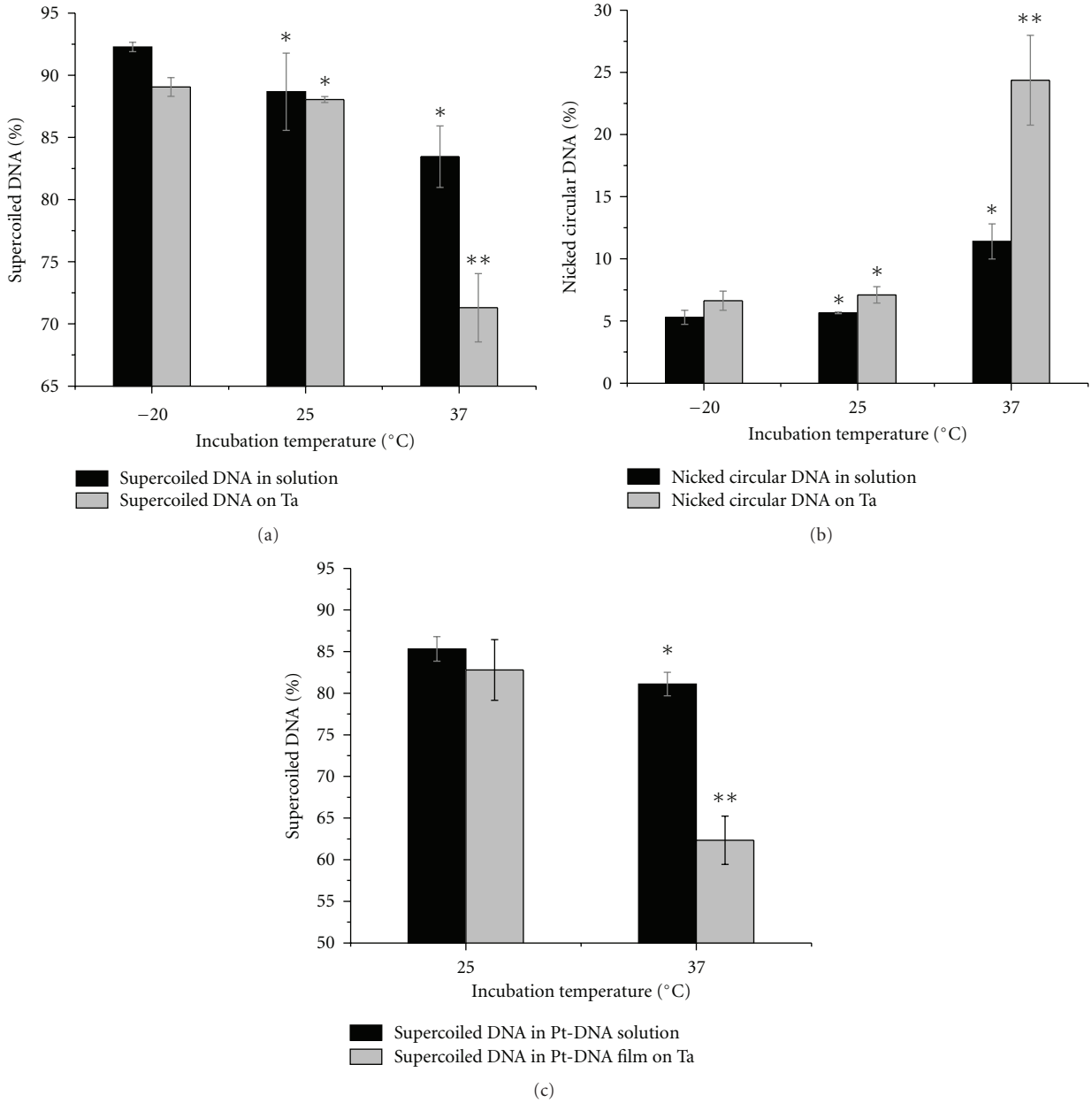

Figure 1: Comparison of the percentages of DNA supercoiled (a), DNA nicked circular (b), and Pt-DNA supercoiled (c) forms in the solution and film samples after incubation at −20°C, 25°C, and 37°C for 24 hours. Data in (a)–(c) are means from three independent experiments; three samples at each temperature are analyzed in each experiment; error bars show standard deviations. *indicates P value >0.05, **indicates P value <0.05.

oxidation mediated by reactive oxygen species (ROS) [31, 41]. Reaction rate constants for formation of 8-oxoguanine and guanine depurination at 37°C are $4.7 \times 10^{-10}\,s^{-1}$ and $1.3 \times 10^{-9}\,s^{-1}$ in DNA solutions, respectively [41]. In our experiment, each plasmid sample contained 0.065 pmole of DNA bases in a volume of 7 μL. After a 24-hour incubation of the plasmid DNA at 37°C, we can estimate that approximately 7% and 18% of the plasmid contain 8-oxoguanine molecules or have undergone guanine depurination, respectively. Such DNA molecules are more susceptible to strand breakage than the original DNA. Furthermore, evacuation and lyophilisation during film preparation induce physical stress and can damage DNA [21]. Therefore, the DNA molecules, which have been kept at 37°C for 24 hours or more, do not have sufficient structural stability to tolerate the process of film preparation. Our results suggest that the samples incubated at 37°C are more sensitive and vulnerable to the film preparation and recovery processes than DNA samples incubated at 25°C and −20°C.

Figure 1(c) shows the comparison of the percentage concentration of supercoiled forms in samples of cisplatin-DNA complexes incubated at 25°C and 37°C for 24 hours.

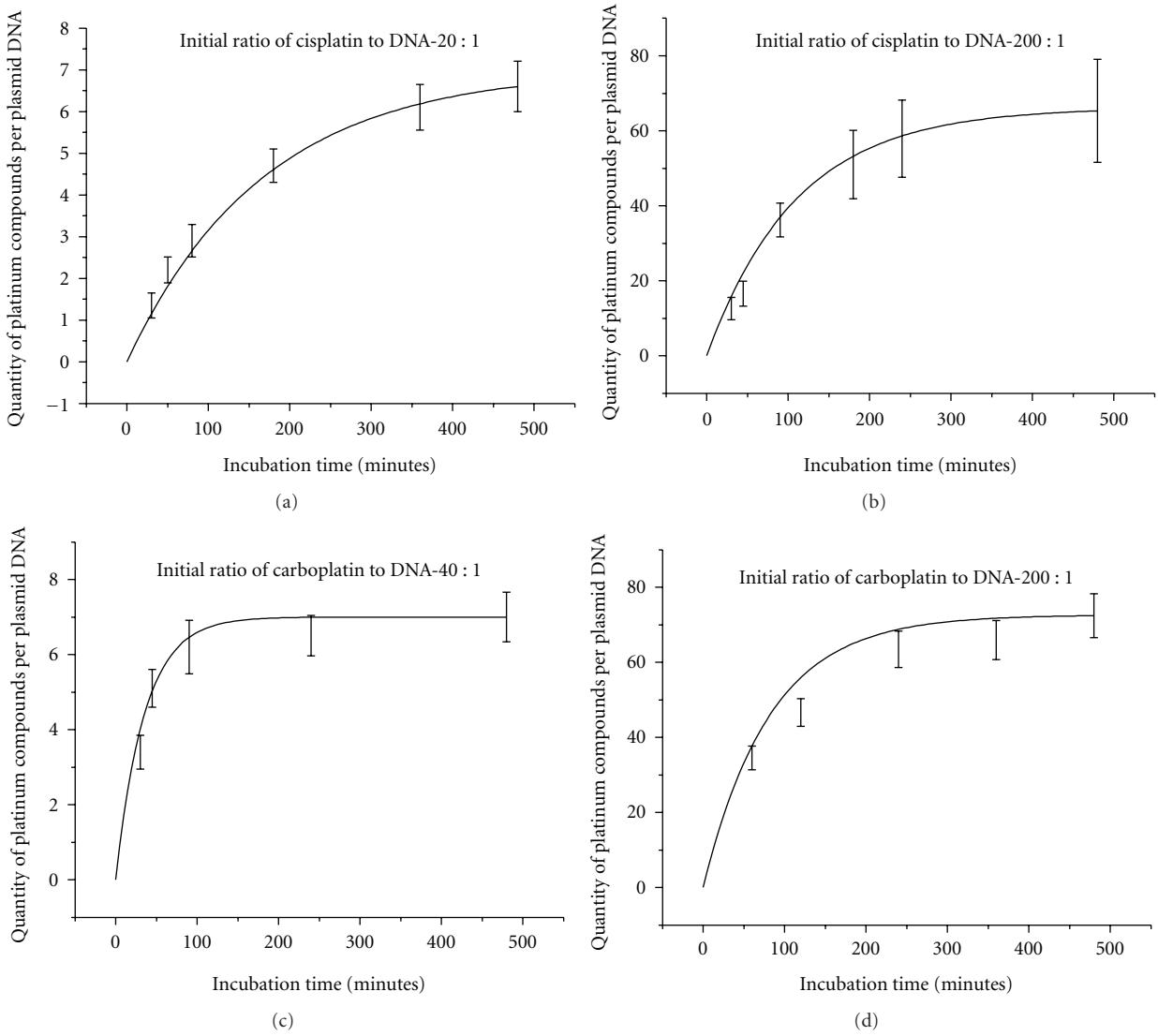

Figure 2: Kinetics of binding of Pt compounds to plasmid DNA. The Pt compounds are: (a) cisplatin with the initial ratios in the solution of 20 : 1, (b) 200 : 1, and (c) carboplatin with the initial ratios of 40 : 1 and (d) 200 : 1. The curves show the quantity of bound Pt compounds per DNA molecule at different incubation times at 25°C. Data in (a)–(d) are means from three measurements; error bars show standard deviations. The continuous black lines are exponential fits to the data.

Again, the analyses were performed for two groups of samples: (i) Pt-DNA solutions and (ii) Pt-DNA films on a Ta substrate. In the solution and film samples, the proportion of the supercoiled form of Pt-DNA is less than those for DNA alone. The molar ratio of cisplatin to DNA in the solutions was 2 : 1. TE buffer was added to the samples in the concentration of three organic ions per nucleotide. Predictably, in both samples the supercoiled form of DNA decreased when the incubation temperature increased. The decrease is small (4.2%) in the samples of Pt-DNA solution. In contrast, there is a large decrease in the supercoiled form of the Pt-DNA film samples (20.5%). Statistical analysis also showed that the decrease is significantly different for the Pt-DNA films with different incubation temperatures (P value: 0.0049). According to our results, the incubation temperature during preparation of the Pt-DNA solution is a substantial factor in determining the composition of Pt-DNA films on Ta substrate for use in irradiation experiments. Moreover, the results suggest that a film composed of cisplatin-DNA complexes with a high proportion of intact DNA molecules (supercoiled form) on a Ta substrate can be obtained when DNA platination occurs at 25°C.

3.2. Kinetics of Binding Pt Compounds to DNA. Following platination at 25°C, DNA has much less damage during the process of deposition and recovery from the Ta substrate. However, the DNA platination reaction proceeds with a slower rate. Increasing the concentration of the Pt compounds can compensate for this lower rate. Figure 2 shows

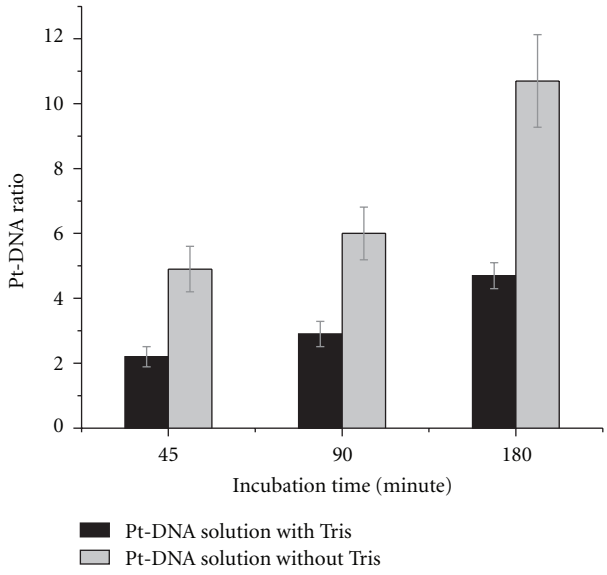

Figure 3: Impact of tris on the reaction of DNA platination. Pt-DNA ratios in the cisplatin-DNA solutions incubated during 45, 90, and 180 minutes at 25°C are compared in the presence and absence of tris. Data are means from three measurements; error bars show standard deviations.

the ratios of bound Pt-compound to DNA for different incubation times at 25°C when the initial concentration ratios of Pt compounds to DNA in solution are 200 : 1, 40 : 1, and 20 : 1. The solution consists of plasmid DNA, cisplatin or carboplatin, and tris with the ratio of 1 : 1 nucleotide. This amount of tris was considered as the minimum amount of buffer which can preserve the stability of DNA during the preparation process. It is clearly seen that the binding kinetics of cisplatin and carboplatin to DNA are similar and exhibit exponential behavior. These curves generally reach saturation prior to 8 hours and show a linear behaviour prior to 2 hours. For the initial concentration ratio of 200 cisplatin molecules per DNA, it is possible to have Pt-DNA samples with the ratios of bound cisplatin to DNA from 16 : 1 to 37 : 1 in 40-minute to 120-minute incubation times, respectively. For the same incubation times, the ratios are 2 : 1 and 3 : 1 when the initial ratio of cisplatin to DNA decreases an order of magnitude (20 : 1). The results demonstrate that various ratios of bound cisplatin or carboplatin to DNA can be obtained in the incubation times of less than 2 hours by increasing the initial concentration of the Pt compounds. Since the kinetics curves obey a linear fit for these incubation times, it is possible to simply extrapolate a variety of Pt-DNA ratios from this part of the curves.

Since Pt compounds can react with most buffers [42], their concentration is also a relevant parameter in the DNA platination process (i.e., buffers compete with DNA for binding Pt compounds). Tris is widely used as a buffer, especially for solutions of nucleic acids. It also reacts with Pt compounds to produce *cis*-$[Pt(NH_3)_2(N\text{-}Tris)(OH)]^+$ and *cis*-$[Pt(NH_3)_2(N,O\text{-}TrisH_{-1})]^+$ [43]. The bar graphs in Figure 3 show a comparison of bound Pt compounds to DNA ratios for three different incubation times at 25°C for two different solutions: (i) a mixture of DNA, cisplatin, and ddH_2O, and (ii) a mixture of DNA, cisplatin, ddH_2O, and tris with the concentration ratio of 1 : 1 nucleotide. The initial concentration ratio of cisplatin to the DNA was 20 : 1 in the solutions. The results demonstrate that the ratio of bound cisplatin to the DNA is more than double when the platination reaction occurs in a ddH_2O solution without tris molecules.

3.3. Effects of Incubation Time on DNA and Pt-DNA Films. The bar graphs in Figure 4 show a comparison of the percentage of supercoiled DNA and Pt-DNA samples that were incubated at 25°C for 2, 4, and 8 hours. The analyses were performed for samples that had been recovered (i) from solution, immediately after incubation (Figure 4(a)), and (ii) from films deposited on Ta (Figure 4(b)). The Pt-DNA samples were prepared with either cisplatin or carboplatin. The initial concentration ratio of the Pt compounds to DNA was 200 : 1 and that of the TE buffer was three organic ions per nucleotide. As seen from Figure 4, more than 90 percent of the DNA, in samples incubated for 2 hours, is in the supercoiled form. The proportion of supercoiled form decreases when the samples are incubated for 4 hours or more. The decrease is statistically significant in all samples except for the pure DNA solution sample. As might be expected, the decrease is greater in Pt-DNA films than in DNA samples. Thus, it is possible to prepare Pt-DNA films with a high proportion of supercoiled DNA at various ratios of bound Pt to DNA, by mixing DNA with high concentrations of Pt-compound solution and restricting the length of the incubation to less than 2 hours, as long as the incubation temperature does not exceed 25°C.

3.4. Effects of Bound Pt to DNA on Pt-DNA Samples Analysis. The distortion of the DNA structure resulting from the formation of Pt-DNA cross-links must be considered in quantification methods such as electrophoresis. Figure 5(a) shows the migration of different forms of cisplatin-DNA in the electrophoresis gel. The mobility of the nicked circular, cancatemeric, and supercoiled bands is changed with increasing numbers of bound Pt molecules per nucleotide (R_b). The change is due to distortion of the different forms of DNA by cisplatin since Pt-DNA crosslinks are known to cause conformational changes in DNA including shortening (bending) and unwinding [44, 45]. The distortion becomes greater as a function of the quantity of bound Pt molecules. Figure 5 shows the dependence of the mobility of the supercoiled, nicked circular, and cancatemeric forms of cisplatin-DNA samples as a function of the ratio R_b in a 1% agarose gel. The mobility of each form of Pt-DNA is normalized to the same form of an unmodified DNA sample (Figure 5(b)). As seen from Figure 5(b), the migration of the nicked circular and supercoiled configurations generally increases with rising R_b. However, the mobility of the nicked circular form increases with a faster rate than that of the supercoiled

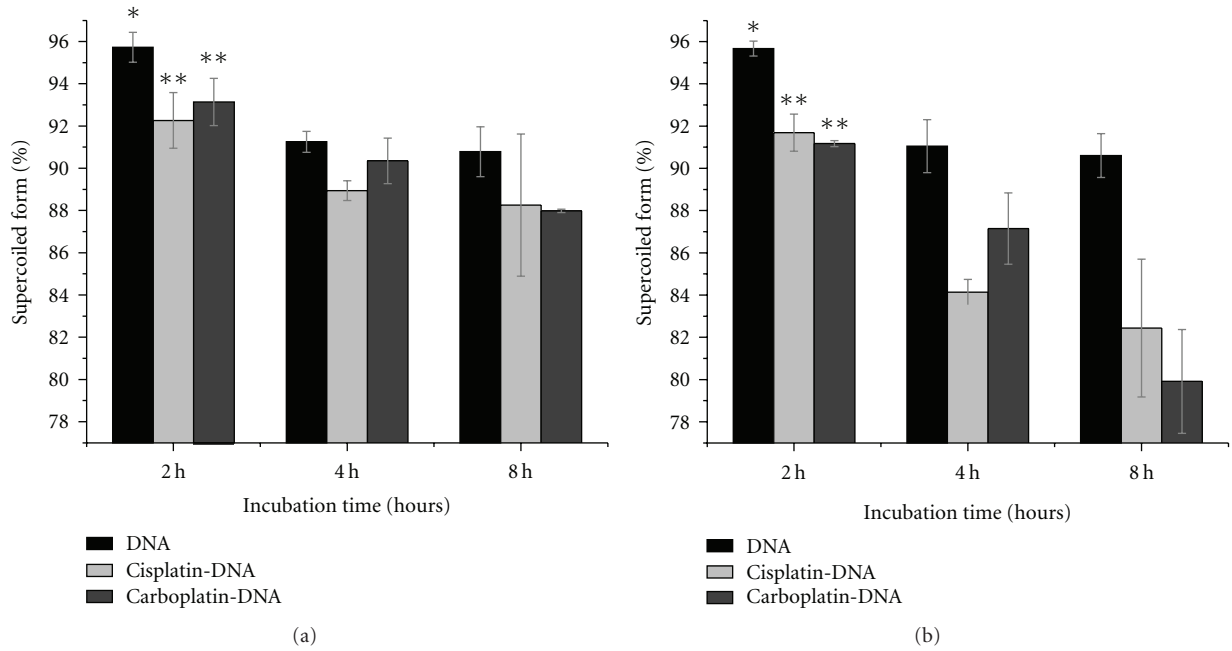

Figure 4: Comparison of the percentages of supercoiled forms in the samples of DNA, cisplatin-DNA, and carboplatin-DNA (a) in solution, and (b) on Ta substrate, after incubation for 2, 4, and 8 hours at 25°C. Data are means from three measurements; error bars show standard deviations.* indicates P value >0.05, ** indicates P value <0.05.

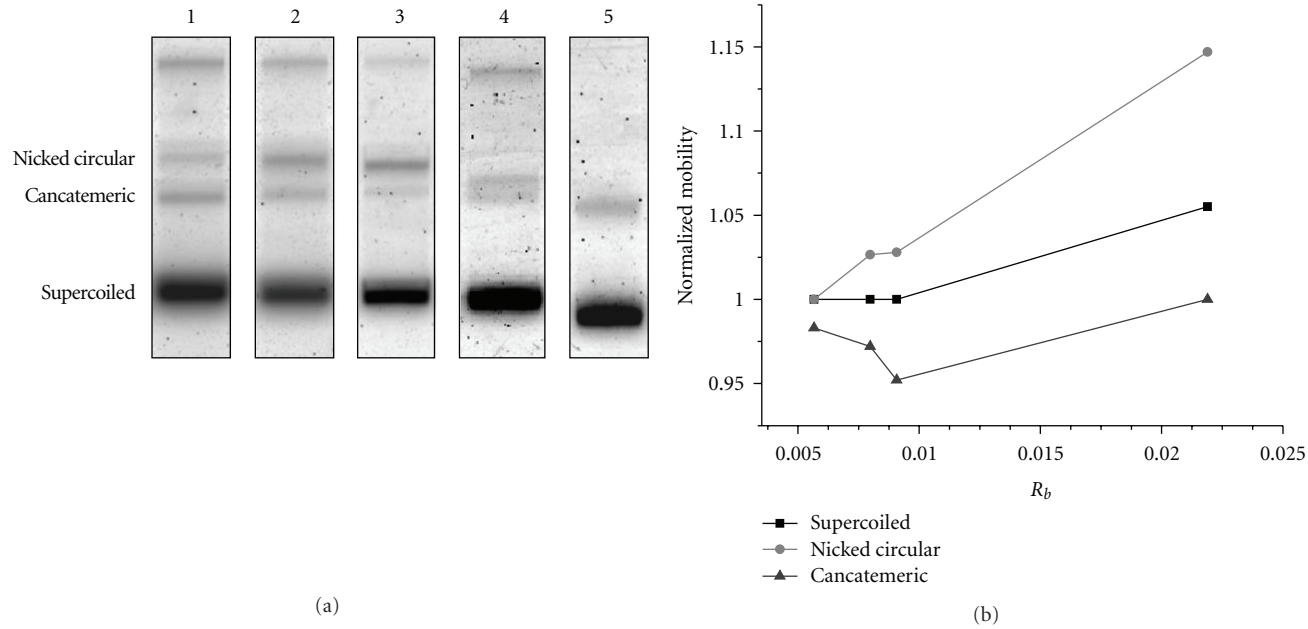

Figure 5: Mobility of cisplatin-DNA molecules in agarose gel. (a) Migration of the different configurations of cisplatin-DNA molecules separated by electrophoresis. Lane 1 is for a DNA sample and lanes 2–5 are for cisplatin-DNA samples with the number of bound cisplatin molecules per nucleotide, R_b, of 0.0057, 0.008, 0.0091, and 0.0219, respectively. (b) Normalized mobility of the nicked circular, supercoiled, and cancatemeric forms of Pt-DNA samples at different R_b in gel electrophoresis.

form. Mobility of the cancatemeric configuration decreases with rising in R_b up to 0.009 and then increases for higher R_b.

Since the number of Pt molecules per plasmid probably represents a Poisson distribution for each Pt-DNA ratio, this would be expected to reduce the resolution of the agarose gels by increasing the dispersion within each band (i.e., the band width). The linear plasmid band lies between the nicked circular and cancatemeric bands; thus an increase in band width could hinder precise quantification of the linear

band which usually is weaker than the others. Furthermore, the nicked circular and cancatemeric bands merge owing to increased band width and form one band at $R_b = 0.022$. Our results show that the mobility changes are substantial for R_b greater than 0.005.

4. Conclusion

Thin films of platinum-DNA adducts can be considered as useful models in irradiation experiments to study the molecular mechanisms of radiosensitization which underlie concomitant chemoradiation therapy. We have investigated the optimum experimental conditions to prepare dry thin films of Pt compounds bound to plasmid DNA on a Ta substrate. Incubation conditions in DNA platination reactions have substantial effects on the stability of Pt-DNA, particularly in the thin film samples preparation. In most in vitro experiments, reaction of Pt compounds with DNA solutions has been performed at 37°C for incubation times varying from 24 to 48 hours. However, our results show that these conditions can induce damage to the DNA and highly sensitize them to manipulations required to form thin films and recover DNA from the Ta substrate. The concentration of intact DNA increases significantly in the film samples when the incubation temperature during reaction with the Pt is reduced to 25°C and the time of incubation is 2 hours. By increasing the concentration of the Pt compounds, it is possible to compensate for the reduced reaction rate at lower temperature. High levels of plasmid platination however affect the quantification of Pt-DNA samples in agarose gel electrophoresis, because Pt-DNA adducts distort the conformation of DNA molecules. Therefore, the optimum condition is obtained from an equilibrium between temperature, time, and Pt compounds concentration during the DNA platination reaction.

By recording the kinetics of binding Pt compounds to DNA, it is possible to extrapolate different Pt-DNA ratios from the kinetics curves. We have found that the proportion of supercoiled DNA is more than 90% in the Pt-DNA film when the DNA platination reaction is performed at 25°C for less than 2 hours in solutions containing the Pt compound with quantities of less than 3×10^{-2} Pt molecules per nucleotide and the minimum concentration of Tris buffer (one tris molecule per nucleotide). Under these conditions, agarose gel electrophoresis is an accurate method for quantification of DNA damage. We have also determined that the maximum number of bound Pt-compound per nucleotide is about 5×10^{-3} under our optimum conditions. This ratio is an order of magnitude higher than those found in biological studies and clinical applications [46]. These high ratios, however, are useful for in vitro mechanistic studies in which substantial quantities of product are required. Hence, we have found that by adjusting the initial concentration of Pt compounds in solution, Pt-DNA films having a known controlled ratio of platinum chemotherapeutic agents to DNA can be obtained while maintaining DNA integrity.

Acknowledgments

Financial support for this work was provided by the Canadian Institute of Health Research (CIHR) and the Marie Curie international incoming fellowship program. The authors wish to thank Dr. Andrew D. Bass, Mr. Pierre Cloutier, and Ms. Sonia Girouard for their helpful comments and suggestions.

References

[1] H. Choy, *Chemoradiation in Cancer Therapy*, Humana Press, Totowa, NJ, USA, 2003.

[2] V. T. Devita Jr., S. Hellman, and S. A. Resenberg, *Cancer: Principle and Practice of Oncology*, Lippincott Williams and Wilkins, New York, NY, USA, 2001.

[3] T. Y. Seiwert, J. K. Salama, and E. E. Vokes, "The concurrent chemoradiation paradigm—general principles," *Nature Clinical Practice Oncology*, vol. 4, no. 2, pp. 86–100, 2007.

[4] C. Schaake-Koning, W. Van den Bogaert, O. Dalesio et al., "Effects of concomitant cisplatin and radiotherapy on inoperable non-small- cell lung cancer," *The New England Journal of Medicine*, vol. 326, no. 8, pp. 524–530, 1992.

[5] G. S. Montana, G. M. Thomas, D. H. Moore et al., "Preoperative chemo-radiation for carcinoma of the vulva with N2/N3 nodes: a gynecologic oncology group study," *International Journal of Radiation Oncology Biology Physics*, vol. 48, no. 4, pp. 1007–1013, 2000.

[6] J. K. Salma, T. Y. Siewert, and E. E. Vokes, "Chemoradiotherapy for locally advanced head and neck cancer," *Journal of Clinical Oncology*, vol. 25, pp. 4118–4126, 2007.

[7] C. C. E. Koning, J. S. A. Belderbos, and A. L. J. Uitterhoeve, "From cisplatin-containing sequential radiochemotherapy towards concurrent treatment for patients with inoperable locoregional non-small cell lung cancer: still unanswered questions," *Chemotherapy Research and Practice*, vol. 2010, Article ID 506047, 5 pages, 2010.

[8] J. W. J. Bergs, N. A. P. Franken, R. Ten Cate, C. Van Bree, and J. Haveman, "Effects of cisplatin and γ-irradiation on cell survival, the induction of chromosomal aberrations and apoptosis in SW-1573 cells," *Mutation Research*, vol. 594, no. 1-2, pp. 148–154, 2006.

[9] G. P. Raaphorst, J. M. Leblanc, and L. F. Li, "A comparison of response to cisplatin, radiation and combined treatment for cells deficient in recombination repair pathways," *Anticancer Research*, vol. 25, no. 1, pp. 53–58, 2005.

[10] G. D. Wilson, S. M. Bentzen, and P. M. Harari, "Biologic basis for combining drugs with radiation," *Seminars in Radiation Oncology*, vol. 16, no. 1, pp. 2–9, 2006.

[11] L. Dewit, "Combined treatment of radiation and cisdiamminedichloroplatinum (II): a review of experimental and clinical data," *International Journal of Radiation Oncology Biology Physics*, vol. 13, no. 3, pp. 403–426, 1987.

[12] S. M. Pimblott and J. A. LaVerne, "Production of low-energy electrons by ionizing radiation," *Radiation Physics and Chemistry*, vol. 76, no. 8-9, pp. 1244–1247, 2007.

[13] L. Sanche, "Low-energy electron interaction with DNA: bond dissociation and formation of transient anions, radicals, and radical anions," in *Radiacal and Radical Ion Reactivity in Nucleic Acid Chemistry*, M. M. Greenberg, Ed., pp. 239–293, John Wiley & Sons, Hoboken, NJ, USA, 2009.

[14] L. Sanche, "Role of secondary low energy electrons in radiobiology and chemoradiation therapy of cancer," *Chemical Physics Letters*, vol. 474, no. 1–3, pp. 1–6, 2009.

[15] B. Boudaïffa, P. Cloutier, D. Hunting, M. A. Huels, and L. Sanche, "Resonant formation of DNA strand breaks by low-energy (3 to 20 eV) electrons," *Science*, vol. 287, no. 5458, pp. 1658–1660, 2000.

[16] É. Brun, P. Cloutier, C. Sicard-Roselli, M. Fromm, and L. Sanche, "Damage induced to DNA by low-energy (0-30 eV) electrons under vacuum and atmospheric conditions," *Journal of Physical Chemistry B*, vol. 113, no. 29, pp. 10008–10013, 2009.

[17] K. M. Prise, M. Folkard, B. D. Michael et al., "Critical energies for SSB and DSB induction in plasmid DNA by low-energy photons: action spectra for strand-break induction in plasmid DNA irradiated in vacuum," *International Journal of Radiation Biology*, vol. 76, no. 7, pp. 881–890, 2000.

[18] C. A. Hunniford, R. W. McCullough, R. J. H. Davies, and D. J. Timson, "DNA damage by low-energy ions," *Biochemical Society Transactions*, vol. 37, no. 4, pp. 893–896, 2009.

[19] G. N. Giaever, L. Snyder, and J. C. Wang, "DNA supercoiling in vivo," *Biophysical Chemistry*, vol. 29, no. 1-2, pp. 7–15, 1988.

[20] D. M. Heithoff, R. L. Sinsheimer, D. A. Low, and M. J. Mahan, "An essential role for DNA adenine methylation in bacterial virulence," *Science*, vol. 284, no. 5416, pp. 967–970, 1999.

[21] M. A. Smialek, R. Balog, N. C. Jones, D. Field, and N. J. Mason, "Preparation of DNA films for studies under vacuum conditions: the influence of cations in buffer solutions," *European Physical Journal D*, vol. 60, no. 1, pp. 31–36, 2010.

[22] A. Dumont, Y. Zheng, D. Hunting, and L. Sanche, "Protection by organic ions against DNA damage induced by low energy electrons," *Journal of Chemical Physics*, vol. 132, no. 4, Article ID 045102, 2010.

[23] L. Sanche, "Nanoscopic aspects of radiobiological damage: fragmentation induced by secondary low-energy electrons," *Mass Spectrometry Reviews*, vol. 21, no. 5, pp. 349–369, 2002.

[24] E. R. Jamieson and S. J. Lippard, "Structure, recognition, and processing of cisplatin-DNA adducts," *Chemical Reviews*, vol. 99, no. 9, pp. 2467–2498, 1999.

[25] S. J. Lippard, "Chemistry and molecular biology of platinum anticancer drugs," *Pure and Applied Chemistry*, vol. 59, no. 6, pp. 731–742, 1987.

[26] C. P. Saris, P. J. M. Van de Vaart, R. C. Rietbroek, and F. A. Blommaert, "In vitro formation of DNA adducts by cisplatin, lobaplatin and oxaliplatin in calf thymus DNA in solution and in cultured human cells," *Carcinogenesis*, vol. 17, no. 12, pp. 2763–2769, 1996.

[27] J. Malina, O. Vrana, and V. Brabec, "Mechanistic studies of the modulation of cleavage activity of topoisomerase I by DNA adducts of mono- and bi-functional PtII complexes," *Nucleic Acids Research*, vol. 37, no. 16, Article ID gkp580, pp. 5432–5442, 2009.

[28] R. J. Knox, F. Friedlos, D. A. Lydall, and J. J. Roberts, "Mechanism of cytotoxicity of anticancer platinum drugs: evidence that cis-diamminedichloroplatinum(II) and cis-diammine-(1,1-cyclobutanedicarboxylato)platinum(II) differ only in the kinetics of their interaction with DNA," *Cancer Research*, vol. 46, no. 4, pp. 1972–1979, 1986.

[29] G. B. Onoa and V. Moreno, "Study of the modifications caused by cisplatin, transplatin, and Pd(II) and Pt(II) mepirizole derivatives on pBR322 DNA by atomic force microscopy," *International Journal of Pharmaceutics*, vol. 245, no. 1-2, pp. 55–65, 2002.

[30] G. Natarajan, R. Malathi, and E. Holler, "Increased DNA-binding activity of cis-1,1-cyclobutanedicarboxylatodiammineplatinum(II) (carboplatin) in the presence of nucleophiles and human breast cancer MCF-7 cell cytoplasmic extracts: activation theory revisited," *Biochemical Pharmacology*, vol. 58, no. 10, pp. 1625–1629, 1999.

[31] A. V. Chernikov, S. V. Gudkov, I. N. Shtarkman, and V. I. Bruskov, "Oxygen effect in heat-induced DNA damage," *Biophysics*, vol. 52, no. 2, pp. 185–190, 2007.

[32] HiSpeed, *Plasmid Purification Handbook*, QIAGEN, 2005.

[33] J. A. Glasel, "Validity of nucleic acid purities monitored by 260 nm/280 nm absorbance ratios," *BioTechniques*, vol. 18, no. 1, pp. 62–63, 1995.

[34] *Gel Filtration- Principles and Methods Handbook*, GE Healthcare, 2007.

[35] M. Macka, J. Borak, L. Semenkova, and F. Kiss, "Decomposition of cisplatin in aqueous solutions containing chlorides by ultrasonic energy and light," *Journal of Pharmaceutical Sciences*, vol. 83, no. 6, pp. 815–818, 1994.

[36] M. Pujol, J. Part, M. Trillas, and X. Domènech, "Stability of aqueous carboplatin solutions under illumination," *Monatshefte für Chemie Chemical Monthly*, vol. 124, no. 11-12, pp. 1077–1081, 1993.

[37] E. E. M. Brouwers, M. Tibben, H. Rosing, J. H. M. Schellen, and J. H. Beijnen, "The application of inductively coupled plasma mass spectrometry in clinical pharmacological oncology research," *Mass Spectrometry Reviews*, vol. 27, no. 2, pp. 67–100, 2008.

[38] J. Huang, X. Hu, J. Zhang, K. Li, Y. Yan, and X. Xu, "The application of inductively coupled plasma mass spectrometry in pharmaceutical and biomedical analysis," *Journal of Pharmaceutical and Biomedical Analysis*, vol. 40, no. 2, pp. 227–234, 2006.

[39] M. A. Huels, B. Boudaïffa, P. Cloutier, D. Hunting, and L. Sanche, "Single, double, and multiple double strand breaks induced in DNA by 3-100 eV electrons," *Journal of the American Chemical Society*, vol. 125, no. 15, pp. 4467–4477, 2003.

[40] B. Boudaïffa, P. Cloutier, D. Hunting, M. A. Huels, and L. Sanche, "Cross sections for low-energy (10-50 eV) electron damage to DNA," *Radiation Research*, vol. 157, no. 3, pp. 227–234, 2002.

[41] V. I. Bruskov, L. V. Malakhova, Z. K. Masalimov, and A. V. Chernikov, "Heat-induced formation of reactive oxygen species and 8-oxoguanine, a biomarker of damage to DNA," *Nucleic Acids Research*, vol. 30, no. 6, pp. 1354–1363, 2002.

[42] S. J. Berners-Price and T. G. Appleton, "The chemistry of cisplatin in aqueous solution," in *Platinum-Based Drugs in Cancer Therapy*, L. R. Kelland and N. Farell, Eds., pp. 3–35, Humana Press, Totowa, NJ, USA, 2000.

[43] P. D. Prenxler and W. D. McFadyen, "Reactions of cisplatin and the cis-diamminediaqua platinum(II) cation with tris and hepes," *Journal of Inorganic Biochemistry*, vol. 68, no. 4, pp. 279–282, 1997.

[44] S. Kobayashi, M. Furukawa, C. Dohi, H. Hamashima, T. Arai, and A. Tanaka, "Topology effect for DNA structure of cisplatin: topological transformation of cisplatin-closed circular DNA adducts by DNA topoisomerase," *Chemical and Pharmaceutical Bulletin*, vol. 47, no. 6, pp. 783–790, 1999.

[45] G. B. Onoa, G. Cervantes, V. Moreno, and M. J. Prieto, "Study of the interaction of DNA with cisplatin and other Pd(II) and Pt(II) complexes by atomic force microscopy," *Nucleic Acids Research*, vol. 26, no. 6, pp. 1473–1480, 1998.

[46] T. Boulikas, G. P. Stathopoulos, N. Volakakis, and M. Vougiouka, "Systemic lipoplatin infusion results in preferential tumor uptake in human studies," *Anticancer Research*, vol. 25, no. 4, pp. 3031–3040, 2005.

Hindawi Publishing Corporation
Bioinorganic Chemistry and Applications
Volume 2012, Article ID 609796, 7 pages
doi:10.1155/2012/609796

Research Article

Synthesis, Crystal Structure, and DNA-Binding Studies of a Nickel(II) Complex with the Bis(2-benzimidazolymethyl)amine Ligand

Huilu Wu, Tao Sun, Ke Li, Bin Liu, Fan Kou, Fei Jia, Jingkun Yuan, and Ying Bai

School of Chemical and Biological Engineering, Lanzhou Jiaotong University, Lanzhou 730070, China

Correspondence should be addressed to Huilu Wu, wuhuilu@163.com

Received 20 May 2011; Revised 7 June 2011; Accepted 8 June 2011

Academic Editor: Santiago Gómez-Ruiz

A V-shaped ligand Bis(2-benzimidazolymethyl)amine (bba) and its nickel(II) picrate (pic) complex, with composition $[Ni(bba)_2](pic)_2 \cdot 3MeOH$, have been synthesized and characterized on the basis of elemental analyses, molar conductivities, IR spectra, and UV/vis measurements. In the complex, the Ni(II) ion is six-coordinated with a N_2O_4 ligand set, resulting in a distorted octahedron coordination geometry. In addition, the DNA-binding properties of the Ni(II) complex have been investigated by electronic absorption, fluorescence, and viscosity measurements. The experimental results suggest that the nickel(II) complex binds to DNA by partial intercalation binding mode.

1. Introduction

Binding studies of small molecules to DNA are very important in the development of DNA molecular probes and new therapeutic reagents [1]. Transition metal complexes have attracted considerable attention as catalytic systems for use in the oxidation of organic compounds [2], probes in electron-transfer reactions involving metalloproteins [3], and intercalators with DNA [4]. Numerous biological experiments have demonstrated that DNA is the primary intracellular target of anticancer drugs; interaction between small molecules and DNA can cause damage in cancer cells, blocking the division and resulting in cell death [5–7].

Since the benzimidazole unit is the key-building block for a variety of compounds which have crucial roles in the functions of biologically important molecules, there is a constant and growing interest over the past few years for the synthesis and biological studies of benzimidazole derivatives [8–10]. Since the characterization of urease as a nickel enzyme in 1975, the knowledge of the role of nickel in bioinorganic chemistry has been rapidly expanding [11]. The interaction of Ni(II) complexes with DNA appears to be mainly dependent on the structure of the ligand exhibiting intercalative behavior [12–14].

In this context, we synthesized and characterized a novel Ni(II) complex. Moreover, we describe the interaction of the novel Ni(II) complex with DNA using electronic absorption and fluorescence spectroscopy and viscosity measurements.

2. Experimental

2.1. Materials and Methods. Calf thymus DNA (CT-DNA) and Ethidium bromide (EB) were purchased from Sigma Chemicals Co. (USA). All chemicals used were of analytical grade. All the experiments involving interaction of the ligand and the complexes with CT-DNA were carried out in doubly distilled water buffer containing 5 mM Tris and 50 mM NaCl and adjusted to pH 7.2 with hydrochloric acid. A solution of CT-DNA gave a ratio of UV absorbance at 260 and 280 nm of about 1.8–1.9, indicating that the CT-DNA was sufficiently free of protein [15]. The CT-DNA concentration per nucleotide was determined spectrophotometrically by employing an extinction coefficient of $6600\,M^{-1}\,cm^{-1}$ at 260 nm [16].

Elemental analyses were performed on Carlo Erba 1106 elemental analyzer. The IR spectra were recorded in the 4000–400 cm^{-1} region with a Nicolet FT-VERTEX

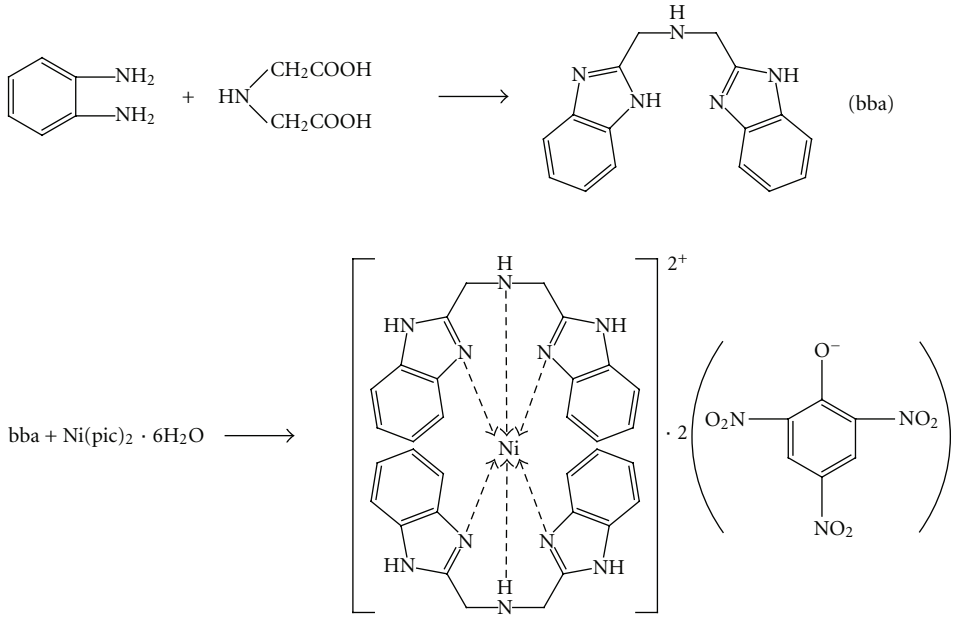

Scheme 1: The synthesis of ligand bba and its Ni(II) complex.

70 spectrometer using KBr pellets. Electronic spectra were taken on a Lab-Tech UV Bluestar spectrophotometer. The fluorescence spectra were recorded on a 970-CRT spectrofluorophotometer. ^{1}HNMR spectra were obtained with a Mercury plus 400 MHz NMR spectrometer with TMS as internal standard and DMSO-d_6 as solvent. Electrolytic conductance measurements were made with a DDS-11A type conductivity bridge using a 10^{-3} mol·L^{-1} solution in DMF at room temperature.

2.2. Electronic Absorption Spectra. Absorption titration experiment was performed with fixed concentrations of the complexes while gradually increasing concentration of CT-DNA. While measuring the absorption spectra, a proper amount of CT-DNA was added to both compound solution and the reference solution to eliminate the absorbance of CT-DNA itself. From the absorption titration data, the binding constant (K_b) was determined using [17]

$$\frac{[\text{DNA}]}{\varepsilon_a - \varepsilon_f} = \frac{[\text{DNA}]}{\varepsilon_b - \varepsilon_f} + \frac{1}{K_b\left(\varepsilon_b - \varepsilon_f\right)}, \tag{1}$$

where [DNA] is the concentration of DNA in base pairs, the apparent absorption coefficient, ε_a, ε_f, and ε_b correspond to $A_{\text{obsd}}/[M]$, the extinction coefficient of the free compounds and the extinction coefficient of the compound when fully bound to DNA, respectively. In plots of $[\text{DNA}]/(\varepsilon_a - \varepsilon_f)$ versus [DNA], K_b is given by the ratio of slope to the intercept.

2.3. Fluorescence Spectra. EB emits intense fluoresence in the presence of CT-DNA due to its strong intercalation between the adjacent CT-DNA base pairs. It was previously reported that the enhanced fluorescence can be quenched by the addition of a second molecule [18]. The extent of fluorescence quenching of EB bound to CT-DNA can be used to determine the extent of binding between the second molecule and CT-DNA. The competitive binding experiments were carried out in the buffer by keeping [DNA]/[EB] = 1 and varying the concentrations of the compounds. The fluorescence spectra of EB were measured using an excitation wavelength of 520 nm and the emission range was set between 550 and 750 nm. The spectra were analyzed according to the classical Stern-Volmer equation [19],

$$\frac{I_0}{I} = 1 + K_{\text{sv}}[Q], \tag{2}$$

where I_0 and I are the fluorescence intensities at 599 nm in the absence and presence of the quencher, respectively, K_{sv} is the linear Stern-Volmer quenching constant, $[Q]$ is the concentration of the quencher.

2.4. Viscosity Measurements. Viscosity experiments were conducted on an Ubbelohde viscometer, immersed in a thermostated water-bath maintained at 25.0 ± 0.1°C. DNA samples approximately 200 bp in average length were prepared by sonicating in order to minimize complexities arising from DNA flexibility [20]. Titrations were performed for the compounds (3 mM), and each compound was introduced into the CT-DNA solution (50 μM) present in the viscometer. Data were presented as $(\eta - \eta_0)^{1/3}$ versus the ratio of the concentration of the compound to CT-DNA, where η is the viscosity of CT-DNA in the presence of the complex, and η_0 is the viscosity of CT-DNA alone. Viscosity values were calculated from the observed flow time of CT-DNA containing solutions corrected from the flow time of buffer alone (t_0), $\eta = (t - t_0)/t_0$.

2.5. Synthesis. The synthetic route for the ligand bba and its Ni(II) complex are shown in Scheme 1.

2.5.1. Bis(2-benzimidazolymethyl)amine (bba). The ligand bba was synthesized according to the procedure reported by Berends and Stephan [21]. The infrared spectra and UV spectra of the bba were almost consistent with the literature. Elemental analysis: $C_{16}H_{15}N_5$ (Mr = 277.33 g·mol^{-1}) calcd: C 69.30; H 5.45; N 25.26%; found: C 69.35; H 5.47; N 25.16%. IR (KBr, pellet, cm^{-1}): 1270s (ν_{C-N}), 1620s ($\nu_{C=N}$), UV-vis (λ, nm): 277, 283, $\varepsilon_{277} = 5.99 \times 10^2$ L·mol^{-1}·cm^{-1}, $\varepsilon_{283} = 5.73 \times 10^2$ L·mol^{-1}·cm^{-1}. ^{1}HNMR (DMSO-d_6, 300 MHz) δ: 12.3 (1H, N-H); 7.144 (m, 4H); 7.5 (d, 4H); 4.0 (s, 4H). Λ_M (DMF, 297 K): 1.29 S·cm^2·mol^{-1}.

2.5.2. [Ni(bba)$_2$](pic)$_2$·3MeOH. The ligand bba (0.4 mmol) and Ni(II) picrate (0.2 mmol) were dissolved in methanol (15 mL). A blue-green crystalline product which formed rapidly was filtered off, washed with methanol and absolute Et_2O, and dried in vacuo. The dried precipitate was dissolved in DMF resulting in a blue-green solution that was allowed to evaporate at room temperature. Blue-green crystals suitable for X-ray diffraction studies were obtained after one week. $C_{47}H_{36}N_{16}Ni\ O_{17}$ (Mr = 1155.63 g·mol^{-1}) calcd: C 48.85; H 3.14; N 19.39%; found: C 48.79; H 3.16; N 19.53%. IR (KBr, pellet, cm^{-1}): 1272s (ν_{C-N}), 1434 ($\nu_{C=N-C=C}$), 1487s ($\nu_{C=N}$), UV-vis (λ, nm): 275, 280, 407, $\varepsilon_{275} = 6.55 \times 10^2$ L·mol^{-1}·cm^{-1}, $\varepsilon_{280} = 6.50 \times 10^2$ L·mol^{-1}·cm^{-1}, $\varepsilon_{407} = 7.99 \times 10^2$ L·mol^{-1}·cm^{-1}. Λ_M (DMF, 297 K): 128.5 S·cm^2·mol^{-1}.

2.6. Crystal Structure Determination. A suitable single crystal was mounted on a glass fiber and the intensity data were collected on a Bruker Smart CCD diffractometer with graphite-monochromated Mo Kα radiation (λ = 0.71073 Å) at 296 K. Data reduction and cell refinement were performed using the SMART and SAINT programs [22]. The structure was solved by direct methods and refined by full-matrix least squares against F^2 of data using SHELXTL software [23]. All H atoms were found in different electron maps and were subsequently refined in a riding-model approximation with C–H distances ranging from 0.95 to 0.99 Å. Basic crystal data, description of the diffraction experiment, and details of the structure refinement are given in Table 1.

Table 1: Crystallographic data and data collection parameters for the Ni(II) complex.

Complex	[Ni(bba)$_2$](pic)$_2$·3MeOH
Molecular formula	$C_{47}H_{36}N_{16}NiO_{17}$
Molecular weight	1155.63
Crystal system	Triclinic
Space group	P-1
a (Å)	10.4758 (9)
b (Å)	16.1097 (13)
c (Å)	17.2302 (14)
α (°)	107.5590 (10)
β (°)	107.5880 (10)
γ (°)	96.9150 (10)
V (Å^3)	2570.1 (4)
Z	2
ρ_{cald} (mg m^{-3})	1.493
Absorption coefficient (mm^{-1})	0.467
F (000)	1188
Crystal size (mm)	0.41 × 0.38 × 0.31
θ range for data collection (°)	2.04–25.00
$h/k/l$ (max, min)	−12, 12/−16, 19/−20, 20
Reflections collected	18579
Independent reflections	8974 [R(int) = 0.0203]
Data/restraints/parameters	8974/6/746
Goodness-of-fit on F^2	1.097
Final R_1, wR_2 indices [$I > 2\sigma(I)$]	0.0383, 0.1135
R_1, wR_2 indices (all data)	0.0466, 0.1194
Largest differences peak and hole (eÅ^{-3})	0.734 and −0.384

3. Results and Discussion

The ligand bba and its Ni(II) complex are very stable in the air. They are remarkably soluble in polar solvents such as DMF, DMSO, and MeCN; slightly soluble in ethanol, methanol, ethyl acetate, and chloroform. The molar conductivities in DMF solution indicate that bba (1.29 S·cm^2·mol^{-1}) is nonelectrolyte compound and its Ni(II) complex is 1 : 2 electrolyte compound [24].

3.1. Spectral Characterization. In the bba ligand, a strong band is found at ca. 1270 cm^{-1} together along with a broad band at 1436 cm^{-1}. By analogy with the assigned bands of imidazole, the former can be attributed to ν(C=N–C=C), while the latter can be attributed to ν(C=N) [25–27]. One of them shift to the higher frequency by around 41 cm^{-1} in the complex, which implies direct coordination of all three imine nitrogen atoms to metal ions. This is the preferred nitrogen atom for coordination as found for other metal complexes with benzimidazoles [28]. Information regarding the possible bonding modes of the picrate and benzimidazole rings may also be obtained from the IR spectra, such as 709, 744, 1272, 1363, 1434, 1487, and 1633 cm^{-1} [29]. This fact agrees with the result determined by X-ray diffraction.

DMF solutions of ligand bba and its complexes show, as expected, almost identical UV spectra. The UV bands of bba (275, 280 nm) are only marginally blue shifted (1-2 nm) in the complexes, which is clear evidence of C=N coordination to the metal ions center. The absorption bands are assigned to $\pi \rightarrow \pi^*$ (imidazole) transitions. The bands of picrate (407 nm) are assigned to $\pi \rightarrow \pi^*$ transitions.

3.2. Crystal Structure of [Ni(bba)$_2$](pic)$_2$·3MeOH. The molecular structure of the Ni(II) complex is shown in Figure 1, selected bond lengths and angles are summarized in Table 2. The Ni(II) atom is six-coordinate with a NiN_4O_2 environment. The bba ligand acts as a tridentate N-donor and O-donor. The coordination geometry of the Ni(II)

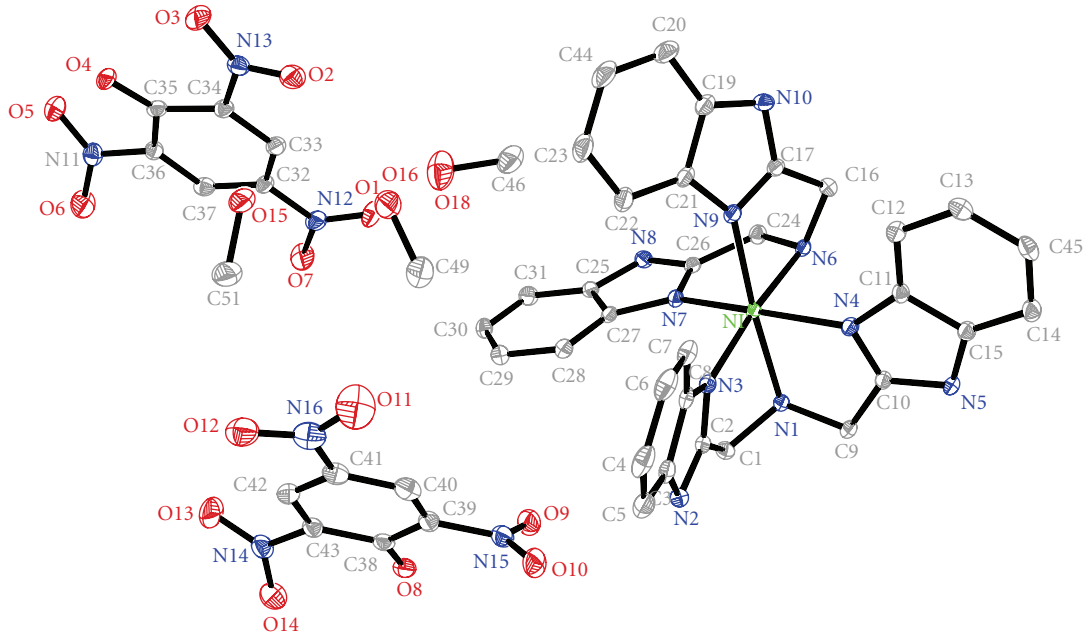

Figure 1: The molecular structure of the Ni(II) complex showing displacement ellipsoids at the 30% probability level. Hydrogen atoms have been omitted for clarity.

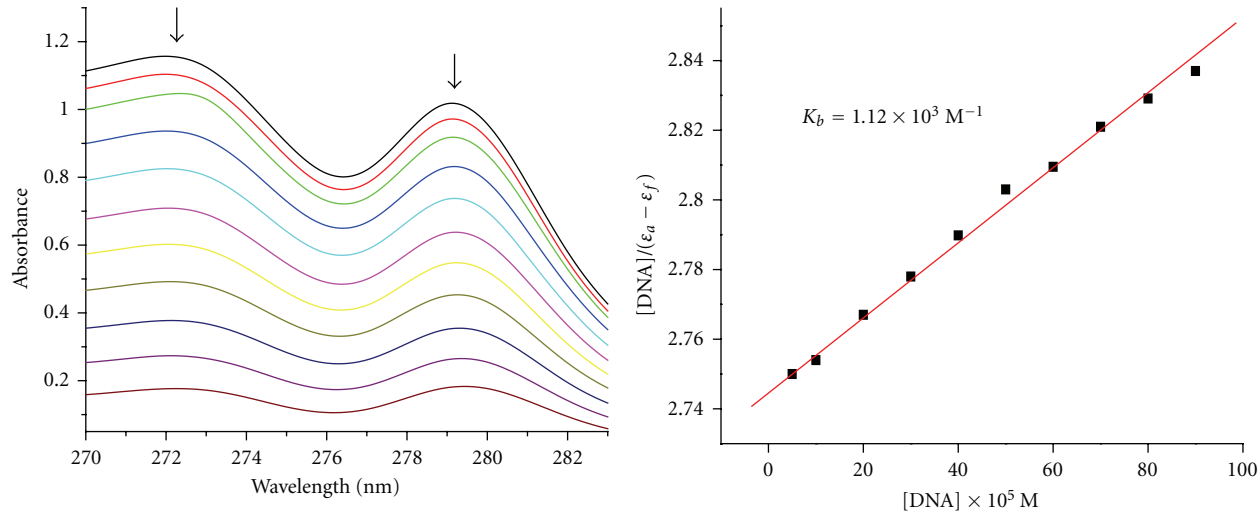

Figure 2: Electronic spectra of the Ni(II) complex (30 μM) in the presence of 0, 5, 10, 20, 30, 40, 50, 60, 70, 80, and 90 μL CT-DNA. [DNA] = 2.5 $\times 10^{-5}$ M. Arrow shows the absorbance changes upon increasing CT-DNA concentration. Plots of [DNA]/($\varepsilon_a - \varepsilon_f$) versus [DNA] for the titration of the Ni(II) complex with CT-DNA.

Table 2: Selected bond lengths (Å) and angles (deg) of the Ni(II) complex.

Bond lengths					
Ni–N(1)	2.1647 (19)	Ni–N(4)	2.0793(18)	Ni–N(6)	2.1788(19)
Ni–N(3)	2.0899 (19)	Ni–N(7)	2.0667 (18)	Ni–N(9)	2.0628 (19)
Bond angles					
N(1)–Ni–N(6)	94.12 (7)	N(9)–Ni–N(7)	173.40 (7)	N(9)–Ni–N(4)	98.11 (7)
N(3)–Ni–N(7)	173.40 (7)	N(3)–Ni–N(1)	79.29 (7)	N(7)–Ni–N(4)	166.55 (7)
N(9)–Ni–N(3)	107.52 (7)	N(7)–Ni–N(3)	98.95 (7)	N(3)–Ni–N(4)	89.98 (7)
N(1)–Ni–N(9)	173.19 (7)	N(7)–Ni–N(1)	90.23 (7)	N(1)–Ni–N(4)	81.52 (7)
N(9)–Ni–N(6)	79.07 (8)	N(7)–Ni–N(6)	81.11 (7)	N(4)–Ni–N(6)	88.87 (7)

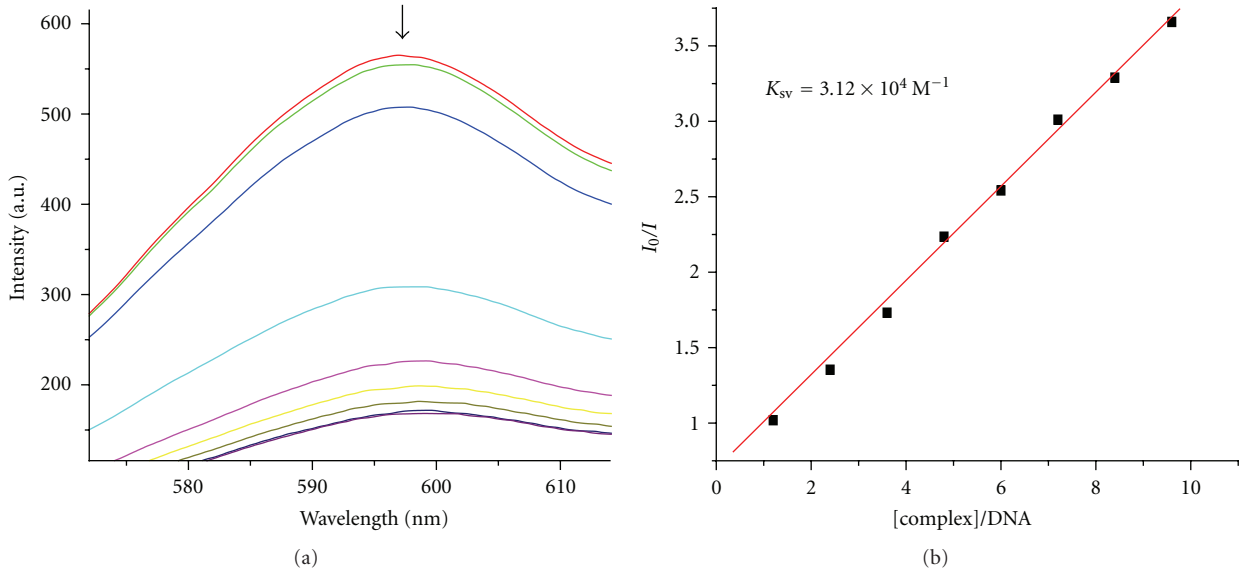

FIGURE 3: Emission spectra of EB bound to DNA in the presence of the complex. [Complex] = 3×10^{-3} M; λ_{ex} = 520 nm. The arrow shows the intensity changes upon increasing concentrations of the complex. Fluorescence quenching curves of EB bound to CT-DNA by the Ni(II) complex. (Plots of I_0/I versus [Complex]/DNA.).

may be best described as distorted octahedral with four coordination nitrogen atoms from an ideal equatorial plane. The maximum deviation (N9) from the plane containing these four N atoms is 0.764 Å. The bond average length between the Ni ion and the apical N atom (N1, N6) is 2.171 Å, which is about 0.097 Å longer than the bond average length between the Ni ion and four coordination N atoms from an equatorial plane. This geometry is assumed by the Ni(II) to relieve the steric crowding. Therefore, compared with a regular octahedron, it reflects a relatively distorted coordination octahedron around Ni(II).

3.3. Spectral Studies of the Interactions with DNA

3.3.1. Electronic Absorption Titration. Electronic absorption spectroscopy is universally employed to determine the binding characteristics of metal complexes with DNA [30–32]. The absorption spectra of the Ni(II) complex in the absence and presence of CT-DNA are given in Figure 2. There are two well-resolved bands at about 272, 278 nm for the complex. The λ for the ligand increases only from 272 to 273, and for the complex from 278 to 279 nm, a slight red shift about 1 nm under identical experimental conditions. The slight red shift suggests that the Ni(II) complex interacts with DNA [33].

The binding constant K_b for the complex has been determined from the plot of [DNA]/($\varepsilon_a - \varepsilon_f$) versus [DNA] and was found to be $1.12 \times 10^3\ M^{-1}$. Compared with those of the so-called DNA-intercalative ruthenium complexes (1.1×10^4–$4.8 \times 10^4\ M^{-1}$) [34], the binding constants (K_b) of the Ni(II) complex suggest that the complex with DNA with an affinity is less than the classical intercalators.

3.3.2. Fluorescence Spectroscopic Studies. intensity in the EB-DNA adduct allows determination of the affinity of the

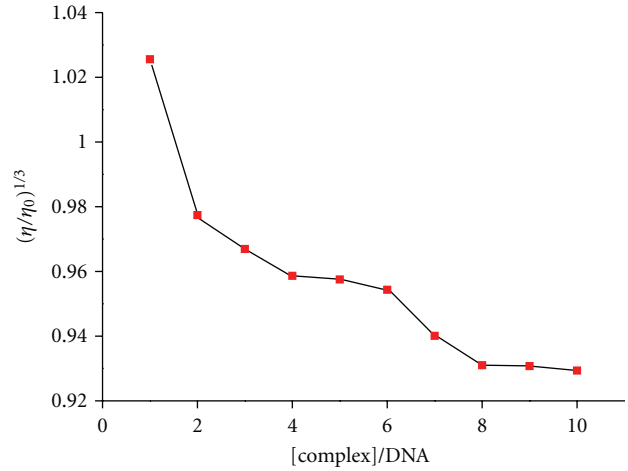

FIGURE 4: Effect of increasing amounts of the Ni(II) complex on the relative viscosity of CT-DNA at 25.0 ± 0.1°C.

complex for DNA, whatever the binding mode may be. If a complex can replace EB from DNA-bound EB, the fluorescence of the solution will be quenched due to the fact that free EB molecules are readily quenched by the surrounding water molecules [35]. For all the compounds, no emission was observed either alone or in the presence of CT-DNA in the buffer. The fluorescence quenching of EB bound to CT-DNA by the Ni(II) complex is shown in Figure 3. The quenching of EB bound to CT-DNA by the Ni(II) complex is in good agreement with the linear Stern-Volmer equation, which provides further evidence that the Ni(II) complex bind to DNA. The quenching plots illustrate that the quenching of EB bound to DNA by the complex is in good agreement with the linear Stern-Volmer equation, which also proves that the complex binds to DNA. The K_{sv}

value for the Ni(II) complex is $3.12 \times 10^4\,M^{-1}$. The data suggest that the Ni(II) complex interacts with DNA.

3.3.3. Viscosity Studies. Optical photophysical techniques are widely used to study the binding model of the ligand, metal complexes, and DNA but not to give sufficient clues to support a binding model. Therefore, viscosity measurements were carried out to further clarify the interaction of metal complexes and DNA. Hydrodynamic measurements that are sensitive to the length change (i.e., viscosity and sedimentation) are regarded as the least ambiguous and the most critical tests of a binding model in solution in the absence of crystallographic structural data [15, 20]. A classical intercalative mode causes a significant increase in viscosity of DNA solution due to increase in separation of base pairs at intercalation sites and hence an increase in overall DNA length. By contrast, complexes that bind exclusively in the DNA grooves by partial and/or nonclassical intercalation, under the same conditions, typically cause less pronounced (positive or negative) or no change in DNA solution viscosity [20]. The values of $(\eta - \eta_0)^{1/3}$ were plotted against [compound]/[DNA] (Figure 4). For the Ni(II) complex, as increasing the amounts of compound, the viscosity of DNA decreases steadily. The decreased relative viscosity of DNA may be explained by a binding mode which produced bends or kinks in the DNA and thus reduced its effective length and concomitantly its viscosity. The results suggest that the Ni(II) complex may bind to DNA by partial intercalation.

4. Conclusions

In this paper, a new Ni(II) complex has been synthesized and characterized. Moreover, the DNA-binding properties of the Ni(II) complex were investigated by electronic absorption, fluorescence, and viscosity measurements. The experimental results indicate that the Ni(II) complex can bind to CT-DNA by partial intercalation mode. Information obtained from our study will be helpful to understand the mechanism of interactions of benzimidazoles and their complexes with nucleic acids and should be useful in the development of potential probes of DNA structure and conformation.

Appendix

Additional Data

CCDC 825141 contains the additional crystallographic data for this paper. These data can be obtained free of charge from The Cambridge Crystallographic Data Centre via http://www.ccdc.cam.ac.uk/data_request/cif.

Acknowledgments

The authors acknowledge the financial support and a grant from "Qing Lan" Talent Engineering Funds by Lanzhou Jiaotong University. The grant from "Long Yuan Qing Nian" of Gansu Province is also acknowledged.

References

[1] M. Mrksich and P. B. Dervan, "Antiparallel side-by-side heterodimer for sequence-specific recognition in the minor groove of DNA by a distamycin/1-methylimidazole-2-carboxamide-netropsin pair," *Journal of the American Chemical Society*, vol. 115, no. 7, pp. 2572–2576, 1993.

[2] C. Kokubo and T. Katsuki, "Highly enantioselective catalytic oxidation of alkyl aryl sulfides using Mn-salen catalyst," *Tetrahedron*, vol. 52, no. 44, pp. 13895–13900, 1996.

[3] S. Schoumacker, O. Hamelin, J. Pécaut, and M. Fontecave, "Catalytic asymmetric sulfoxidation by chiral manganese complexes: acetylacetonate anions as chirality switches," *Inorganic Chemistry*, vol. 42, no. 24, pp. 8110–8116, 2003.

[4] C. M. Dupureur and J. K. Barton, "Structural Studies of Λ- and Δ-$[Ru(phen)_2dppz]^{2+}$ Bound to $d(GTCGAC)_2$: characterization of Enantioselective Intercalation," *Inorganic Chemistry*, vol. 36, no. 1, pp. 33–43, 1997.

[5] C. Hemmert, M. Pitié, M. Renz, H. Gornitzka, S. Soulet, and B. Meunier, "Preparation, characterization and crystal structures of manganese(II), iron(III) and copper(II) complexes of the bis[di-1,1-(2-pyridyl)ethyl] amine (BDPEA) ligand; evaluation of their DNA cleavage activities," *Journal of Biological Inorganic Chemistry*, vol. 6, no. 1, pp. 14–22, 2001.

[6] V. S. Li, D. Choi, Z. Wang, L. S. Jimenez, M. Tang, and H. Kohn, "Role of the C-10 substituent in mitomycin C-1-DNA bonding," *Journal of the American Chemical Society*, vol. 118, no. 10, pp. 2326–2331, 1996.

[7] G. Zuber, J. C. Quada, and S. M. Hecht, "Sequence selective cleavage of a DNA octanucleotide by chlorinated bithiazoles and bleomycins," *Journal of the American Chemical Society*, vol. 120, no. 36, pp. 9368–9369, 1998.

[8] A. Gellis, H. Kovacic, N. Boufatah, and P. Vanelle, "Synthesis and cytotoxicity evaluation of some benzimidazole-4,7-diones as bioreductive anticancer agents," *European Journal of Medicinal Chemistry*, vol. 43, no. 9, pp. 1858–1864, 2008.

[9] Ö. Ö. Güven, T. Erdoğan, H. Göker, and S. Yildiz, "Synthesis and antimicrobial activity of some novel phenyl and benzimidazole substituted benzyl ethers," *Bioorganic and Medicinal Chemistry Letters*, vol. 17, no. 8, pp. 2233–2236, 2007.

[10] K. Kopańska, A. Najda, J. Zebrowska et al., "Synthesis and activity of 1*H*-benzimidazole and 1*H*-benzotriazole derivatives as inhibitors of Acanthamoeba castellanii," *Bioorganic and Medicinal Chemistry*, vol. 12, no. 10, pp. 2617–2624, 2004.

[11] K. C. Skyrianou, F. Perdih, I. Turel, D. P. Kessissoglou, and G. Psomas, "Nickel-quinolones interaction—part 2: interaction of nickel(II) with the antibacterial drug oxolinic acid," *Journal of Inorganic Biochemistry*, vol. 104, no. 2, pp. 161–170, 2010.

[12] K. C. Skyrianou, C. P. Raptopoulou, V. Psycharis, D. P. Kessissoglou, and G. Psomas, "Structure, cyclic voltammetry and DNA-binding properties of the bis(pyridine)bis(sparfloxacinato)nickel(II) complex," *Polyhedron*, vol. 28, no. 15, pp. 3265–3271, 2009.

[13] Y. Jin, M. A. Lewis, N. H. Gokhale, E. C. Long, and J. A. Cowan, "Influence of stereochemistry and redox potentials on the single- and double-strand DNA cleavage efficiency of Cu(II)-and Ni(II)·Lys-Gly-his-derived ATCUN metallopeptides," *Journal of the American Chemical Society*, vol. 129, no. 26, pp. 8353–8361, 2007.

[14] F. Bisceglie, M. Baldini, M. Belicchi-Ferrari et al., "Metal complexes of retinoid derivatives with antiproliferative activity: synthesis, characterization and DNA interaction studies," *European Journal of Medicinal Chemistry*, vol. 42, no. 5, pp. 627–634, 2007.

[15] J. B. Chaires, "Tris(phenanthroline)ruthenium(II) enantiomer interactions with DNA: mode and specificity of binding," *Biochemistry*, vol. 32, no. 10, pp. 2573–2584, 1993.

[16] J. Marmur, "A procedure for the isolation of deoxyribonucleic acid from microorganisms," *Methods in Enzymology*, vol. 6, pp. 726–738, 1963.

[17] A. Wolfe, G. H. Shimer, and T. Meehan, "Polycyclic aromatic hydrocarbons physically intercalate into duplex regions of denatured DNA," *Biochemistry*, vol. 26, no. 20, pp. 6392–6396, 1987.

[18] M. Chauhan, K. Banerjee, and F. Arjmand, "DNA binding studies of novel copper(II) complexes containing L-tryptophan as chiral auxiliary: in vitro antitumor activity of Cu-Sn_2 complex in human neuroblastoma cells," *Inorganic Chemistry*, vol. 46, no. 8, pp. 3072–3082, 2007.

[19] J. R. Lakowicz and G. Weber, "Quenching of fluorescence by oxygen. A probe for structural fluctuations in macromolecules," *Biochemistry*, vol. 12, no. 21, pp. 4161–4170, 1973.

[20] S. Satyanarayana, J. C. Dabrowiak, and J. B. Chaires, "Neither Δ- nor Λ-tris(phenanthroline)ruthenium(II) binds to DNA by classical intercalation," *Biochemistry*, vol. 31, no. 39, pp. 9319–9324, 1992.

[21] H. P. Berends and D. W. Stephan, "Copper(I) and copper(II) complexes of biologically relevant tridentate ligands," *Inorganica Chimica Acta*, vol. 93, no. 4, pp. 173–178, 1984.

[22] Bruker, *Smart Saint and Sadabs*, Bruker Axs, Inc., Madison, Wisc, USA, 2000.

[23] G. M. Sheldrick, *SHELXTL*, Siemmens Analytical X-Ray Instruments, Inc., Madison, Wisc, USA, 1996.

[24] W. J. Geary, "The use of conductivity measurements in organic solvents for the characterisation of coordination compounds," *Coordination Chemistry Reviews*, vol. 7, no. 1, pp. 81–122, 1971.

[25] C. Y. Su, B. S. Kang, C. X. Du, Q. C. Yang, and T. C. W. Mak, "Formation of mono-, bi-, tri-, and tetranuclear Ag(I) complexes of C_3-symmetric tripodal benzimidaxole ligands," *Inorganic Chemistry*, vol. 39, no. 21, pp. 4843–4849, 2000.

[26] R. J. Sundberg and R. B. Martin, "Interactions of histidine and other imidazole derivatives with transition metal ions in chemical and biological systems," *Chemical Reviews*, vol. 74, no. 4, pp. 471–517, 1974.

[27] V. McKee, M. Zvagulis, and C. A. Reed, "Further insight into magnetostructural correlations in binuclear copper(II) species related to methemocyanin: X-ray crystal structure of a 1,2-μ-nitrito complex," *Inorganic Chemistry*, vol. 24, no. 19, pp. 2914–2919, 1985.

[28] T. J. Lane, I. Nakagawa, J. L. Walter, and A. J. Kandathil, "Infrared investigation of certain imidazole derivatives and their metal chelates," *Inorganic Chemistry*, vol. 1, pp. 267–276, 1962.

[29] H. Wu, R. Yun, K. Li, K. Wang, X. Huang, and T. Sun, "Synthesis, crystal structure and spectra properties of the nickel (II) complex with 1,3-bis(1-benzylbenzimidazol2-yl)-2-oxopropane," *Synthesis and Reactivity in Inorganic, Metal-Organic and Nano-Metal Chemistry*, vol. 39, no. 9, pp. 614–617, 2009.

[30] H. Li, X. Y. Le, D. W. Pang, H. Deng, Z. H. Xu, and Z. H. Lin, "DNA-binding and cleavage studies of novel copper(II) complex with L-phenylalaninate and 1,4,8,9-tetraaza-triphenylene ligands," *Journal of Inorganic Biochemistry*, vol. 99, no. 11, pp. 2240–2247, 2005.

[31] V. G. Vaidyanathan and B. U. Nair, "Synthesis, characterization, and DNA binding studies of a chromium(III) complex containing a tridentate ligand," *European Journal of Inorganic Chemistry*, no. 19, pp. 3633–3638, 2003.

[32] V. G. Vaidyanathan and B. U. Nair, "Nucleobase oxidation of DNA by (terpyridyl)chromium(III) derivatives," *European Journal of Inorganic Chemistry*, no. 9, pp. 1840–1846, 2004.

[33] J. Liu, T. Zhang, T. Lu et al., "DNA-binding and cleavage studies of macrocyclic copper(II) complexes," *Journal of Inorganic Biochemistry*, vol. 91, no. 1, pp. 269–276, 2002.

[34] A. M. Pyle, J. P. Rehmann, R. Meshoyrer, C. V. Kumar, N. J. Turro, and J. K. Barton, "Mixed-ligand complexes of ruthenium(II): factors governing binding to DNA," *Journal of the American Chemical Society*, vol. 111, no. 8, pp. 3051–3058, 1989.

[35] B. C. Baguley and M. Le Bret, "Quenching of DNA-ethidium fluorescence by amsacrine and other antitumor agents: a possible electron-transfer effect," *Biochemistry*, vol. 23, no. 5, pp. 937–943, 1984.